



**BINGHAM YIELD STRESS AND BINGHAM PLASTIC VISCOSITY OF  
HOMOGENEOUS NON-NEWTONIAN SLURRIES**

---

by

Brian Tonderai Zengeni

Student Number: 210233265

Dissertation submitted in partial fulfilment of the requirements for the degree and  
which counts towards 50% of the final mark

**Master of Technology Mechanical Engineering**

in the Faculty of Engineering

**at the Cape Peninsula University of Technology**

Supervisor: Prof. Graeme John Oliver

Bellville Campus

October 2016

**CPUT copyright information**

The dissertation/thesis may not be published either in part (in scholarly, scientific or technical journals), or as a whole (as a monograph), unless permission has been obtained from the University

**DECLARATION**

I, Brian Tonderai Zengeni, declare that the contents of this dissertation represent my own unaided work, and that the dissertation has not previously been submitted for academic examination towards any qualification. Furthermore, it represents my own opinions and not necessarily those of the Cape Peninsula University of Technology.

**October 2016**

\_\_\_\_\_  
**Signed**

\_\_\_\_\_  
**Date**

## ABSTRACT

This dissertation presents how material properties (solids densities, particle size distributions, particle shapes and concentration) of gold tailings slurries are related to their rheological parameters, which are yield stress and viscosity. In this particular case Bingham yield stresses and Bingham plastic viscosities. Predictive models were developed from analysing data in a slurry database to predict the Bingham yield stresses and Bingham plastic viscosities from their material properties. The overall goal of this study was to develop a validated set of mathematical models to predict Bingham yield stresses and Bingham plastic viscosities from their material properties.

The interaction of the non-Newtonian material properties is very complex at varying mass solids concentrations. The evaluation of these interactions in terms of constitutive equations is almost impossible and the relationship between material properties, mass solids concentration and rheology can only be modelled in a statistical manner. The validity of each model is checked to ensure that predictions and interpretations are unbiased and efficient. This is done by comparing the resulting models to experimental data generated from test work. An in-depth analysis was conducted to see the interrelationship between the material properties and how they affect the yield stress and viscosity values.

Regression analysis was used as an analysis tool to come up with the relationships as well as to develop the predictive models. Two coefficients Beta ( $\beta$ ) and Zeta ( $\zeta$ ) were used in the prediction of Bingham plastic viscosity and yield stress respectively. The freely settled bed packing concentration  $C_{\text{free}}$  was found to be a very important parameter as it is a function of a solids density, particle size distribution, particle shape and concentration.

The feasibility of the developed predictive models was validated by testing six different gold tailings samples with different material properties. Flow curves of the different gold tailings samples were generated and the Bingham plastic model was used to analyse the flow curves. The measured Bingham yield stress and plastic viscosity values were compared to the predicted yield stress and plastic viscosity values from the developed models using the material properties as inputs. Future work should be performed to improve the accuracy of the predictions of the Bingham yield stress and the Bingham plastic viscosity using these models.

## **ACKNOWLEDGEMENTS**

I wish to firstly thank God almighty, for granting me wisdom, power and a sound mind in compiling these ideas together into this work with the help of the following people:

- Dr Angus Paterson from Paterson and Cooke Consulting Engineers for his guidance and support with the resources for me to complete this dissertation.
- Professor Graeme Oliver for his supervision and critical evaluation as well as his support during my dissertation preparation.
- My colleague and friend Bruno Salvodi for his continuous encouragement and motivation for me to finish this dissertation.
- I would lastly like to thank my wife Memory for her continued support, motivation and constructive criticism to see this dissertation to completion.

## **DEDICATION**

This dissertation is dedicated to my wife Memory and my son Kutenda, for they have been my source of inspiration during my compilation of my dissertation. I would also like to dedicate this work to my loving parents for their continuous encouragement and support.

## TABLE OF CONTENTS

DECLARATION.....	i
ABSTRACT.....	ii
ACKNOWLEDGEMENTS.....	iii
DEDICATION.....	iv
TABLE OF CONTENTS.....	v
NOMENCLATURE.....	ix
1. CHAPTER ONE.....	1
1.1 Introduction.....	1
1.2 Problem Statement.....	1
1.3 Background.....	2
1.4 Objectives.....	3
1.5 Research Methodology.....	3
1.5.1 <i>Experimental Work</i> .....	3
1.5.2 <i>Analysis of Data</i> .....	3
1.5.3 <i>Research Design</i> .....	3
1.6 Research Delineation.....	3
1.7 Research Significance.....	4
1.8 Structure of Dissertation.....	4
2. CHAPTER TWO.....	5
2.1 Rheology.....	5
2.2 Definition of Rheological Parameters.....	5
2.2.1 <i>Viscosity</i> .....	5
2.2.2 <i>Shear Rate</i> .....	6
2.2.3 <i>Shear Stress</i> .....	6
2.3 Newtonian Fluid Behaviour.....	7
2.4 Non-Newtonian Fluid Behaviour.....	8
2.4.1 <i>Time independent versus time-dependent fluid</i> .....	8
2.4.2 <i>Newtonian versus non-Newtonian fluids</i> .....	8
2.5 Rotational Rheometry.....	9
2.6 Factors Affecting Rheology.....	15
2.6.1 <i>Shape Factors</i> .....	16
2.7 Yield Stress.....	17
2.8 Viscosity.....	20
3. CHAPTER THREE.....	23
3.1 Experimental Work.....	23
3.2 Rotational Viscometer Tests.....	23
3.2.1 <i>Viscosity Check with Calibration Oil</i> .....	24

3.3	Material Properties .....	24
3.3.1	<i>Particle Size Distribution</i> .....	25
3.3.2	<i>Slurry pH and Temperature</i> .....	25
3.3.3	<i>Particle Micrographs</i> .....	25
3.3.4	<i>Solids Density Measurements</i> .....	25
3.3.5	<i>Slurry Mixture Density Measurement</i> .....	26
3.3.6	<i>Mass Solids Concentration</i> .....	26
3.3.7	<i>Volumetric Solids Concentration</i> .....	26
3.3.8	<i>Freely Settled Bed Packing Concentration</i> .....	26
4.	CHAPTER FOUR .....	27
4.1	Data Analysis and Discussion .....	27
4.2	Particle Size Distribution.....	27
4.3	Effect of Solids Concentration .....	27
4.4	Summary of Material Properties .....	28
4.5	Rotational Viscometer Results.....	29
4.6	Determining the Beta Coefficient from Regression Analysis .....	38
4.6.1	<i>Using The Calculated Beta Coefficient to Predict Plastic Viscosity</i> .....	39
4.6.2	<i>Calculating Zeta Coefficient to Predict Bingham Yield Stress</i> .....	42
4.6.3	<i>The Relationship between Beta and Zeta Coefficient</i> .....	44
5.	CHAPTER FIVE .....	45
5.1	Results .....	45
5.1.1	<i>Comparison of Tested Data to Model Predictions</i> .....	45
5.2	Evaluation of Model Predictions.....	61
5.3	Summary of Model Predictions .....	63
6.	CHAPTER SIX .....	64
6.1	Discussion and Conclusions.....	64
6.1.1	<i>Summary of This Research</i> .....	64
6.1.2	<i>Limitations to the Study</i> .....	65
6.1.3	<i>Future Work</i> .....	65
	REFERENCES.....	66
	Appendix A : PARTICLE SIZE DISTRIBUTION DATA.....	70
	Appendix B : ROTATIONAL VISCOMETER TEST DATA.....	76
	Appendix C : VISCOSITY AND DENSITY REFERENCE STANDARD .....	114

## LIST OF TABLES

Table 2-I: Different Flow Models (Bird et al, 1960; Shook and Roco, 1991).....	11
Table 4-I:Material Property Summary .....	28
Table 4-II: Measured Bingham Yield Stress and Plastic Viscosity in Database.....	29

Table 4-III: Predicted Plastic Viscosity Using Calculated Beta Coefficient .....	39
Table 4-IV: Calculated Beta Coefficients and $C_{bfree}$ for all Samples .....	40
Table 4-V: Comparison of Calculated Beta and Predicted Beta Coefficients .....	41
Table 4-VI: Calculation of Zeta Coefficient for Sample 1 .....	42
Table 4-VII: Calculated Yield Stress Using Zeta Coefficient .....	43
Table 5-I: Summary of Material Properties for the Six Gold Tailings Samples .....	46
Table 5-II: Sample A Rheology Test Results .....	47
Table 5-III: Comparison of Predicted and Measured Data for Sample A .....	47
Table 5-IV: Sample B Rheology Test Results .....	49
Table 5-V: Comparison of Predicted and Measured Data for Sample B .....	50
Table 5-VI: Sample C Rheology Test Results .....	52
Table 5-VII: Comparison of Predicted and Measured Data for Sample C .....	52
Table 5-VIII: Sample 4 Rheology Test Results .....	54
Table 5-IX: Comparison of Predicted and Measured Data for Sample D .....	55
Table 5-X: Sample E Rheology Test Results .....	57
Table 5-XI: Comparison of Predicted and Measured Data for Sample E .....	57
Table 5-XII: Sample F Rheology Test Results .....	59
Table 5-XIII: Comparison of Predicted and Measured Data for Sample F .....	60
Table 5-XIV: Average Relative Errors of Samples Tested .....	61

## LIST OF FIGURES

Figure 2-1: The Two-Plate-Model Definition of Viscosity (Coghill, 2003; Paterson & Cooke, 2000 and Slatter et al, 2002). .....	6
Figure 2-2: Comparison of Newtonian Flow Behaviour .....	7
Figure 2-3: Comparison of Newtonian Flow Behaviour - Constant Viscosity .....	8
Figure 2-4: Geometry of the Searle system (Anton Paar Measuring System Data Sheet) .....	9
Figure 2-5: Rheograms of Different Time-Independent Flow (Chhabra & Richardson, 2008) .....	10
Figure 2-6: Rheogram Data at 61.3% $m$ .....	13
Figure 2-7: Pseudo Shear Comparison of Pipe Loop Data with Rotational Viscometer Data .....	14
Figure 2-8: Pressure Gradient Comparison of Pipelooop and Rotational Viscometer Data .....	15
Figure 2-9: Effects of Particle Concentration and Interparticle Attraction on Fluid Rheology (Brown and Heywood, 1991) .....	15
Figure 2-10: Different Particle Shapes and Shape Factors (Macdonald 1983) .....	17
Figure 3-1: An Anton Paar Rheolab QC Rotational Viscometer .....	23
Figure 3-2: Calibration Oil Viscosity Results .....	24
Figure 3-3: The SEM Microscope .....	25
Figure 4-1: Particle Size Distribution Comparison .....	27
Figure 4-2: Yield Stress versus Mass Solids Concentration Comparison .....	36
Figure 4-3: Plastic Viscosity versus Mass Solids Concentration Comparison .....	37
Figure 4-4: Plot of LOG (Viscosity Ratio) vs Volume Ratio with Y-intercept not Adjusted .....	38
Figure 4-5: Plot of LOG (Viscosity Ratio) vs Volume Ratio Adjusted to Zero .....	38
Figure 4-6: Comparison of Measured and Predicted Plastic Viscosity Data .....	39
Figure 4-7: Beta Coefficient ( $\beta$ ) v $C_{bfree}$ for All 30 Samples .....	41



Figure 4-8: Relationship between Beta and Zeta Coefficient .....	44
Figure 5-1: Particle Size Distribution Comparison.....	45
Figure 5-2: Rheogram of Sample A .....	46
Figure 5-3: Comparison of Measured and Predicted Yield Stress for Sample A .....	48
Figure 5-4: Comparison of Measured and Predicted Plastic Viscosity for Sample A.....	48
Figure 5-5: Rheogram of Sample B .....	49
Figure 5-6: Comparison of Measured and Predicted Yield Stress for Sample B .....	50
Figure 5-7: Comparison of Measured and Predicted Plastic Viscosity for Sample B.....	51
Figure 5-8: Rheogram of Sample C .....	51
Figure 5-9: Comparison of Measured and Predicted Yield Stress for Sample C .....	53
Figure 5-10: Comparison of Measured and Predicted Plastic Viscosity for Sample C.....	53
Figure 5-11: Rheogram of Sample D .....	54
Figure 5-12: Comparison of Measured and Predicted Yield Stress for Sample D .....	55
Figure 5-13: Comparison of Measured and Predicted Plastic Viscosity for Sample D.....	56
Figure 5-14: Rheogram of Sample E .....	56
Figure 5-15: Comparison of Measured and Predicted Yield Stress for Sample E .....	58
Figure 5-16: Comparison of Measured and Predicted Plastic Viscosity for Sample E .....	58
Figure 5-17: Rheogram of Sample F .....	59
Figure 5-18: Comparison of Measured and Predicted Yield Stress for Sample F.....	60
Figure 5-19: Comparison of Measured and Predicted Plastic Viscosity of Sample F .....	61

## NOMENCLATURE

Symbol	Description	Units
A	correlating parameter	-
B	correlating parameter	-
$C_{bfree}$	freely settled bed packing concentration	(%)
$C_v$	volumetric solids concentration	(%)
$C_m$	mass solids concentration	(%)
d	particle size	( $\mu\text{m}$ )
D	pipeline internal diameter	(m)
F	force	(N)
K	fluid consistency index	( $\text{Pa}\cdot\text{s}^n$ )
$K_B$	Bingham viscosity	( $\text{Pa}\cdot\text{s}$ )
M	mass	(kg)
n	flow behaviour index	-
$\rho$	density	( $\text{kg}/\text{m}^3$ )
T	torque	(Nm)
$\tau$	shear stress	(Pa)
$\tau_{yB}$	Bingham yield stress	(Pa)
$\tau_y$	yield stress	(Pa)
$\mu$	viscosity	( $\text{Pa}\cdot\text{s}$ )
$\mu_a$	apparent viscosity	( $\text{Pa}\cdot\text{s}$ )
V	pipeline velocity	(m/s)
$V_R$	Volume ratio	-
$\eta_R$	Viscosity ratio	
$\dot{\gamma}$	shear rate	( $\text{s}^{-1}$ )
$\Omega$	angular velocity	( $\text{rads}^{-1}$ )

### Subscripts

m	mixture (slurry), mass
s	solids
v	volumetric
w	conveying fluid
p	pycnometer
b	beaker

# 1. CHAPTER ONE

This chapter gives the background to the research problem. It also gives an outline of the objectives, methodology and the importance of the research being carried out.

## 1.1 Introduction

This project presents a comparison of rheology test work conducted on homogeneous non-Newtonian slurries of gold tailings to model predictions. The slurries were tested in a commercial test facility over several years using an Anton Paar Rheolab QC rotational viscometer at varying mass solids concentrations and compared with data. The slurry rheology is required for evaluating the various hydraulic parameters such as optimum design velocity, transport concentration, pumping power and specific power consumption (Govier and Aziz, 1972).

The Searle system was used for the rotational viscometer tests. It is a system where the bob rotates and the cup is stationary and is used to measure the rheology of the different homogeneous non-Newtonian slurries. Specifically, the CC35/HR (measuring bob radius = 17.5 mm, measuring cup radius = 21.0 mm, gap length = 52.5 mm, cone angle 120 °) measuring system will be selected for this work. Models for predicting Bingham yield stresses and Bingham plastic viscosities as a function of mass solids concentration will be generated from the correlations of the slurries tested and also from literature from other scholars of thought.

The purpose of the study is to advise an organisation on the advantages of the project and to investigate whether the project is feasible under the current economic conditions, with the intention of developing the project into a feasible mining operation. The need for this scoping study is also to establish high-level estimates of the capital and operating costs that may be associated with a project of this nature.

## 1.2 Problem Statement

For pump and pipeline pre-feasibility studies it is necessary to estimate the system capital and operating costs to a defined accuracy of typically  $\pm 25\%$ . It is, therefore, important to establish the cost implication of increasing solids concentration on pumping requirements and to balance this with reduced water consumption. In order to do this for mineral slurries, it is necessary to estimate the rheology of the homogeneous non-Newtonian slurries with reasonable certainty. However representative samples are

not always available at the pre-feasibility level, and so direct viscometer measurements cannot be made. This lack of information complicates the design and reliable operation of these systems. This project analyses a large amount of measured data from a commercial laboratory's slurry database and aims to develop a series of correlations utilising basic solids properties data to predict the slurry yield stress and plastic viscosity *a priori* to a reasonable accuracy commensurate with typical pre-feasibility study requirements.

### 1.3 Background

When working on proposals for pre-feasibility studies of pipeline projects, it is of utmost importance to come up with project capital and operating costs that are within range of  $\pm 25\%$  of the final cost of the project. During conceptual engineering, the rheological properties of slurries need to be determined with reasonable accuracy. The pumping system design engineer will use these rheological parameters to establish the number of pump sets required and to complete the preliminary pump and pipeline sizing. The aim is to produce this design information efficiently without the need for extensive and time-consuming test work if the material properties of the slurry are known. Being able to produce quick estimates of pipe sizes, pump sizes and pump power is very useful in conceptual engineering as part of comparing various scenarios in order to optimise the design. This information is generated from the accurate prediction of the rheological properties of the slurry, which typically are the Bingham yield stress and Bingham plastic viscosities.

Therefore, it will be of tremendous value to develop empirical models that *a priori* predict the Bingham yield stress and Bingham plastic viscosity with varying mass solids concentration using easily measured material properties. The rheological parameters of gold tailings slurries can be estimated using a series of correlations that will be developed by assessing a comprehensive database of results that contain measured data of rheology and the solids properties. The correlations developed using the database will utilise the solids properties and chemistry of the slurry. This data will be used to estimate the Bingham parameters that will be compared with measured rheological properties of specific samples prepared in the laboratory.

## 1.4 Objectives

The objectives of this project are to:

- To develop correlations that predict Bingham yield stresses and Bingham plastic viscosities as a function of mass solids concentration. The predicted data should be within reasonable accuracy ( $\pm 25\%$ ) of the actual tested data so that it can be used during pre-feasibility studies.
- Provide a means of estimating the slurry rheological properties based on the rheological properties of the slurry, and physical properties of the material.
- Ensure that the results of the study formulated are applicable to industry.

## 1.5 Research Methodology

The following steps were undertaken with the above objectives in mind:

### 1.5.1 *Experimental Work*

The experimental work was conducted at commercial test facility in Cape Town using an Anton Paar Rheolab QC rotational viscometer.

### 1.5.2 *Analysis of Data*

The Bingham plastic model was used to analyse the rotational viscometer laminar flow data. The model was used to determine the Bingham yield stress and Bingham plastic viscosity.

### 1.5.3 *Research Design*

Correlational research design was used in coming up with the relationships among the tested variables.

## 1.6 Research Delineation

Below are some of the considerations that are anticipated, although the research scope may evolve depending on data quality and availability.

- The research is limited to testing gold tailings only, although results are expected to be generic and applicable to other non-Newtonian slurries.

- The analysis will be done using the Bingham plastic model to come up with yield stresses and plastic viscosity values.
- The models to predict the Bingham yield stress and Bingham plastic viscosity will be validated against actual tested data of control samples that will be made up to specific particle size distributions.
- The predictive models will be valid for slurries that lie within the envelope of the particle size distributions of the materials tested.
- The depth of the details presented in the research project report will be at a dissertation level.

## **1.7 Research Significance**

The slurry test work and successive modelling performed in this study has a direct impact on the hydraulic design and operation of industrial tailings slurry pipelines and the overall disposal systems. Inadequate or inaccurate mineral slurry testing and modelling could lead to the design of highly inefficient, unreliable and even inoperable systems. It is, therefore, imperative that accurate methods of estimating Bingham yield stresses and Bingham plastic viscosities of slurries be predicted from their material properties with reasonable accuracy.

## **1.8 Structure of Dissertation**

Chapter 2: This chapter mainly focuses on a literature survey of rheology and models developed to date. It basically sets the background for later chapters. Chapter 3: Defines and discusses the various experimental equipment and procedures that were used throughout the study to determine slurry material properties and the rheological properties of the slurries. Chapter 4: Presents a summary of the slurry database used in this study and the results of the test work performed on other slurry samples. Some of the results are represented in graphical form to achieve a better understanding for the reader. Chapter 4 also presents the steps taken in the predictive model development. Chapter 5: Presents the results of the tested data to the predicted data from the prediction models and Chapter 6: Discussion and conclusion.

## 2. CHAPTER TWO

This chapter reviews the literature on rheology. It differentiates Newtonian and non-Newtonian fluids. It explains rotational rheometry, the different flow models available which are applicable to the study of slurry rheology. It outlines factors that affect the flow behaviour of mineral tailings slurries. It also gives an overview of the work done to date on the predictions of yield stress and viscosities of mineral tailings slurries.

### 2.1 Rheology

At the beginning of the 20<sup>th</sup> century, the characteristics of many non-Newtonian fluids motivated Professor Eugene Bingham to come up with the term rheology and to define it as the study of the deformation and flow of matter (Barnes et al 1989). The word rheology is derived from the Greek words “rheo”, which means flow and “logus”, which means science or study of (Coghill, 2003 and Slatter et al, 2002).

Deformation is the relative displacement of points of a body. It is divided into two types: elasticity and flow. Elasticity is reversible deformation; the deformed body recovers its original shape, and the applied work is largely recoverable. Flow is irreversible deformation; when the stress is removed, the material does not revert to its original form. This means that work is converted to heat. Viscoelastic materials show both elasticity and flow.

### 2.2 Definition of Rheological Parameters

The rheological parameters of viscosity, shear stress and shear rate are defined in the following paragraphs.

#### 2.2.1 Viscosity

Viscosity is defined as the measure of a fluid's resistance to flow and is best described by the Two-Plate-Model in Figure 2-1 (Coghill, 2003; Paterson & Cooke, 2000 and Slatter et al, 2002). Figure 2-1 describes the shearing of a fluid between two parallel plates. The space between two parallel plates, a distance (H) apart, is filled with a fluid. The upper plate, with surface area (A), is moved with a velocity (V) under the force (F), while the lower plate remains stationary. The top layer of the fluid adjacent to the upper plate moves with the plate at a velocity (V), while the bottom layer of the fluid adjacent to the lower plate remains stationary at zero velocity. As a result, a velocity gradient ( $dV/dH$ )

develops across the space between the two plates, where  $dV$  refers to the velocity differential between adjacent layers of fluid and  $dH$  refers to the differential thickness of a layer of fluid (Coghill,2003; Paterson & Cooke, 2000 and Slatter et al,2002).

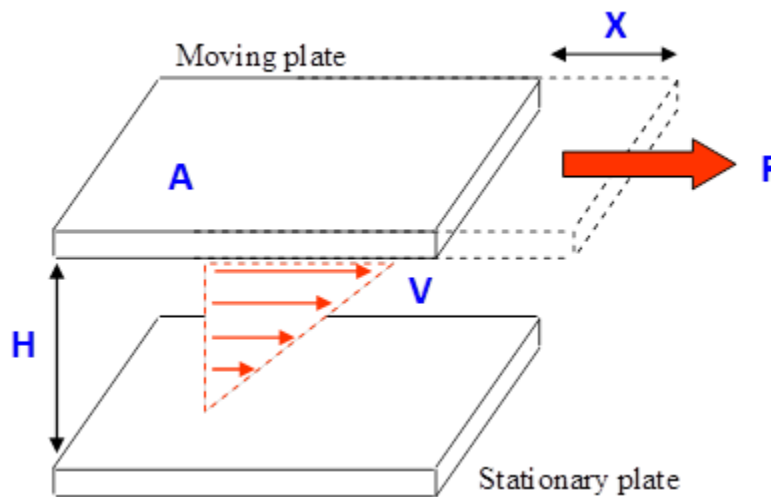


Figure 2-1: The Two-Plate-Model Definition of Viscosity (Coghill, 2003; Paterson & Cooke, 2000 and Slatter et al, 2002).

### 2.2.2 Shear Rate

The velocity gradient,  $dV/dH$ , is a measure of the speed at which the intermediate layers move with respect to each other. It describes the shearing effect the liquid experiences and is called shear rate ( $\dot{\gamma}$ ) and its unit of measure is called reciprocal second ( $s^{-1}$ ).

### 2.2.3 Shear Stress

The force per unit area ( $F/A$ ) required to produce the shearing action is called shear stress ( $\tau$ ) and its unit of measure is  $N/m^2$ . Equation 2-1 is used to calculate shear stress.

$$\tau = F/A \quad \text{Equation 2-1}$$

Therefore the dynamic viscosity ( $\mu$ ) can be defined as follows using Equation 2-2:

$$\mu = \tau / \dot{\gamma} \quad \text{Equation 2-2}$$

The unit of dynamic viscosity is the (Pa.s) for a Newtonian liquid. For a non-Newtonian liquid it is called the apparent viscosity ( $\mu_a$ ).



### 2.3 Newtonian Fluid Behaviour

It is important to make a distinction between Newtonian and non-Newtonian rheological behaviour. Newtonian fluids exhibit a linear relationship between shear stress and shear rate, as presented in Figure 2-2. This means that when shear stress is plotted against shear rate at a given temperature, the plot shows a straight line with a constant slope that is independent of shear rate. The slope of the relationship in Figure 2-2 represents the fluid viscosity according to Newton's equation for an ideal fluid Equation 2-2.

Newtonian fluids, therefore, exhibit a constant viscosity over a wide range of shear rates, as described in Figure 2-3, under constant temperature and pressure conditions. Figure 2-2 shows a comparison of two Newtonian fluids, fluid 1 and 2. It is evident that the steeper the slope is the higher is the constant viscosity value as shown in Figure 2-3 (Coghill, 2003; Jewell et al, 2002; Paterson & Cooke, 2000 and Slatter et al, 2002).

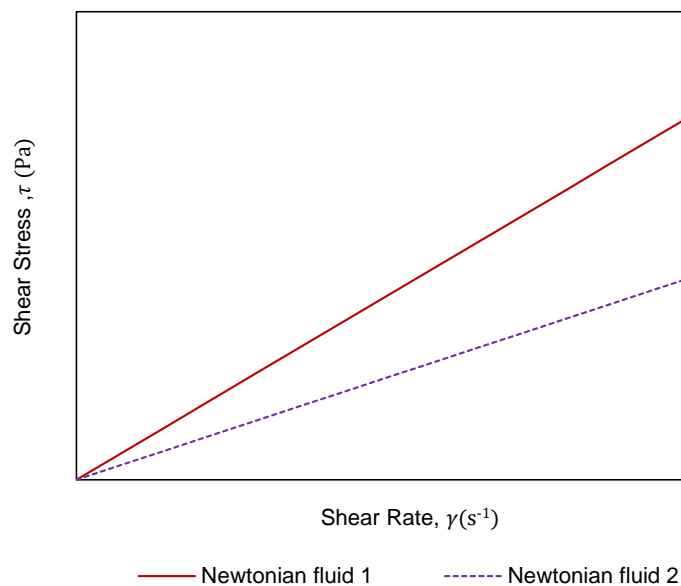


Figure 2-2: Comparison of Newtonian Flow Behaviour

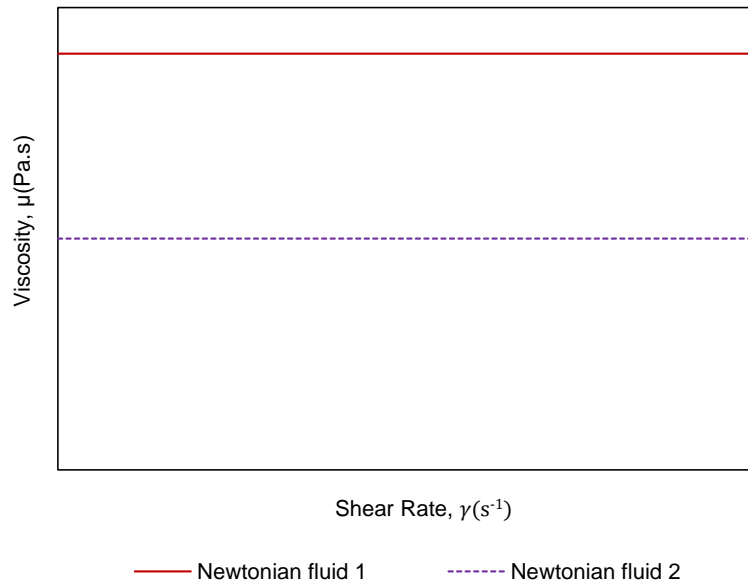


Figure 2-3: Comparison of Newtonian Flow Behaviour - Constant Viscosity

## 2.4 Non-Newtonian Fluid Behaviour

A non-Newtonian fluid is a fluid that does not have a constant apparent viscosity (ratio of shear stress to rate of shear). The apparent viscosity (ratio of shear stress to rate of shear) of a non-Newtonian fluid varies with the shear rate, and shear rate history. Two important distinctions are made in categorising the rheology of fluids (Chhabra & Richardson, 1999):

### 2.4.1 Time independent versus time-dependent fluid.

The rheological properties of a time-independent fluid do not vary with time. With time-dependent fluids, the fluid rheology is dependent on the earlier shear history experienced by the fluid.

### 2.4.2 Newtonian versus non-Newtonian fluids.

With a Newtonian fluid, the shear stress associated with the fluid is related to the shear rate by a single constant, the Newtonian viscosity. To model the rheology of a non-Newtonian fluid, at least two constants are required. The fluid behaviour may follow a power law model. Some fluids exhibit a yield stress where a net shear stress must be applied before any shear occurs. These fluids are known as visco-elastic fluids.

## 2.5 Rotational Rheometry

A group of experimental techniques for investigating the rheological behaviour of materials is called rheometry. At the very beginning, it was referred to a set of standard techniques for measuring shear viscosity, then, with the rapid increase in interest, in non-Newtonian fluids, other techniques for measuring the normal stresses and the elongational viscosity were developed. Nowadays rheometry is usually understood as the area encompassing any technique which involves measuring mechanical or rheological properties of a material. In most cases, the shear viscosity is the primary variable characterising the behaviour of a fluid (Ancy 2001).

The objective of this thesis is not about rheological characterisation methods of fluids as this is a science on its own. An Anton Paar Rheolab QC rotational viscometer and standard methods of rheological characterization were used to characterise the fluids. The Searle system viscometer was considered in this investigation because it is the one that was used in generating the rheological properties of the slurries in the slurry database used. It is a system where the outer cylinder (cup radius,  $R_c$ ) is stationary, while the inner cylinder (bob radius,  $R_b$ ) rotates at an angular velocity ( $\Omega$ ) (Steffe 1996). The shear rate of the fluid, therefore, varies from  $\Omega$  at the rotating bob, to zero at the cup wall. The device measures the torque ( $T$ ), required to rotate the inner cylinder at the set angular velocity or speed. Figure 2-4 shows the Searle viscometer geometry used to conduct the test work.

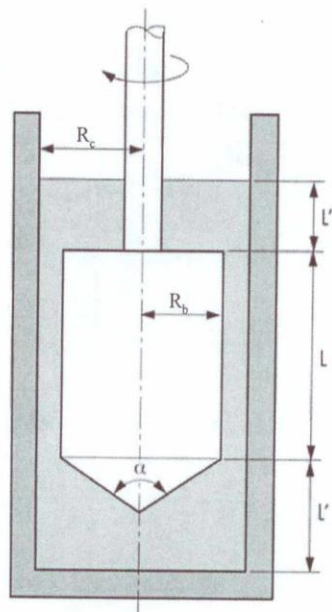


Figure 2-4: Geometry of the Searle system (Anton Paar Measuring System Data Sheet)

The yield stress and the shear rate are determined or calculated using the torque and the speed output values from the rotational viscometer respectively. Equation 2-3 and Equation 2-4 are used to calculate the yield stress and shear rate respectively from the measured torque and speed parameters.

$$\tau = \frac{T}{2 \cdot \pi \cdot R_b^2 \cdot L} \quad \text{Equation 2-3}$$

$$\dot{\gamma} = \frac{2 \cdot \pi \cdot N}{60} \cdot \frac{(Rr^2 + 1)}{(Rr^2 - 1)} \quad \text{Equation 2-4}$$

Where

Rr = Radius Ratio ( $R_c/R_b$ ), the ratio of the cup radius to the bob radius

A plot of shear stress versus shear rate for laminar flow conditions is called a rheogram. Figure 2-5 shows some of these relationships graphically (Chhabra & Richardson, 2008).

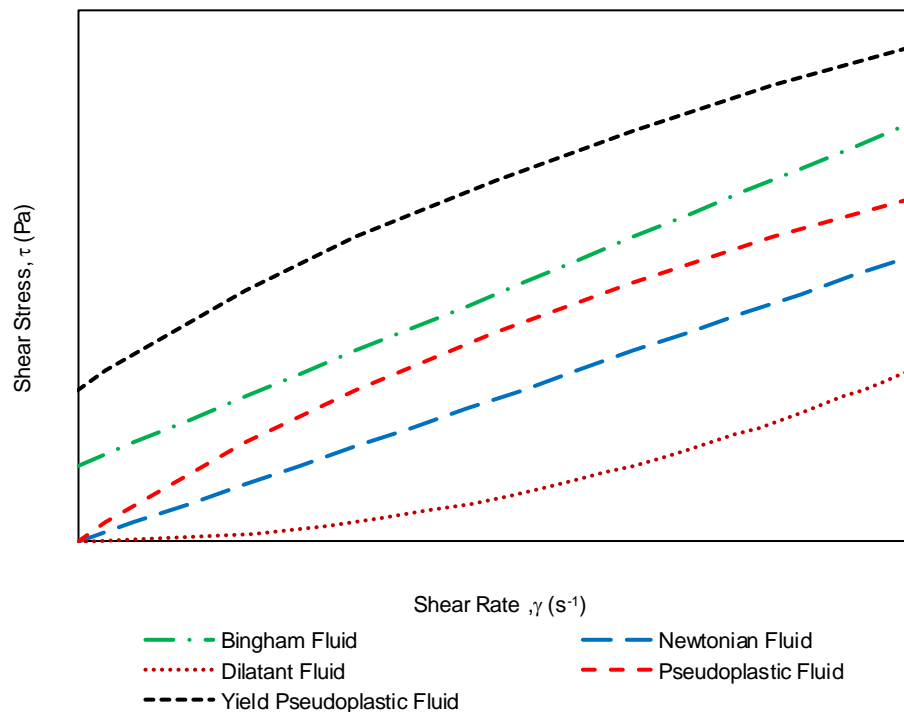


Figure 2-5: Rheograms of Different Time-Independent Flow (Chhabra & Richardson, 2008)

The rheological models in Figure 2-5 are only valid within the regions of laminar or streamline flow (Alderman, 1996). Slurries consist of two distinct phases, namely the solids, and liquid phases. Slurries studied in this investigation are considered to be

homogeneous mixtures. The term homogeneous is used to imply a uniform spatial distribution of the solid particles and uniform concentration of solids (Wilson et al, 1992). This condition assumes that the two phases are homogeneously distributed over the cross section of the test apparatus for the duration of the test work while the slurry is flowing. The rheology of the slurry is also considered to be time independent such that any variation in the resistance to the flow of the slurry with respect to time is considered to be negligible.

Any fluid that obeys Sir Isaac Newton's relationship is said to be a Newtonian fluid and any fluid that does not is said to be a Non-Newtonian fluid. Slurries encountered in industrial problems have a yield stress, a critical value of stress below which they do not flow. They are sometimes called viscoplastic materials or Bingham plastics after Bingham (Bingham, 1922), who first described paints in this way in 1919. A number of rheological models exist that are used to model the flow behaviour obtained from viscometry test work. The constitutive model equations for certain non-Newtonian fluids are shown in Table 2-1 (Bird et al, 1960; Shook and Roco, 1991). These rheological models can be described by the Herschel-Bulkley model Equation 2-5.

$$\tau = \tau_y + \left( K \dot{\gamma} \right)^n \quad \text{Equation 2-5}$$

Table 2-1: Different Flow Models (Bird et al, 1960; Shook and Roco, 1991).

Flow Model	Flow Equation
Casson	$\tau^{1/2} = \tau_y^{1/2} + \left( K \dot{\gamma} \right)^{1/2}$ Equation 2-6
Yield Pseudo-Plastic	$\tau = \tau_y + K \dot{\gamma}^n$ Equation 2-7
Bingham	$\tau = \tau_{yB} + K_B \dot{\gamma}$ Equation 2-8
Newtonian	$\tau = \mu \dot{\gamma}$ Equation 2-9
Dilatant	$\tau = \mu \dot{\gamma}^n$ Equation 2-10

The Bingham model is the simplest of the viscoelastic rheological models containing a yield stress. The model represents a linear relationship between the shear stress and rate of shear strain, offset by the yield stress. Changes in the concentration, chemical

addition, temperature or pH can be directly correlated to the two parameters of the Bingham model. Although the three parameters of the Herschel-Bulkley model may provide a better fit to the specific experimental data collected, it may not always be the most appropriate choice or provide the most meaningful rheological parameters or results. It is important to remember that experimental data will always be better fit by the inclusion of an additional parameter, and such additional parameters add complexity and must be treated with care.

Since the Bingham plastic model (Equation 2-8 in Table 2-1) has been used to analyse the slurries in the slurry database, it was used to represent the rheology of the gold tailings slurries considered in this study. The rheological parameters in the Bingham model parameters are determined directly from the flow curves and are therefore dynamic. The data from the test work was analysed by applying the Bingham plastic model which is a two-parameter model describing the slurry rheology (Bingham, 1922). The two parameters are the Bingham plastic viscosity ( $K_B$ ) and Bingham yield stress ( $\tau_{yB}$ ) which are calculated from the gradient of the flow curve and intercept of the linear relationship between shear stress and shear rate respectively.

To measure the rheology of slurries, (Goodwin, 1975; He and Forssberg, 2004; Nguyen and Boger, 1987 and Sumner et al, 2000) have all successfully used Couette viscometry to classify non-Newtonian fluids with yield stresses. In general, if slurries are carefully prepared the results are often quite similar to those observed in pipelines. In order to compare rotational viscometer data to measured pipeline test data, all data is plotted on a pseudo shear diagram. A pseudo shear diagram is a plot of wall shear stress versus pseudo shear rate and a rheogram is a plot of shear stress versus shear rate. Figure 2-6 presents the rheogram data of typical homogeneous mineral tailings at 61.3%*m*.

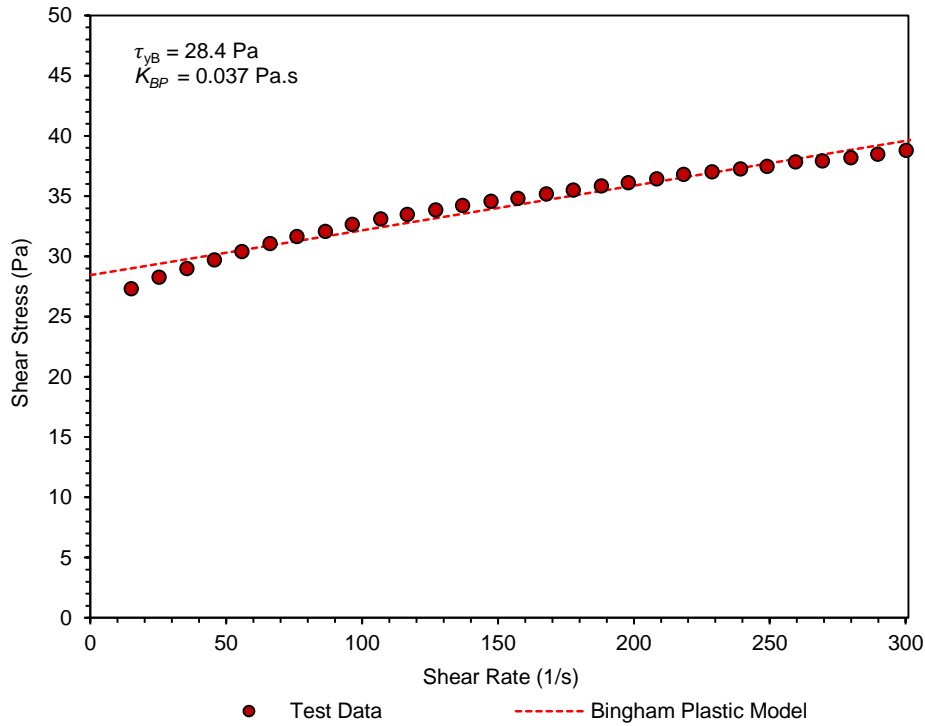


Figure 2-6: Rheogram Data at 61.3% m

Figure 2-7 presents a comparison of actual pressure loss data measured in a 150 NB pipeline to predictions estimated from the rotational viscometer data at a mass solids concentration of 61.3% m. Analysis of the constitutive equation for pipe flow of Herschel Bulkley mixtures results in the following generalised equation relating pseudo shear rate to wall shear stress (Govier and Aziz 1972):

$$\frac{8V}{D} = \frac{4n}{\tau_0^3} \left( \frac{1}{K} \right)^{\frac{1}{n}} (\tau_0 - \tau_y)^{\frac{n+1}{n}} \left[ \left( \frac{\tau_0 - \tau_y}{3n+1} \right)^2 + 2\tau_y \left( \frac{\tau_0 - \tau_y}{2n+1} \right) + \frac{\tau_y^2}{n+1} \right] \quad \text{Equation 2-11}$$

The measured rheogram data obtained from the viscometer were analysed to obtain the best fit Bingham plastic parameters of yield stress and plastic viscosity. The viscometer data was converted to a pseudo shear diagram using the Buckingham Equation, which is a special case of Equation 2-11 when  $n = 1$ . The Buckingham equation uses the Bingham plastic model parameters (yield stress and plastic viscosity) from Equation 2-8 to convert the true shear rate from a rotational viscometer to pseudo shear rate as follows (Govier and Charles 1961).

$$\frac{8V}{D} = \left( \frac{\tau}{K_{BP}} \right) \left[ 1 - \frac{4}{3} \left( \frac{\tau_{yB}}{\tau} \right) + \frac{1}{3} \left( \frac{\tau_{yB}}{\tau} \right)^4 \right] \quad \text{Equation 2-12}$$

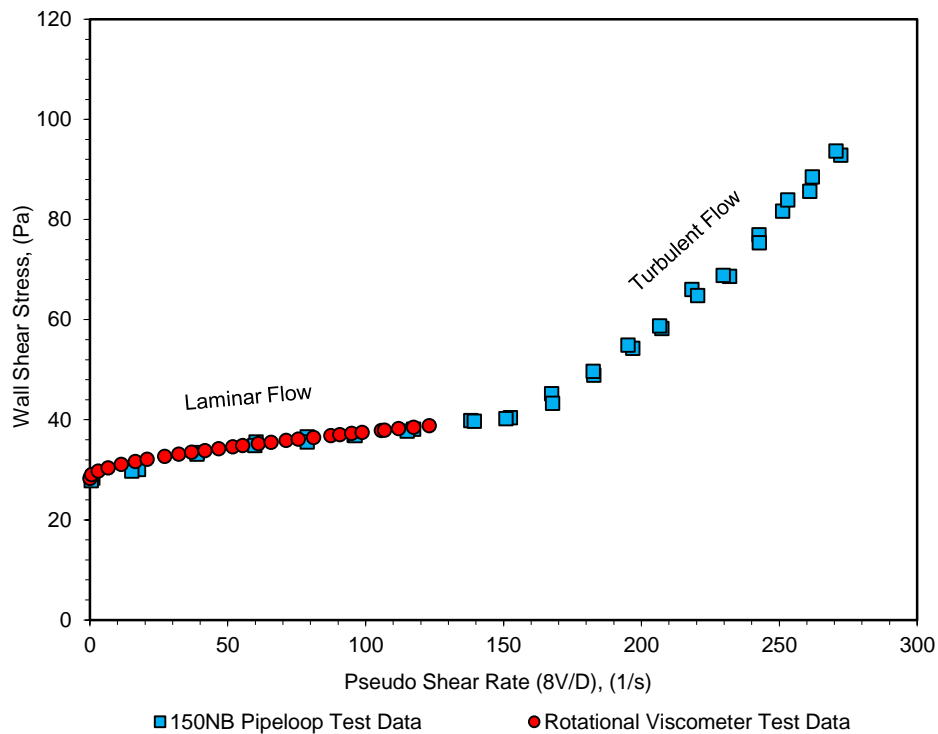


Figure 2-7: Pseudo Shear Comparison of Pipe Loop Data with Rotational Viscometer Data

From the pseudo shear diagram, there is a good agreement of pipe loop and rotational viscometer data for this data set in the laminar flow region. The yield stress from the pipe loop and rotational viscometer data are both approximately 28 Pa. The rotational viscometer has an advantage of requiring only a small amount of sample compared to pipe loop tests. However, the shear rates and shear stress distributions between the pipe loop and rotational viscometers differ and it should be ensured that similar shear rate ranges are used when comparing the devices (Paterson & Cooke 2007).

Figure 2-8 presents pipeline pressure gradient comparisons of the 150NB pipe loop data to the rotational viscometer data at the same solids mass concentration of 61.3%*m*. It can clearly be seen that the rotational viscometer does not show the onset of turbulent flow as the pipe loop test data does, it is only valid for laminar flow conditions. Some researchers, such as (Litzenberger, 2003) reported a substantial dissimilarity in plastic viscosities between Couette measurements and the pipeline results for the same slurry concentration, indicating that care must be taken if the viscometer results are to be scaled to larger pipelines, as well as in the interpretation of the pipeline data.



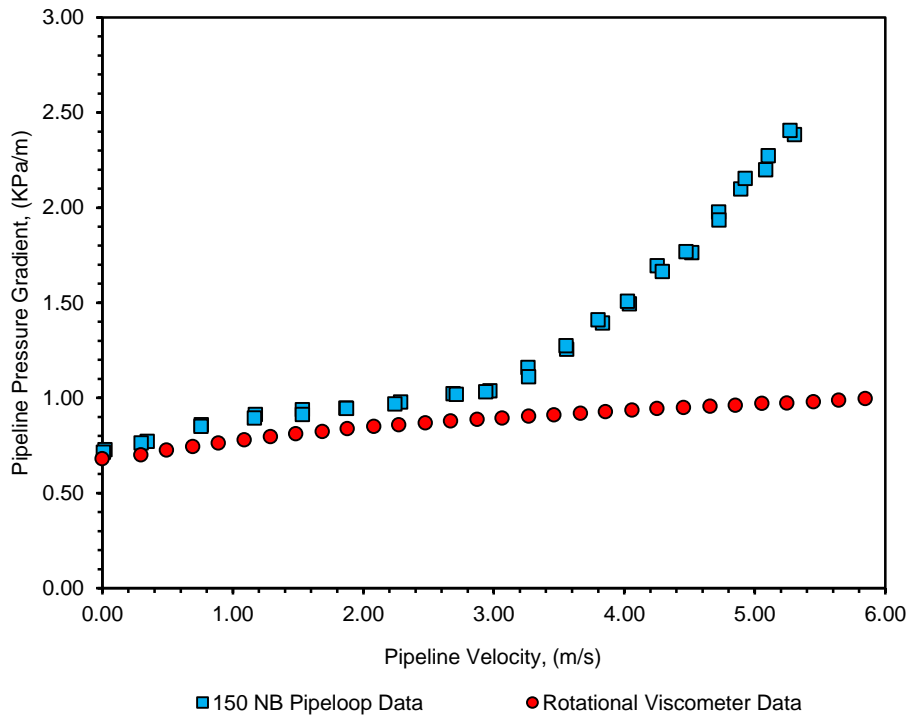


Figure 2-8: Pressure Gradient Comparison of Pipeloop and Rotational Viscometer Data

## 2.6 Factors Affecting Rheology

Some of the factors that affect rheological properties are the shear rate, concentration, pH and temperature. The most obvious factor that can have an effect on the rheological behaviour of a material is temperature. Some materials are quite sensitive to temperature, and a relatively small variation will result in a significant change in viscosity (D. McClung and P. Schaerer, 1993). Figure 2-9 shows how particle concentration and interparticle attraction affects fluid rheology.

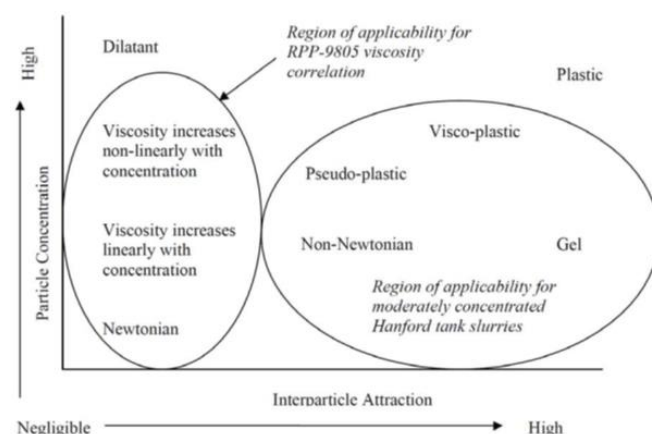


Figure 2-9: Effects of Particle Concentration and Interparticle Attraction on Fluid Rheology (Brown and Heywood, 1991)

Various physical and chemical properties of slurry, such as solids concentration, particle size distribution, pH, temperature and shape factors have significant influences on the slurry rheology due to change or modification in surface property (Weltmann and Green, 1943).

The electrostatic forces in clays are of importance because these particles are generally very small in size and can often be considered to be colloids (Litzenberger, 2004). Many particles have surface charges associated with them. The combination of a high degree of surface charge associated with the significant surface area, combined with a small particle size and mass results in high charge to mass ratios leading to the important effects observed with clays.

Surface chemistry is an important area in aqueous clay mixtures. Most clay particles have a plate-like particle shape with specific charges on the faces and edges of the particle. When they are placed in an aqueous solution they tend to form agglomerates in a face to edge manner which increases the mechanical strength of the agglomerate and thus the yield stress of the mixture (Xu et al, 1993). Certain chemical additions (i.e. flocculants or coagulants) can cause ion exchange to occur between the solution and the particles, which further increases the strength of these structures (Nguyen and Boger, 1987). This can increase the yield stress and plastic viscosity of the mixture.

(Nguyen and Boger, 1987) have also shown that yield stress and the plastic viscosity are functions of the volumetric concentration of fine particles. For kaolin clay slurries, (He and Forssberg, 2004) have shown that this dependence is exponential. This exponential dependency is also valid for the mineral slurries in this dissertation. They also showed that the rheological parameters are strong functions of pH and chemical additive concentration. He and Forssberg (2004) demonstrate that for a given mineral, the yield stress is known to be a strong function of particle diameter and solids concentration. They showed that the addition of clay or sand will cause a nearly cubic increase in yield stress with concentration.

### *2.6.1 Shape Factors*

There are many descriptive terms that are applied to particle shape. The initial shape of weathered particles is affected by mineralogy: micas tend to be platy, feldspars are often tabular, and quartz tends to be equant (Macdonald 1983). Ellipsoidal, cylindrical

and spherical particles are generated by abrasion. Figure 2-10 shows some of the different particle shapes and shape factors.













	Very angular	Angular	Sub angular	Sub rounded	Rounded	Well rounded	
Sphericity							High 1.00
							Low 0
	0.12 - 0.17	0.17 - 0.25	0.25 - 0.35	0.35 - 0.49	0.49 - 0.70	0.70 - 1.00	

Figure 2-10: Different Particle Shapes and Shape Factors (Macdonald 1983)

The mechanical strength of granular medium relies on friction between particles. In general, angular particles with low sphericity tend to mobilise more friction than rounded particles. On the other hand, rounded or spherical particles tend to pack together more effectively to create denser sediments.

## 2.7 Yield Stress

Bingham and Green (1919) first introduced the concept of yield stress ( $\tau_y$ ) for a class of fluids known as viscoplastic fluids. After their initial work, many different equations have been proposed to describe the relationship between shear stress and shear rate for different viscoplastic materials (Nguyen and Boger, 1992). The yield stress was simply defined as the minimum stress required for producing a shear flow in many models. Cheng et al. (1998) pointed out that, for yield stress fluids in general the yield stress is a time-dependent property. Upon yielding, the flow properties show time dependency indicating a degradation of structure with continued shear, finally developing equilibrium or time-independent flow properties which still exhibit a yield stress which can be represented using the Bingham model.

Thomas (1963) obtained the relationship based on a number of Kaolin slurry tests and found the yield stress of flocculated suspensions has been found to be a direct function of the particle size and solids volume concentration, which could be represented as follows by Equation 2-13:

$$\tau_y = A \frac{C_v^3}{d_p^2} \quad \text{Equation 2-13}$$

Coussot and Piau, (1995) proposed a number of empirical correlations to describe the dependence of yield stress on suspension volume concentration. The general form of this correlations is as shown by Equation 2-14 below:

$$\tau_y = A \exp^{BC_v} \quad \text{Equation 2-14}$$

Where A and B are empirical coefficients to be fitted to the yield stress data. More recently (Zhou et al. 1999) elaborated on a potential model for the yield stress based on mean field theory for particles governed by Van der Waal's forces. In this model the yield stress is computed as the sum of all pairwise inter-particle forces. Zhou et al. (1999) then applied this to a range of particle sizes. The geometric resistance, which produces the yield stress, is related to the number of particle contacts.

Spelay, (200) and Talmon et al., (2014) stated that the theoretical framework to describe sand-fines slurry flow and segregation behaviour includes a dual rheology approach. They indicated that the rheology of the sand-fines mixture is quantified for flow momentum simulations. Thomas (2010) indicated that the rheology (inherent viscosity), of the carrier fluid (fines+water) determines sand segregation (e.g. settling of coarse particles within the carrier fluid), which includes shear induced settling. The carrier fluid constituents are found below 44  $\mu\text{m}$  (fines) fraction, and (settling) coarse above 44  $\mu\text{m}$  fraction whilst the dispersed clays are found below 2  $\mu\text{m}$ .

Kranenburg, (1994) developed a rheological model for yield stress based on fractal-dimension theory Equation 2-15.

$$\tau_y = A_y \left( \frac{\phi_{\text{clay}}}{\phi_{\text{water}} + \phi_{\text{clay}}} \right)^{2/(3-n_f)} \exp(\beta\lambda) \quad \text{Equation 2-15}$$

Where  $\phi_{\text{clay}}$  and  $\phi_{\text{water}}$  are volume fractions of clay and water,  $A_y$  is the yield stress constant,  $n_f$  is the fractal dimension,  $\beta$  is the constant linear concentration and  $\lambda$  is the linear solids concentration.

Equation 2-15 by Kranenburg, (1994) was derived based on a shear-thinning model, assuming self-similarity of the cohesive structure (the mud flocs which constitute the carrier fluid). Self-similarity entails that the larger particle aggregates have an analogous

structure as the smaller aggregates. This assumption generally yields a power law behaviour. The arrangement of such self-similar mixtures can be expressed by the fractal dimension  $n_f$ . Depending on the clay composition the value of  $n_f$  in Equation 2-15 varies between 2.5 and 2.8 Kranenburg, (1994). An increase in clay content raises the rheological properties. The increase of internal friction induced by sand particles is captured by an exponential term containing the linear sand concentration ( $\lambda$ ), Bagnold, (1956).

Jacobs et al., (2008) derived a yield stress model based on a similar approach for associated Bingham plastic viscosity Equation 2-16.

$$\tau_y = K_y \left( \frac{W}{PI} \right)^{B_y} \exp(\alpha \lambda) \quad \text{Equation 2-16}$$

Where  $K_y$  is the yield stress constant,  $W$  is the water content (mass water/mass solids),  $PI$  is the plasticity index,  $\alpha$  is the constant linear concentration,  $\lambda$  is the linear solids concentration and  $B_y$  is a yield power function.

The fundamental idea is that the water content with respect to the clay is the governing parameter for baseline rheological behaviour without sand. Therefore, the model utilises the ratio between the water content ( $W$ ) and the plasticity index ( $PI$ ) of the carrier fluid. An increase in water content decreases the rheological properties. Like in Equation 2-15, the increase in friction due to sand is represented by an exponential function with the linear sand concentration ( $\lambda$ ) Jacobs et al., (2008).

Thomas, (1999), presented a Bingham model developed for sand-slime mixtures in mining processes Equation 2-17 below.

$$\tau_y = C_y \left( \frac{\phi_{fines}}{\phi_{water} + \phi_{fines}} \right)^p \left( 1 - \frac{\phi_{sand}}{K_{yield} \phi_{sandmax}} \right)^{-2.5} \quad \text{Equation 2-17}$$

Thomas describes the influence of the fines in the carrier fluid by a power function for the yield strength. Equation 2-17 consists of two parts, the first describes the yield strength of the carrier fluid and the second describes the effect of sand particles. The addition of sand is accounted for with respect to the maximum sand concentration and parameters  $K_{yield}$ .

Where  $C_y$  is the yield stress constant,  $\Phi_{\text{fines}}$ ,  $\Phi_{\text{water}}$ ,  $\Phi_{\text{sand}}$  are the fines, water and sand volume fractions respectively,  $K_{\text{yield}}$  is the yield constant,  $\Phi_{\text{sandmax}}$  is the sand maximum concentration and  $p$  is a yield power function.

## 2.8 Viscosity

As mentioned earlier a Newtonian fluids viscosity is represented by the gradient of the rheogram and is constant for all shear rates, whilst the viscosity of Non-Newtonian fluids is referred to as the apparent viscosity as the viscosity varies with shear rate. The Newtonian viscosity of the slurry is given by the relative viscosity ( $\mu_r$ ), the ratio of the slurry viscosity ( $\mu$ ) to the dynamic viscosity of the carrier medium or suspended liquid which is generally water ( $\mu_w$ ). Equation 2-18 shows the relationship between  $\mu_r$ ,  $\mu$  and  $\mu_w$  Paterson & Cooke, (2000).

$$\mu_r = \mu / \mu_w \quad \text{Equation 2-18}$$

$\mu_r$  is a function of many parameters that include:

- Particle properties of size, shape, density and size distribution,
- Solids concentration,
- Temperature,
- Physio-chemical effects, including surface charge, zeta potentials and chemical properties
- Shear strain rate,
- Shear history.

Viscosity is very dependent on concentration. Einstein (1911) found that for dilute slurries, the relative viscosity could be calculated by using Equation 2-19, assuming the particles are large enough to ignore electro-kinetic effects. Where  $C_v$  is the volumetric solids concentration.

$$\mu_r = 1 + 2.5C_v \quad \text{Equation 2-19}$$

Equation 2-19 is only valid for very dilute slurries, or mixtures with very little solids about 5% or less. Numerous other equations now exist for calculating viscosity which are all refinements or improvements of Einstein's equation.

Michaels and Bolger, (1962) historically based the plastic viscosity term on the Einstein relation for dispersed non-attracting particles by the use of Equation **2-20**.

$$\frac{\mu}{\mu_w} = 1 + 2.5C_v \quad \text{Equation 2-20}$$

Equation **2-20** has often been the starting point for semi-empirical relationships for the viscosity term. Thomas (1963) further states that the viscosity term for any given suspension is constant when expressed as  $\ln(\mu/\mu_w)$  vs  $C_v$ . A number of empirical relationship expansions for the above relationships have been proposed. Equation **2-21** for example, was proposed by Thomas (1965) for low and moderate concentration non-interacting spheres:

$$\frac{\mu}{\mu_w} = 1 + 2.5C_v + 10C_v^2 + 0.00273e^{16.6C_v} \quad \text{Equation 2-21}$$

Thomas (1963) published a study of factors affecting Bingham rheological parameters of fine particle slurries. He reported that in the case where slurry particles approach colloidal size, such as kaolin clay in water, the yield stress and plastic viscosity vary with concentration. He found that the plastic viscosity varied exponentially with volumetric concentration and the yield stress varied with volumetric solids concentration to the third power. Equation **2-22** an empirical equation suggested by Thomas (1999), however, is the most common method of representing the effect of solids concentration on the Bingham viscosity term.

$$K_B = Ae^{BC_v} \quad \text{Equation 2-22}$$

Where A, and B are empirical coefficients.

Studies conducted by Thomas (1999) suggested that the ratio  $C_v/C_{vmax}$  where  $C_{vmax}$  is the volume concentration of the solids at maximum packing is important for representing the effect of particle shape and size distributions. Landel, Moser, and Bauman (1965) found that the viscosity increase due to the addition of a range of spherical and non-spherical particles of both narrow and wide particle size distributions could be represented as follows by Equation **2-23**:

$$\frac{\mu}{\mu_w} = \left(1 - \frac{C_v}{C_{vmax}}\right)^{-2.5} \quad \text{Equation 2-23}$$

Weltmann and Green (1943); Goodwin (1975) developed a number of theoretical and empirical equations to predict the viscosity of concentrated suspensions. Each equation has achieved some agreement between prediction and measurement, but with limits to factors such as solids concentration and slurry characteristics, in a variety of suspension systems.

Kranenburg, (1994) developed a rheological model for plastic viscosity ( $\mu$ ) based on the fractal dimension theory. The equation was derived based on the same shear-thinning model as explained for Equation 2-15.

$$\mu = \left[ \mu_w + A_\mu \left( \frac{\phi_{clay}}{\phi_{water} + \phi_{clay}} \right)^{\frac{2(a+1)}{3}} \left( \frac{1}{\gamma} \right)^{\frac{(a+1)(3-n_f)}{3}} \right] \exp(\beta\lambda) \quad \text{Equation 2-24}$$

Where  $A_\mu$  is a viscosity constant,  $\gamma$  is the shear rate and  $a$  is an anisometric parameter.

Jacobs et al., (2008) also developed a rheological model for plastic viscosity ( $\mu$ ) based on fractal dimension theory as did Kranenburg, (1994). The model was also derived based on the shear-thinning model Equation 2-25.

$$\mu = \left[ \mu_w + K_\mu \left( \frac{W}{PI} \right)^{B_\mu} \right] \exp(\alpha\lambda) \quad \text{Equation 2-25}$$

Where  $K_\mu$  is a viscosity constant,  $W$  is the water content (mass water/mass solids),  $PI$  is the plasticity index,  $B_\mu$  is the viscosity power function,  $\alpha$  is the constant linear concentration and  $\lambda$  is the linear solids concentration.



### 3. CHAPTER THREE

#### 3.1 Experimental Work

This chapter aims to define and discuss the various experimental equipment and procedures that were used throughout the study. This includes the details of sample preparation, principles of rheological measurements used in the course of experimental work and data analysis.

#### 3.2 Rotational Viscometer Tests

The Searle system was used for the rotational viscometer tests. Specifically, the CC35/HR (measuring bob radius = 17.5 mm, measuring cup radius = 21.0 mm, gap length = 52.5 mm, cone angle 120 °) measuring system was selected for this work. The objective of the rotational viscometer tests is to determine the rheological properties of the slurries at different mass solids concentrations. Flow curves were generated by the rotational viscometer by plotting shear stress versus shear rate from shear rates of 5 s<sup>-1</sup> to 300 s<sup>-1</sup>. The yield stress and plastic viscosity of the gold tailings samples were determined using the rotational viscometer laminar flow data. The data were analysed by applying the Bingham plastic model. An Anton Paar Rheolab QC rotational viscometer with a temperature control bath was used for the test work. Figure 3-1 presents the Anton Paar Rheolab QC used to conduct the rheology tests.



Figure 3-1: An Anton Paar Rheolab QC Rotational Viscometer

The rotational viscometer test sequence to produce a rheogram, plot of shear stress versus shear rate data was analysed according to the methods prescribed in ISO 3219: 1993E which is based on the German standard DIN 53019.

### 3.2.1 Viscosity Check with Calibration Oil

The rotational viscometer is serviced after every six months by technicians from Anton Paar and before a test campaign, an in-service check is done with calibration oil. This is done to ensure that the instrument is giving accurate results. Figure 3-2 presents the results of the in-service check done before the test campaign. Calibration oil is a Newtonian fluid and the viscosity varies with temperature. This test was done at 22°C and the measured viscosity which is the gradient of the graph was 0.0437 Pa.s as compared to 0.0459 Pa.s from the viscosity and density reference standard table. Appendix D presents the viscosity and density reference standard for the calibration oil.

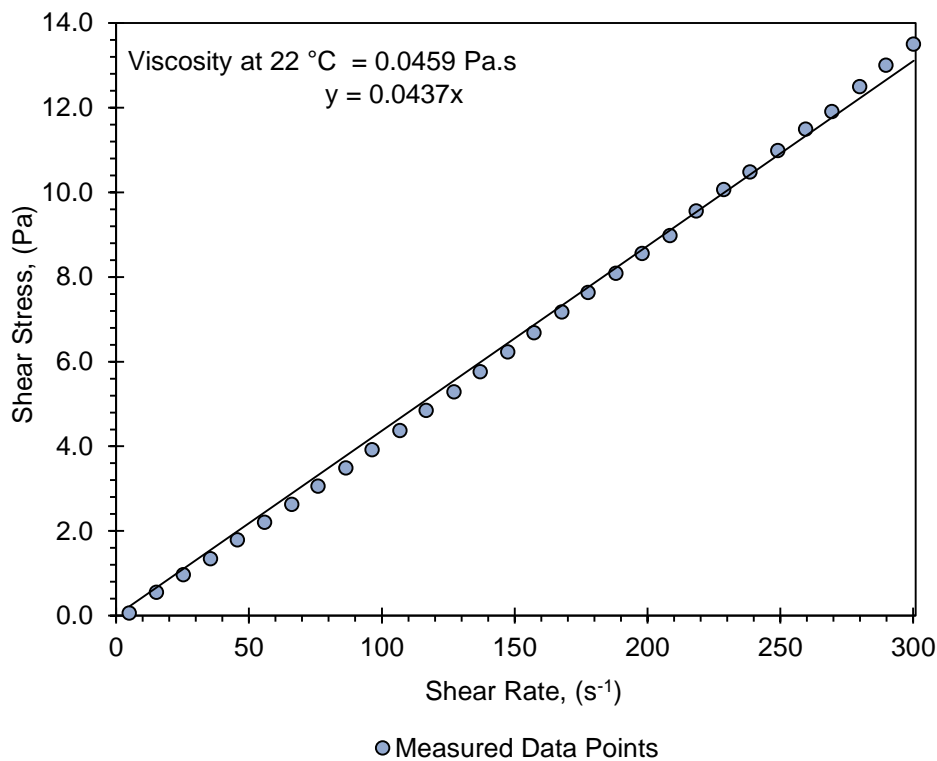


Figure 3-2: Calibration Oil Viscosity Results

### 3.3 Material Properties

The first step in the design of a slurry pipeline is a characterization of the material properties. The material properties that enable any slurry to be characterised are discussed in this chapter.

### 3.3.1 Particle Size Distribution

The particle size distribution (PSD) were outsourced and were measured according to the method detailed in ASTM D 422-63 “Standard Test Method for Particle Size Analysis of Soils” and by the use of Malvern laser diffraction.

### 3.3.2 Slurry pH and Temperature

The pH and temperature of the slurry were measured by using a handheld pH meter. The pH meter was calibrated by a two-point calibration using buffer solutions at pH values of 4.01 and 7.01.

### 3.3.3 Particle Micrographs

The particle micrographs were done at the department of chemical engineering at the University of Cape Town and were generated as follows. A small amount of dried sample is sprinkled onto an aluminium stub coated with carbon glue. The stub is then coated with a carbon film in the evaporation coater (to make it conductive). The sample is inserted into the Scanning Electron Micrograph (SEM) and viewed at set magnifications of 100x, 1000x and 5000x. The SEM is an FEI Nova nano SEM with an FEG tip for high resolution. The micrographs were used to illustrate the difference in the shape of the different ore body particles tested. Figure 3-3 shows the SEM microscope used for taking the electronic micrographs.



Figure 3-3: The SEM Microscope

### 3.3.4 Solids Density Measurements

The solids density of the materials was determined using a helium gas pycnometer. The helium gas pycnometer determines the skeletal solids density of the particles.

### 3.3.5 Slurry Mixture Density Measurement

The slurry mixture density was measured by using a 250 ml volumetric flask. The density of water was assumed to be 1000 kg/m<sup>3</sup> in the slurry density calculations. Equation 3-1 was used to calculate the mixture density of the samples tested.

$$\rho_m = \frac{M_{\text{slurry}}}{250 - (M_{\text{water}} / \rho_w)} \quad \text{Equation 3-1}$$

### 3.3.6 Mass Solids Concentration

The mass solids concentration ( $C_m$ ) of the slurries was determined by oven drying the samples. Equation 3-2 calculates the solids mass concentration.  $C_m$  is the ratio of the mass of solids ( $M_s$ ) to the mass of the mixture ( $M_m$ ).

$$C_m = \frac{M_s}{M_m} \quad \text{Equation 3-2}$$

### 3.3.7 Volumetric Solids Concentration

The volumetric solids concentration ( $C_v$ ) is a function of the mixture density ( $\rho_m$ ), the mass solids concentration ( $C_m$ ) and the solids density ( $\rho_s$ ) of the material and it calculated using Equation 3-3.

$$C_v = \frac{\rho_m}{\rho_s} \times C_m \quad \text{Equation 3-3}$$

### 3.3.8 Freely Settled Bed Packing Concentration

The freely settled bed packing concentration by volume is calculated from the volume of the freely settled bed formed by a known volume of solids. A slurry sample prepared from the dried and pre-weighed solids is allowed to settle in a measuring cylinder. It is the ratio of the volume of solids to the volume of the freely settled bed. Equation 3-4 calculates the freely settled bed concentration.

$$C_{\text{bfree}} = \frac{(\text{Volume of solid})}{(\text{Volume of freely settled bed})} \quad \text{Equation 3-4}$$

## 4. CHAPTER FOUR

### 4.1 Data Analysis and Discussion

This chapter focuses on the presentation and analysis of data obtained from the slurry database. The database consists of 30 different thickened gold tailings samples from different ore bodies. The material properties of the samples were measured using the methods described in Chapter 3. For anonymity, the samples are going to be presented as sample 1 to 30. In this chapter, the effect of the material properties on the rheology of the thickened tailings is going to be investigated, with an anticipation of unlocking the underlying key relationships between material properties and rheology.

### 4.2 Particle Size Distribution

Figure 4-1 presents the particle size distribution (PSD) of the samples tested in the slurry database. All the samples have a top size of approximately 600  $\mu\text{m}$ . The coarsest and finest samples have a  $d_{50}$  of approximately 50  $\mu\text{m}$  and 8  $\mu\text{m}$  respectively.

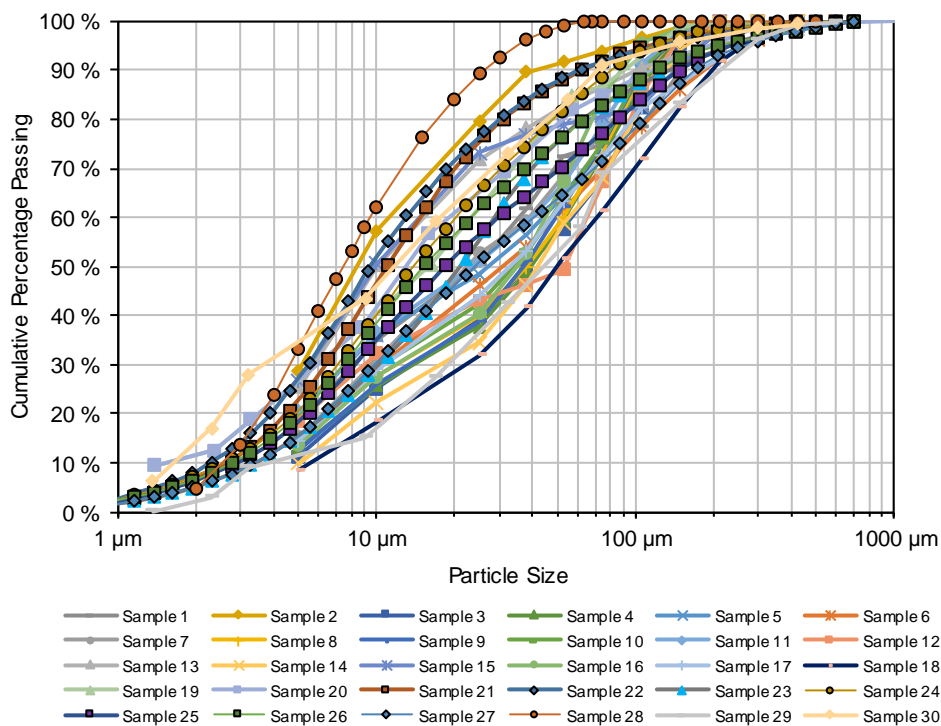


Figure 4-1: Particle Size Distribution Comparison

### 4.3 Effect of Solids Concentration

One of the factors that contribute to non-Newtonian flow behaviour of a fluid is varying the solids concentration. As the solids concentration increases, the particles are brought closer to each other, which restricts their movement. As a result, the yield stress

and plastic viscosity of the material increases due to the increased particle-particle interaction and network structure strength. The presence of and the increase in the concentration of solids have been given as the primary reason for the increased viscosity in Einstein's Law of Viscosity Equation 2-19. Einstein's theory correlates the dispersion viscosity with the volume fractions of solids suspended in that fluid for spherical, non-interacting, unsolvated and rigid particles.

#### 4.4 Summary of Material Properties

Table 4-I presents a summary of the material properties of the 30 samples tested in the slurry database.

Table 4-I:Material Property Summary

Sample Name	Solids Density (kg/m <sup>3</sup> )	C <sub>bfree</sub>	d <sub>90</sub> (µm)	d <sub>50</sub> (µm)	d <sub>25</sub> (µm)	pH	Temperature (°C)
Sample 1	2770	22%v(44% <i>m</i> )	149	25	7	4.0	21.6
Sample 2	2791	25%v(48% <i>m</i> )	40	9	-	3.7	21.5
Sample 3	2760	34%v(60% <i>m</i> )	130	38	10	7.5	22.1
Sample 4	2686	43%v(68% <i>m</i> )	117	39	10	4.2	28.1
Sample 5	2672	32%v(57% <i>m</i> )	107	27	6	7.3	23.4
Sample 6	2770	43%v(67% <i>m</i> )	184	31	8	3.8	23.7
Sample 7	2720	29%v(52% <i>m</i> )	131	22	4	7.4	23.5
Sample 8	2760	40%v(64% <i>m</i> )	111	38	9	4.3	20.6
Sample 9	2770	28%v(52% <i>m</i> )	108	37	9	4.0	22.4
Sample 10	2790	42%v(67% <i>m</i> )	106	34	8	7.7	21.9
Sample 11	2770	35%v(60% <i>m</i> )	102	23	6	3.9	23.2
Sample 12	2730	45%v(69% <i>m</i> )	122	54	7	4.1	23.8
Sample 13	3150	30%v(57% <i>m</i> )	100	10	5	5.8	20.0
Sample 14	2730	45%v(69% <i>m</i> )	132	42	12	6.9	22.0
Sample 15	2800	26%v(50% <i>m</i> )	144	10	5	3.8	20.0
Sample 16	3550	33%v(58% <i>m</i> )	89	35	9	6.1	19.7
Sample 17	2790	27%v(50% <i>m</i> )	181	33	8	4.2	23.9
Sample 18	2750	36%v(61% <i>m</i> )	198	50	16	7.3	23.0
Sample 19	2726	35%v(60% <i>m</i> )	91	16	5	7.1	19.6
Sample 20	2719	35%v(60% <i>m</i> )	117	13	4	7.0	18.9
Sample 21	2541	17%v(34% <i>m</i> )	62	11	5	11.3	26.7
Sample 22	2614	25%v(46% <i>m</i> )	61	9	5	11.2	27.8
Sample 23	2247	11%v(22% <i>m</i> )	135	21	8	10.2	24.1
Sample 24	2717	43%v(67% <i>m</i> )	80	14	6	8.2	27.0
Sample 25	2737	42%v(66% <i>m</i> )	149	18	7	9.4	25.4

Sample 26	2683	37%v(61%m)	119	15	6	9.6	28.0
Sample 27	2670	45%v(69%m)	171	24	8	8.1	26.7
Sample 28	2790	25%v(49%m)	26	7	4	9.5	16.8
Sample 29	2902	43%v(68%m)	214	44	15	9.0	24.7
Sample 30	2633	26%v(48%m)	72	11	3	9.6	26.4

#### 4.5 Rotational Viscometer Results

An Anton Paar Rheolab QC rotational viscometer with a temperature control bath was used for the test work. All the samples were tested and analysed using the ISO 3219 method. The samples were all fully sheared before testing and all data were corrected for end effects. Table 4-II presents the Bingham yield stress and Bingham plastic viscosity data of the gold tailings slurries tested in the slurry database. It presents the relationships between mass solids concentration (Cm), volumetric solids concentration (Cv), yield stress ( $\tau_y$ ), plastic viscosity ( $K_B$ ) volume ratio and the viscosity ratio of the 30 samples tested.

Two other parameters that are of utmost importance are the Volume Ratio ( $V_R$ ) and the Viscosity Ratio ( $\eta_R$ ). Equation 4-1 is used to calculate the Volume Ratio and Equation 4-2 is used to calculate the Viscosity Ratio.

$$V_R = 1/(1 - Cv) - 1 \quad \text{Equation 4-1}$$

$$\eta_R = MPV / \mu_w \quad \text{Equation 4-2}$$

Where:

MPV – Measured plastic viscosity (Pa.s)

$\mu_w$  – Viscosity of water at 25°C (0.000894 Pa.s)

MYS – Measured yield stress (Pa)

Table 4-II: Measured Bingham Yield Stress and Plastic Viscosity in Database

Sample 1					
Cm	Cv	MYS	MPV	Vol Ratio	Vis Ratio
0.545	0.302	27.5	0.030	0.433	33.56

0.543	0.300	25.0	0.029	0.428	32.44
0.539	0.297	22.3	0.028	0.423	31.32
0.534	0.293	19.2	0.027	0.414	30.20
0.527	0.287	16.0	0.025	0.403	27.96
0.517	0.279	13.0	0.020	0.387	22.37
0.503	0.268	10.2	0.016	0.366	17.90
0.484	0.253	7.0	0.013	0.338	14.54
0.460	0.235	4.2	0.011	0.308	12.30
0.437	0.219	1.8	0.010	0.281	11.19
<b>Sample 2</b>					
Cm	Cv	MYS	MPV	Vol Ratio	Vis Ratio
0.529	0.287	37.2	0.045	0.403	50.34
0.527	0.285	32.0	0.043	0.399	48.10
0.518	0.278	27.0	0.036	0.386	40.27
0.512	0.273	22.5	0.028	0.376	31.32
0.501	0.265	17.0	0.024	0.360	26.85
0.481	0.249	11.0	0.015	0.332	16.78
0.454	0.230	7.0	0.010	0.298	11.19
0.415	0.203	3.3	0.008	0.254	8.95
0.376	0.177	1.5	0.007	0.216	7.83
<b>Sample 3</b>					
Cm	Cv	MYS	MPV	Vol Ratio	Vis Ratio
0.698	0.456	58.0	0.125	0.838	139.82
0.658	0.411	18.0	0.050	0.698	55.93
0.639	0.391	11.0	0.032	0.641	35.79
0.620	0.372	8.5	0.028	0.591	31.32
0.604	0.356	5.0	0.020	0.552	22.37
0.547	0.304	1.7	0.012	0.437	13.42
0.492	0.260	0.6	0.008	0.351	8.95
<b>Sample 4</b>					
Cm	Cv	MYS	MPV	Vol Ratio	Vis Ratio
0.709	0.475	77.0	0.140	0.905	156.60
0.697	0.461	50.0	0.105	0.856	117.45
0.678	0.439	26.5	0.066	0.783	73.83
0.662	0.421	16.0	0.048	0.728	53.69
0.640	0.399	9.8	0.031	0.663	34.68
0.608	0.366	4.8	0.022	0.578	24.61
0.570	0.331	2.3	0.013	0.494	14.54
<b>Sample 5</b>					
Cm	Cv	MYS	MPV	Vol Ratio	Vis Ratio
0.682	0.445	32.0	0.085	0.801	95.08
0.634	0.394	9.5	0.029	0.650	32.44



0.601	0.361	5.1	0.019	0.564	21.25
0.580	0.341	3.0	0.016	0.517	17.90
0.551	0.315	1.8	0.012	0.459	13.42
0.502	0.274	0.7	0.009	0.377	10.07
<b>Sample 6</b>					
Cm	Cv	MYS	MPV	Vol Ratio	Vis Ratio
0.667	0.419	19.7	0.057	0.722	63.76
0.649	0.400	11.6	0.041	0.668	45.86
0.636	0.386	8.5	0.030	0.630	33.56
0.622	0.373	6.4	0.024	0.594	26.85
0.611	0.362	4.6	0.022	0.568	24.61
0.575	0.328	1.6	0.019	0.488	21.25
0.534	0.293	0.6	0.012	0.414	13.42
<b>Sample 7</b>					
Cm	Cv	MYS	MPV	Vol Ratio	Vis Ratio
0.693	0.454	81.0	0.130	0.832	145.41
0.674	0.432	41.5	0.080	0.760	89.49
0.649	0.405	20.8	0.049	0.681	54.81
0.628	0.383	13.5	0.030	0.621	33.56
0.598	0.353	6.8	0.021	0.547	23.49
0.548	0.309	2.7	0.013	0.446	14.54
0.500	0.269	1.1	0.009	0.368	10.07
<b>Sample 8</b>					
Cm	Cv	MYS	MPV	Vol Ratio	Vis Ratio
0.677	0.432	56.0	0.110	0.761	123.04
0.651	0.403	22.0	0.060	0.676	67.11
0.632	0.383	13.0	0.042	0.622	46.98
0.604	0.356	6.5	0.025	0.553	27.96
0.575	0.329	3.1	0.019	0.489	21.25
0.549	0.306	1.9	0.013	0.441	14.54
0.508	0.272	0.7	0.011	0.374	12.30
<b>Sample 9</b>					
Cm	Cv	MYS	MPV	Vol Ratio	Vis Ratio
0.694	0.450	70.5	0.135	0.818	151.01
0.685	0.440	48.0	0.105	0.787	117.45
0.656	0.409	18.4	0.056	0.692	62.64
0.635	0.387	9.7	0.038	0.631	42.51
0.603	0.355	4.8	0.023	0.550	25.73
0.570	0.325	2.1	0.017	0.480	19.02
0.531	0.291	0.8	0.012	0.411	13.42
<b>Sample 10</b>					
Cm	Cv	MYS	MPV	Vol Ratio	Vis Ratio
0.692	0.446	111.0	0.200	0.806	223.71
0.689	0.445	86.5	0.170	0.802	190.16

0.660	0.413	33.0	0.077	0.702	86.13
0.641	0.392	19.0	0.052	0.645	58.17
0.622	0.372	12.1	0.035	0.593	39.15
0.600	0.351	7.8	0.024	0.542	26.85
0.556	0.311	3.0	0.017	0.452	19.02
0.519	0.280	1.6	0.011	0.390	12.30
<b>Sample 11</b>					
Cm	Cv	MYS	MPV	Vol Ratio	Vis Ratio
0.699	0.456	77.0	0.140	0.838	156.60
0.680	0.434	39.0	0.088	0.768	98.43
0.665	0.418	21.5	0.058	0.717	64.88
0.639	0.390	10.7	0.037	0.639	41.39
0.617	0.368	6.6	0.025	0.582	27.96
0.590	0.342	3.3	0.020	0.519	22.37
0.544	0.301	1.1	0.012	0.430	13.42
<b>Sample 12</b>					
Cm	Cv	MYS	MPV	Vol Ratio	Vis Ratio
0.708	0.470	59.0	0.130	0.887	145.41
0.693	0.453	30.9	0.095	0.828	106.26
0.674	0.431	13.7	0.062	0.758	69.35
0.645	0.399	7.6	0.034	0.664	38.03
0.614	0.368	2.3	0.022	0.582	24.61
0.582	0.337	1.3	0.013	0.509	14.54
0.548	0.307	0.5	0.012	0.444	13.42
<b>Sample 13</b>					
Cm	Cv	MYS	MPV	Vol Ratio	Vis Ratio
0.594	0.318	24.8	0.040	0.465	44.74
0.589	0.313	22.7	0.039	0.455	43.62
0.585	0.309	19.3	0.036	0.447	40.27
0.576	0.301	16.0	0.031	0.431	34.68
0.571	0.297	13.0	0.028	0.422	31.32
0.550	0.280	9.3	0.019	0.388	21.25
0.519	0.255	5.4	0.014	0.343	15.66
0.483	0.229	2.7	0.011	0.297	12.30
0.436	0.197	1.0	0.009	0.246	10.07
<b>Sample 14</b>					
Cm	Cv	MYS	MPV	Vol Ratio	Vis Ratio
0.719	0.484	82.0	0.230	0.937	257.27
0.707	0.469	46.2	0.155	0.884	173.38
0.698	0.459	36.0	0.110	0.847	123.04
0.688	0.447	23.9	0.092	0.808	102.91
0.673	0.430	16.3	0.063	0.754	70.47
0.645	0.399	7.8	0.036	0.665	40.27
0.569	0.326	1.6	0.017	0.483	19.02

<b>Sample 15</b>					
Cm	Cv	MYS	MPV	Vol Ratio	Vis Ratio
0.561	0.313	54.0	0.045	0.456	50.34
0.552	0.305	41.0	0.044	0.440	49.22
0.546	0.300	36.9	0.043	0.430	48.10
0.537	0.293	28.7	0.037	0.415	41.39
0.524	0.282	21.2	0.029	0.393	32.44
0.507	0.269	14.9	0.026	0.367	29.08
0.484	0.251	9.8	0.014	0.335	15.66
0.457	0.231	6.3	0.010	0.300	11.19
0.381	0.180	1.6	0.009	0.219	10.07
<b>Sample 16</b>					
Cm	Cv	MYS	MPV	Vol Ratio	Vis Ratio
0.645	0.338	44.5	0.100	0.511	111.86
0.637	0.331	34.0	0.093	0.495	104.03
0.631	0.325	25.2	0.070	0.482	78.30
0.624	0.319	19.8	0.053	0.468	59.28
0.610	0.306	13.8	0.036	0.441	40.27
0.582	0.282	6.8	0.021	0.392	23.49
0.539	0.248	2.4	0.014	0.330	15.66
0.498	0.219	0.8	0.011	0.280	12.30
<b>Sample 17</b>					
Cm	Cv	MYS	MPV	Vol Ratio	Vis Ratio
0.614	0.363	162.0	0.170	0.569	190.16
0.609	0.358	128.0	0.160	0.559	178.97
0.602	0.351	101.0	0.120	0.541	134.23
0.593	0.343	78.5	0.090	0.522	100.67
0.582	0.333	60.5	0.075	0.500	83.89
0.555	0.309	31.8	0.037	0.448	41.39
0.524	0.283	15.5	0.025	0.395	27.73
0.467	0.239	5.8	0.010	0.314	11.19
0.387	0.185	1.7	0.004	0.226	4.47
<b>Sample 18</b>					
Cm	Cv	MYS	MPV	Vol Ratio	Vis Ratio
0.681	0.437	88.0	0.145	0.776	162.19
0.677	0.433	76.0	0.140	0.763	156.60
0.672	0.426	59.0	0.118	0.743	131.99
0.662	0.416	43.5	0.092	0.713	102.91
0.651	0.405	32.0	0.078	0.680	87.25
0.634	0.386	20.4	0.045	0.630	49.84
0.611	0.364	12.4	0.026	0.572	29.41
0.481	0.252	1.3	0.009	0.338	9.51
<b>Sample 19</b>					
Cm	Cv	MYS	MPV	Vol Ratio	Vis Ratio

0.676	0.438	85.1	0.156	0.781	174.85
0.654	0.414	48.0	0.088	0.706	98.08
0.633	0.392	24.3	0.051	0.643	57.43
0.612	0.370	13.8	0.034	0.586	38.31
0.588	0.347	9.0	0.020	0.531	22.32
0.558	0.319	5.3	0.012	0.468	13.91
<b>Sample 20</b>					
Cm	Cv	MYS	MPV	Vol Ratio	Vis Ratio
0.596	0.356	20.0	0.065	0.552	73.11
0.566	0.327	10.8	0.030	0.486	33.43
0.541	0.305	6.9	0.020	0.439	22.09
0.515	0.283	4.2	0.013	0.396	14.94
<b>Sample 21</b>					
Cm	Cv	MYS	MPV	Vol Ratio	Vis Ratio
0.336	0.172	9.5	0.021	0.208	23.16
0.310	0.155	5.5	0.011	0.184	12.13
0.243	0.115	1.6	0.007	0.130	8.26
0.431	0.241	48.9	0.094	0.318	105.26
0.371	0.196	13.2	0.029	0.244	32.29
0.498	0.298	81.1	0.169	0.424	188.49
<b>Sample 22</b>					
Cm	Cv	MYS	MPV	Vol Ratio	Vis Ratio
0.486	0.275	23.8	0.061	0.380	68.23
0.468	0.261	16.5	0.038	0.352	42.35
0.446	0.244	11.7	0.025	0.322	28.49
0.418	0.222	7.3	0.018	0.285	19.92
0.389	0.201	3.9	0.012	0.252	13.54
0.338	0.167	1.6	0.007	0.200	7.27
<b>Sample 23</b>					
Cm	Cv	MYS	MPV	Vol Ratio	Vis Ratio
0.201	0.106	12.9	0.010	0.119	11.49
0.304	0.177	89.4	0.190	0.216	212.53
0.280	0.159	48.1	0.052	0.189	58.13
0.253	0.140	28.9	0.025	0.163	27.83
0.179	0.093	3.9	0.007	0.102	7.42
0.216	0.115	17.2	0.014	0.130	15.48

<b>Sample 24</b>					
Cm	Cv	MYS	MPV	Vol Ratio	Vis Ratio
0.623	0.383	44.8	0.086	0.620	95.89
0.609	0.369	28.7	0.047	0.584	52.75
0.590	0.350	20.5	0.031	0.539	35.09
0.565	0.327	10.4	0.019	0.485	21.56
0.539	0.304	5.6	0.012	0.436	13.49
0.634	0.394	54.8	0.111	0.651	124.00
<b>Sample 25</b>					
Cm	Cv	MYS	MPV	Vol Ratio	Vis Ratio
0.654	0.411	64.2	0.130	0.697	145.57
0.638	0.394	41.1	0.074	0.650	82.31
0.626	0.381	30.7	0.052	0.616	58.37
0.615	0.370	22.5	0.035	0.588	39.38
0.595	0.350	14.4	0.026	0.540	29.56
0.559	0.318	6.5	0.013	0.466	14.32
<b>Sample 26</b>					
Cm	Cv	MYS	MPV	Vol Ratio	Vis Ratio
0.637	0.406	70.6	0.142	0.683	159.15
0.622	0.390	51.4	0.099	0.639	110.25
0.609	0.377	37.9	0.064	0.605	71.12
0.593	0.360	26.4	0.037	0.563	41.05
0.570	0.338	14.7	0.024	0.510	26.50
<b>Sample 27</b>					
Cm	Cv	MYS	MPV	Vol Ratio	Vis Ratio
0.674	0.452	41.7	0.103	0.824	115.16
0.663	0.439	27.4	0.068	0.781	76.21
0.641	0.414	16.5	0.038	0.707	42.86
0.627	0.399	10.9	0.031	0.663	34.15
0.571	0.342	3.4	0.002	0.519	1.75
<b>Sample 28</b>					
Cm	Cv	MYS	MPV	Vol Ratio	Vis Ratio
0.603	0.348	181.0	0.195	0.534	218.12
0.564	0.313	89.9	0.150	0.456	167.79
0.559	0.309	72.9	0.135	0.447	151.01
0.527	0.282	33.3	0.065	0.393	72.27
0.497	0.259	17.6	0.035	0.349	39.40
<b>Sample 29</b>					
Cm	Cv	MYS	MPV	Vol Ratio	Vis Ratio
0.696	0.413	72.0	0.103	0.703	115.18
0.681	0.398	62.3	0.069	0.662	77.10
0.656	0.374	41.1	0.040	0.598	45.04
0.642	0.361	29.4	0.029	0.565	32.62
0.620	0.341	16.6	0.017	0.517	18.55

0.586	0.312	11.2	0.011	0.454	11.82
0.511	0.254	3.0	0.005	0.341	5.06
<b>Sample 30</b>					
Cm	Cv	MYS	MPV	Vol Ratio	Vis Ratio
0.541	0.321	146.9	0.311	0.473	347.71
0.529	0.310	128.0	0.241	0.450	269.04
0.515	0.297	95.1	0.152	0.423	170.21
0.465	0.256	34.1	0.055	0.344	61.45
0.419	0.221	14.3	0.023	0.283	25.97
0.359	0.179	5.1	0.013	0.218	14.54

Figure 4-2 and Figure 4-3 show the Bingham yield stress and plastic viscosity versus mass solids concentration respectively for the 30 samples in the slurry database.

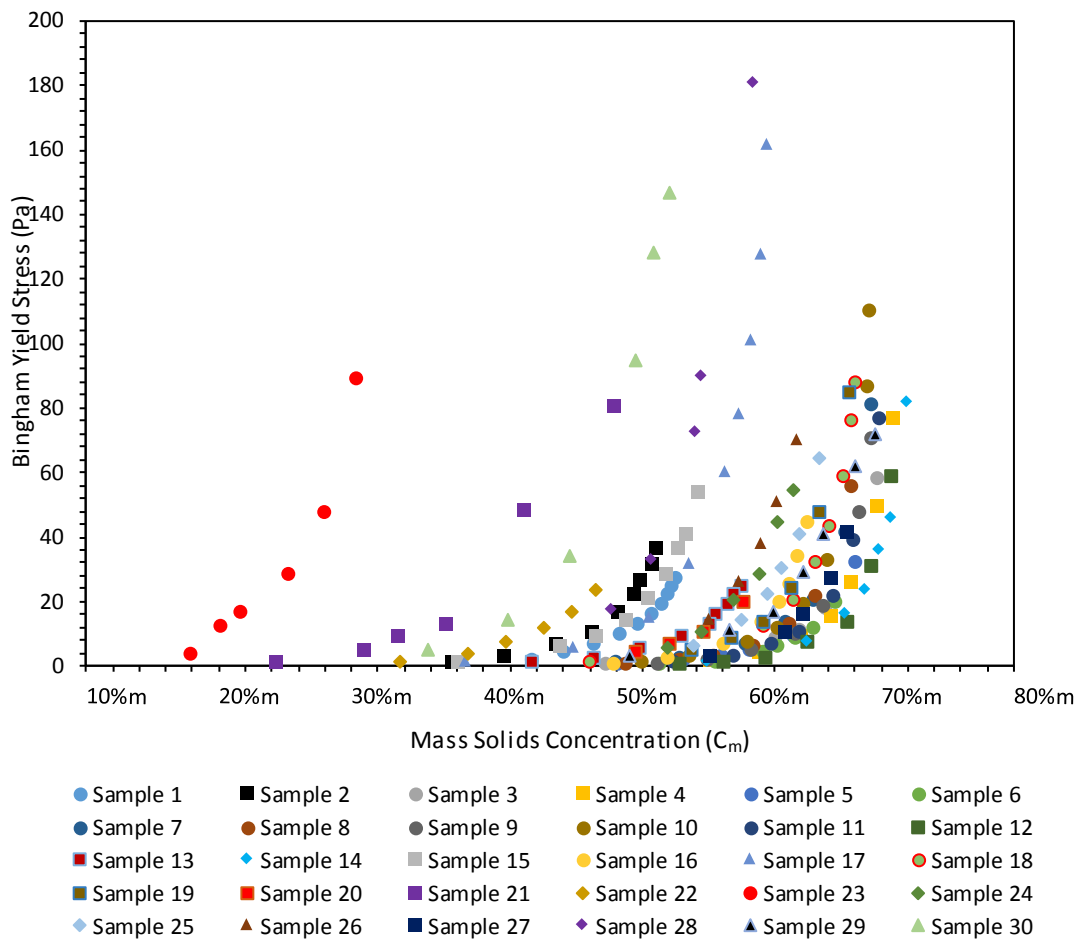


Figure 4-2: Yield Stress versus Mass Solids Concentration Comparison

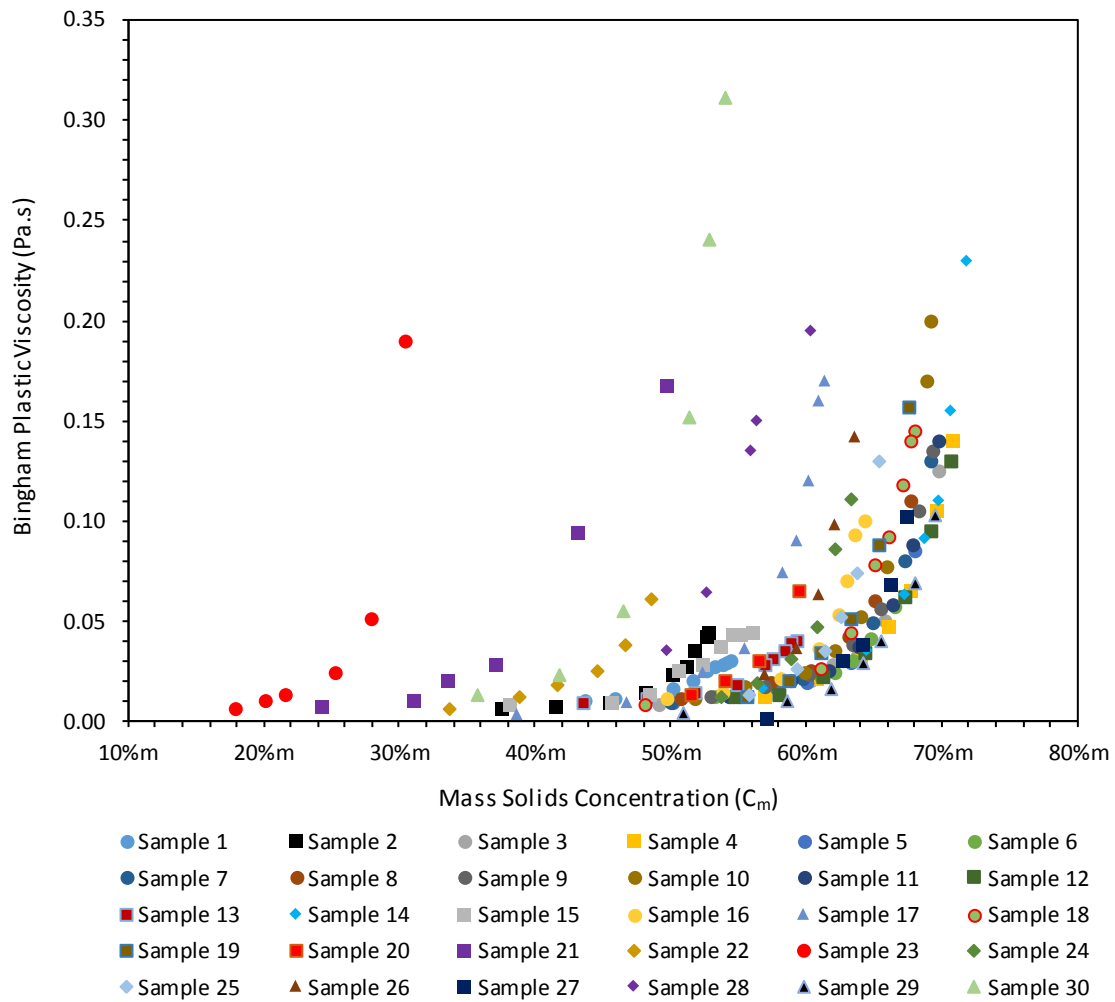


Figure 4-3: Plastic Viscosity versus Mass Solids Concentration Comparison

Although the curves are spread out along the x-axis, they all exhibit an exponential increase in yield stress and plastic viscosity with an increase in mass solids concentration. Sample 23 has the highest yield stress and plastic viscosity, whilst sample 14 has the lowest yield stress and plastic viscosity. From Table 4-1 sample 23 has the lowest  $C_{bfree}$  of 11%v(22% $m$ ) whilst samples 12,14 and 27 have the highest  $C_{bfree}$  value of 45%v(69% $m$ ). It can also be clearly seen that if a sample has a high  $C_{bfree}$  it will exhibit low yield stress and plastic viscosity values respectively.

The  $C_{bfree}$  takes into account the particle size distribution and the shape of the particles. As explained in chapter three it is the ratio of the volume of solids to the volume of settled bed. In order to calculate the volume of solids from a known mass, the solids density of the material is used. Therefore, the  $C_{bfree}$  takes into account the material properties of the sample or material being tested. The packing of the particles is dependent on the particle size distribution, particle shape, solids density and the

intermolecular forces of attraction between particles. This, in turn, affects the rheological properties of the slurry.

#### 4.6 Determining the Beta Coefficient from Regression Analysis

Least squares linear regression analysis was done on each data set to determine the Beta coefficient ( $\beta$ ). By forcing the intercept to zero, the slope of the linear line is referred to as the Beta coefficient. Figure 4-4 and Figure 4-5 present plots of LOG (Viscosity Ratio) vs Volume Ratio for the non-adjusted and adjusted slope respectively for sample 1.

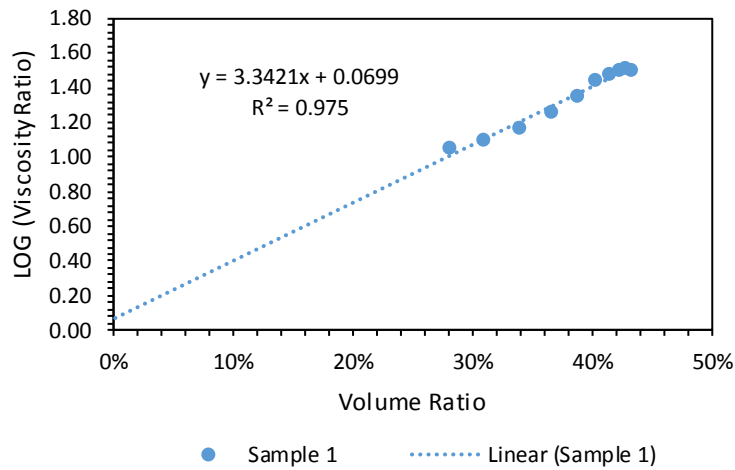


Figure 4-4: Plot of LOG (Viscosity Ratio) vs Volume Ratio with Y-intercept not Adjusted

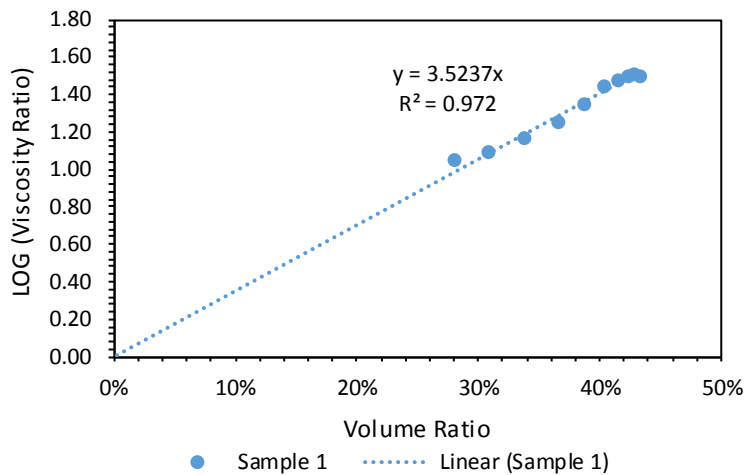


Figure 4-5: Plot of LOG (Viscosity Ratio) vs Volume Ratio Adjusted to Zero

The slope of the plot of LOG (Viscosity Ratio) vs Volume Ratio changes from 3.34 to 3.52 as illustrated in Figure 4-4 and Figure 4-5 respectively. If the intercept is set to zero, the slope 3.52 is referred to as the calculated Beta coefficient.



#### 4.6.1 Using The Calculated Beta Coefficient to Predict Plastic Viscosity

The calculated Beta coefficient ( $\beta$ ) can be used to predict the Bingham plastic viscosity ( $K_B$ ) by the use of Equation 4-3. Table 4-III presents how the predicted plastic viscosity values for sample 1 can be calculated using the Beta coefficient.

$$K_B = 10^{V_R \beta} \mu_w \quad \text{Equation 4-3}$$

Where  $\mu_w = 0.000894 \text{ Pa} \cdot \text{s}$  at  $25 \text{ }^\circ\text{C}$

Table 4-III: Predicted Plastic Viscosity Using Calculated Beta Coefficient

Sample 1					
MPV	Volume Ratio ( $V_R$ )	Viscosity Ratio ( $\eta_R$ )	$\log(\eta_R)$	Calculated Beta ( $\beta$ )	Predicted PV
0.030	0.433	33.56	1.493	3.52	0.030
0.029	0.428	32.44	1.511		0.029
0.028	0.423	31.32	1.496		0.028
0.027	0.414	30.20	1.480		0.026
0.025	0.403	27.96	1.447		0.023
0.020	0.387	22.37	1.350		0.021
0.016	0.366	17.90	1.253		0.017
0.013	0.338	14.54	1.163		0.014
0.011	0.308	12.30	1.090		0.011
0.010	0.281	11.19	1.049		0.009

Figure 4-6 presents the comparison of the measured data to the predicted data using the Beta coefficient.

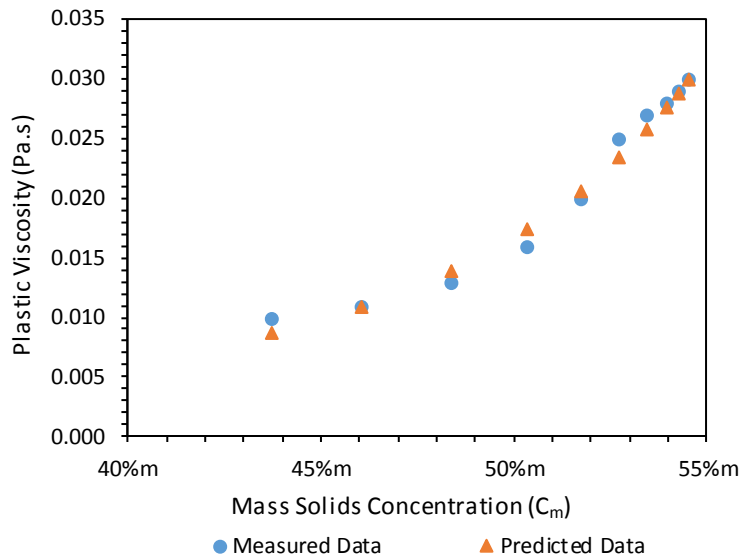


Figure 4-6: Comparison of Measured and Predicted Plastic Viscosity Data

The Beta coefficients of all the samples were calculated as shown in Table 4-III for sample 1 and Table 4-IV presents the results of the calculated Beta coefficients and  $C_{bfree}$  values for all 30 samples.

Table 4-IV: Calculated Beta Coefficients and  $C_{bfree}$  for all Samples

Sample Name	Calculated Beta	$C_{bfree}$
Sample 1	3.52	22%v(44%m)
Sample 2	4.00	25%v(48%m)
Sample 3	2.52	34%v(60%m)
Sample 4	2.39	43%v(68%m)
Sample 5	2.43	32%v(57%m)
Sample 6	2.49	43%v(67%m)
Sample 7	2.56	29%v(52%m)
Sample 8	2.71	40%v(64%m)
Sample 9	2.63	28%v(52%m)
Sample 10	2.79	42%v(67%m)
Sample 11	2.57	35%v(60%m)
Sample 12	2.42	45%v(69%m)
Sample 13	3.55	30%v(57%m)
Sample 14	2.51	45%v(69%m)
Sample 15	3.83	26%v(50%m)
Sample 16	3.84	33%v(58%m)
Sample 17	3.82	27%v(50%m)
Sample 18	2.81	36%v(61%m)
Sample 19	2.73	35%v(60%m)
Sample 20	3.13	35%v(60%m)
Sample 21	5.93	17%v(34%m)
Sample 22	4.61	25%v(46%m)
Sample 23	9.58	11%v(22%m)
Sample 24	2.99	43%v(67%m)
Sample 25	2.85	42%v(66%m)
Sample 26	3.06	37%v(61%m)
Sample 27	2.19	45%v(69%m)
Sample 28	4.67	25%v(49%m)
Sample 29	2.69	43%v(68%m)
Sample 30	5.30	26%v(48%m)

After all the Beta coefficients of the 30 samples was determined, the researcher tried to find out if there was any correlation between Beta and the  $C_{bfree}$  of the samples. Figure 4-7 presents a graph of Beta coefficients vs  $C_{bfree}$  plotted to test this hypothesis.

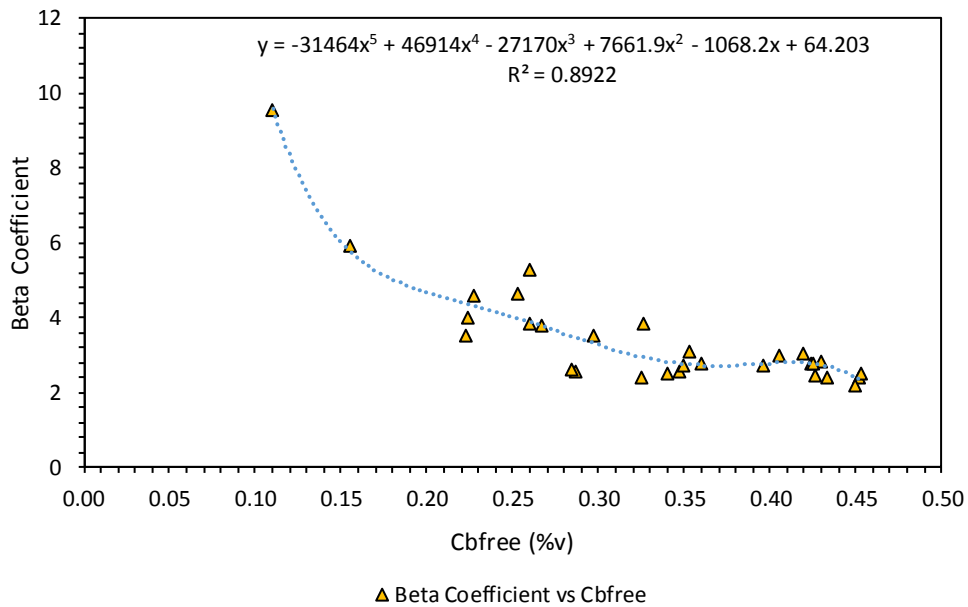


Figure 4-7: Beta Coefficient ( $\beta$ ) v  $C_{bfree}$  for All 30 Samples

The graph shows that there is a good correlation between the Beta coefficients and the  $C_{bfree}$  values of the 30 samples in the slurry database with an  $R^2$  value of 0.89.

The polynomial equation displayed in Figure 4-7 was used by the researcher to predict the Beta coefficients of the 30 samples tested. Table 4-V presents a comparison of the calculated Beta and measured Beta coefficients. It also presents the percentage error calculated by Equation 4-4 showing how accurate the polynomial equation predicts Beta.

$$\%Error = \frac{(\text{Predicted} - \text{Calculated})}{\text{Calculated}} \times 100 \quad \text{Equation 4-4}$$

Table 4-V: Comparison of Calculated Beta and Predicted Beta Coefficients

Sample Name	Calculated Beta	Predicted Beta	Error
Sample 1	3.52	4.37	23.7%
Sample 2	4.00	4.37	9.2%
Sample 3	2.52	2.81	11.7%
Sample 4	2.39	2.67	11.8%
Sample 5	2.43	2.95	21.6%
Sample 6	2.49	2.73	10.0%
Sample 7	2.56	3.48	35.7%
Sample 8	2.71	2.74	1.3%
Sample 9	2.63	3.50	33.0%

Sample 10	2.79	2.74	-1.7%
Sample 11	2.57	2.76	7.5%
Sample 12	2.42	2.28	-5.8%
Sample 13	3.55	3.32	-6.4%
Sample 14	2.51	2.24	-10.6%
Sample 15	3.83	3.89	1.4%
Sample 16	3.84	2.94	-23.4%
Sample 17	3.82	3.77	-1.5%
Sample 18	2.81	2.71	-3.4%
Sample 19	2.73	2.75	0.6%
Sample 20	3.13	2.74	-12.6%
Sample 21	5.93	5.80	-2.3%
Sample 22	4.61	4.31	-6.4%
Sample 23	9.58	9.61	0.3%
Sample 24	2.99	2.76	-7.4%
Sample 25	2.85	2.71	-5.1%
Sample 26	3.06	2.76	-9.8%
Sample 27	2.19	2.35	7.4%
Sample 28	4.67	3.98	-14.8%
Sample 29	2.69	2.74	-1.0%
Sample 30	5.30	3.88	-26.8%

#### 4.6.2 Calculating Zeta Coefficient to Predict Bingham Yield Stress

Another constant Zeta ( $\zeta$ ) was calculated in order to predict the Bingham yield stress ( $\tau_{YB}$ ). Equation 4-5 was used to calculate the constant Zeta for all the 30 samples tested in the slurry database. The constant Zeta is only applicable for yield stresses greater than 5 Pa.

$$\zeta = \ln(\tau_{YB}) / V_R \quad \text{Equation 4-5}$$

Table 4-VI shows how Zeta was calculated for sample 1 and the same was applied to the remaining 29 samples.

Table 4-VI: Calculation of Zeta Coefficient for Sample 1

<b>Cm</b>	<b>Cv</b>	<b>MYS</b>	<b>Vol Ratio (<math>V_R</math>)</b>	<b>Zeta (<math>\zeta</math>)</b>	<b>Average Zeta</b>
0.545	0.302	27.5	0.433	7.66	6.91
0.543	0.300	25.0	0.428	7.52	

0.539	0.297	22.3	0.423	7.34	
0.534	0.293	19.2	0.414	7.13	
0.527	0.287	16.0	0.403	6.89	
0.517	0.279	13.0	0.387	6.63	
0.503	0.268	10.2	0.366	6.35	
0.484	0.253	7.0	0.338	5.76	
0.460	0.235	4.2	0.308	4.66	
0.437	0.219	1.8	0.281	2.09	

The last two tests in Table 4-VI were excluded in the calculation of Zeta as their yield stress is less than 5 Pa, therefore Zeta for sample 1 is 6.91. Equation 4-6 is used to calculate the Bingham yield stress, it presents the relationship between yield stress, volume ratio and Zeta.

$$\tau_{yB} = e^{(V_R \times \zeta)} \quad \text{Equation 4-6}$$

Table 4-VII presents the comparison of the measured yield stress to the calculated yield stress for sample 1 using the Zeta coefficient by the use of Equation 4-6.

Table 4-VII: Calculated Yield Stress Using Zeta Coefficient

<b>Cm</b>	<b>Cv</b>	<b>MYS</b>	<b>Calculated YS</b>	<b>Error</b>
0.545	0.302	27.5	19.9	-28%
0.543	0.300	25.0	19.3	-23%
0.539	0.297	22.3	18.6	-17%
0.534	0.293	19.2	17.5	-9%
0.527	0.287	16.0	16.1	1%
0.517	0.279	13.0	14.5	11%
0.503	0.268	10.2	12.5	23%
0.484	0.253	7.0	10.3	48%

### 4.6.3 The Relationship between Beta and Zeta Coefficient

A relationship was sought between Beta and Zeta coefficients. After calculating all Zeta coefficients for the 30 samples in the slurry database, Equation 4-7 was produced which relates Beta and Zeta coefficients. The calculated Beta coefficient is used to generate Zeta, which is used to calculate the Bingham yield stress. Figure 4-8 presents the relationship between Beta and Zeta coefficient.

$$\zeta = 2.2505\beta - 1.4757$$

Equation 4-7

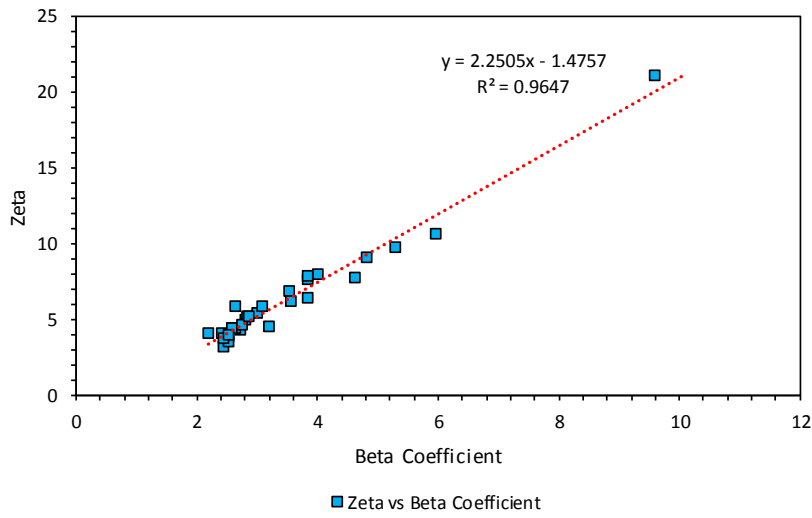


Figure 4-8: Relationship between Beta and Zeta Coefficient

Equation 4-3 and Equation 4-6 are used on six different samples that lie within the envelope of the samples tested in the slurry database to see how accurately they predict the plastic viscosity and yield stress respectively.

5. CHAPTER FIVE

5.1 Results

This chapter presents the results of the comparison of the actual tested data to the developed model predictions data, to validate the performance and compare the rheological models with experimental data.

5.1.1 Comparison of Tested Data to Model Predictions

Figure 5-1 presents the particle size distribution of the six gold tailings samples tested. For the prediction models to be applicable, the six gold tailings slurries tested should lie within the envelope of the samples tested in the slurry database.

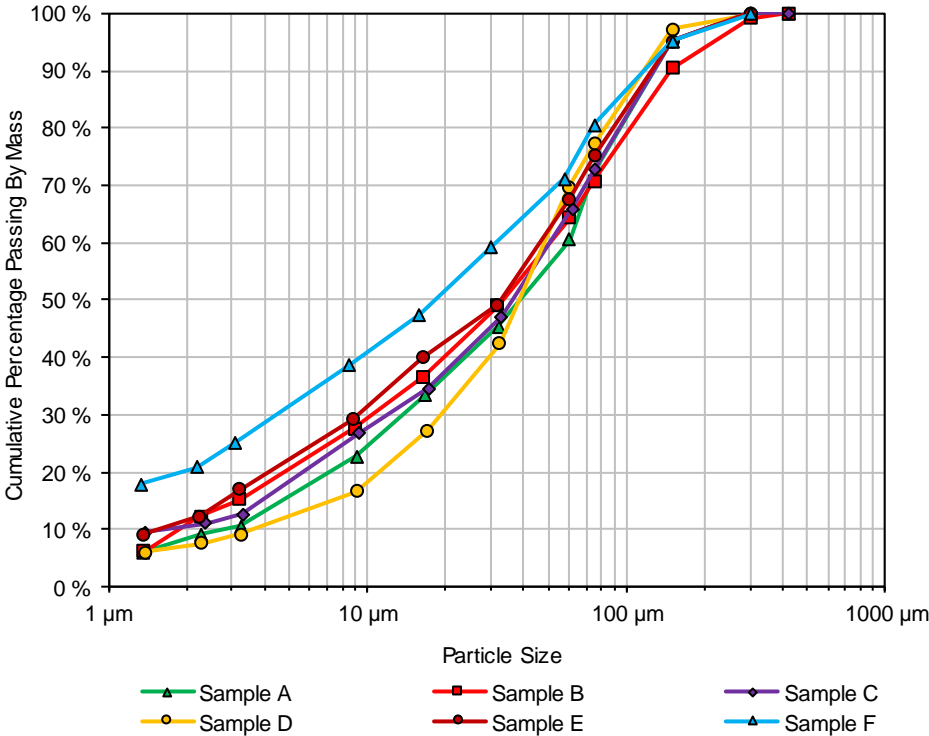


Figure 5-1: Particle Size Distribution Comparison

Table 5-1 presents a summary of the material properties of the six samples tested and the predicted Beta and Zeta coefficients from the  $C_{bfree}$  as discussed in chapter four.

Table 5-I: Summary of Material Properties for the Six Gold Tailings Samples

Sample Name	Solids Density (kg/m <sup>3</sup> )	C <sub>bfree</sub>	d <sub>90</sub> (μm)	d <sub>50</sub> (μm)	d <sub>25</sub> (μm)	pH	Temp (°C)	Beta (β)	Zeta (ζ)
Sample A	2.839	44.7%v or 69.6%m	129	39	10	8.5	17.3	2.43	4.00
Sample B	2.875	44.3%v or 68.6%m	148	33	7	8.4	17.6	2.75	4.71
Sample C	2.788	44.4%v or 68.4%m	128	36	8	8.7	16.4	2.70	4.60
Sample D	2.853	42.5%v or 68.6%m	117	38	15	7.8	14.9	2.74	4.69
Sample E	2.825	30.1%v or 54.1%m	125	33	6	8.1	18.3	3.26	5.85
Sample F	2.585	26.1%v or 51.9%m	117	18	3	8.6	15.2	3.86	7.22

Figure 5-2 shows the rheogram of sample A for mass solids concentrations ranging from 62.4%m to 75.0%m. The average pH and temperature measured were 8.5 at 17.3°C respectively for sample A.

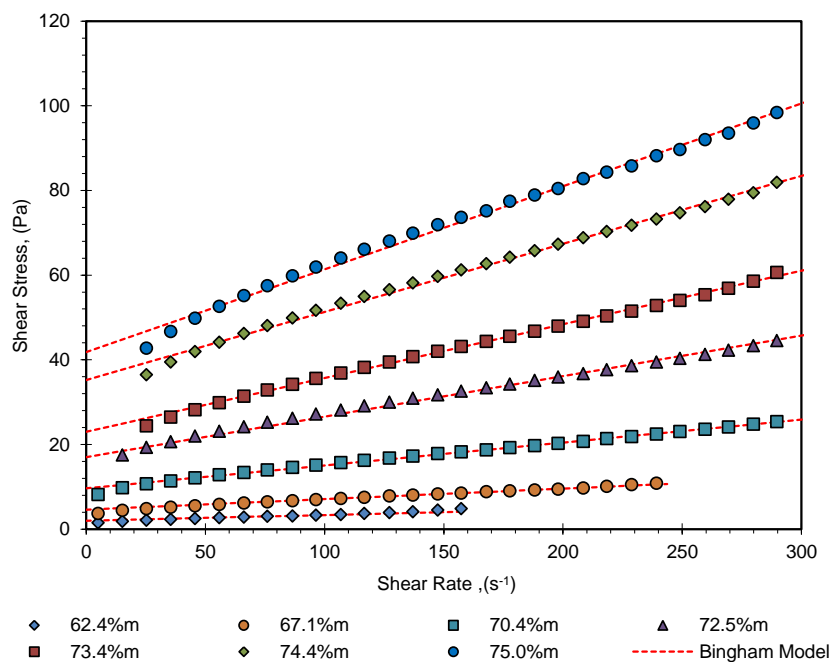


Figure 5-2: Rheogram of Sample A



The Bingham plastic model was applied to the tested data and Table 5-II summarises the Bingham plastic parameters for the range of mass solids concentrations tested for sample A.

Table 5-II: Sample A Rheology Test Results

<b>Test Results for Sample A</b>			
Mass Solids Concentration (%m)	Volume Solids Concentration (%v)	Bingham Yield Stress, $\tau_{yB}$ (Pa)	Bingham Plastic Viscosity, $K_B$ (Pa.s)
62.4	35.7	2.0	0.013
67.1	40.3	4.6	0.025
70.4	43.8	9.6	0.054
72.5	46.2	17.0	0.096
73.4	47.2	23.0	0.127
74.4	48.4	35.2	0.161
75.0	49.1	41.8	0.196

The Bingham plastic viscosity and yield stress were calculated as explained in the previous chapter and the comparison between the measured and predicted data for sample A is presented in Table 5-III.

Table 5-III: Comparison of Predicted and Measured Data for Sample A

<b>Sample A</b>			
MPV	Predicted PV	MYS	Predicted YS
0.013	0.020	2.0	9.2
0.025	0.039	4.6	14.8
0.054	0.070	9.6	22.5
0.096	0.109	17.0	30.8
0.127	0.134	23.0	35.7
0.161	0.171	35.2	42.5
0.196	0.199	41.8	47.4

Figure 5-3 and Figure 5-4 present the comparison of the yield stress and plastic viscosity graphically.

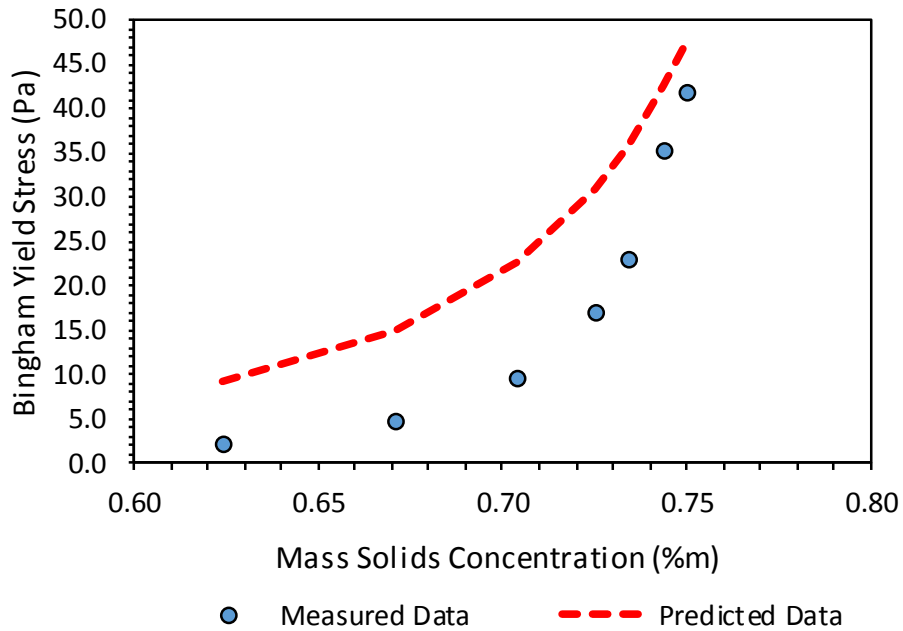


Figure 5-3: Comparison of Measured and Predicted Yield Stress for Sample A

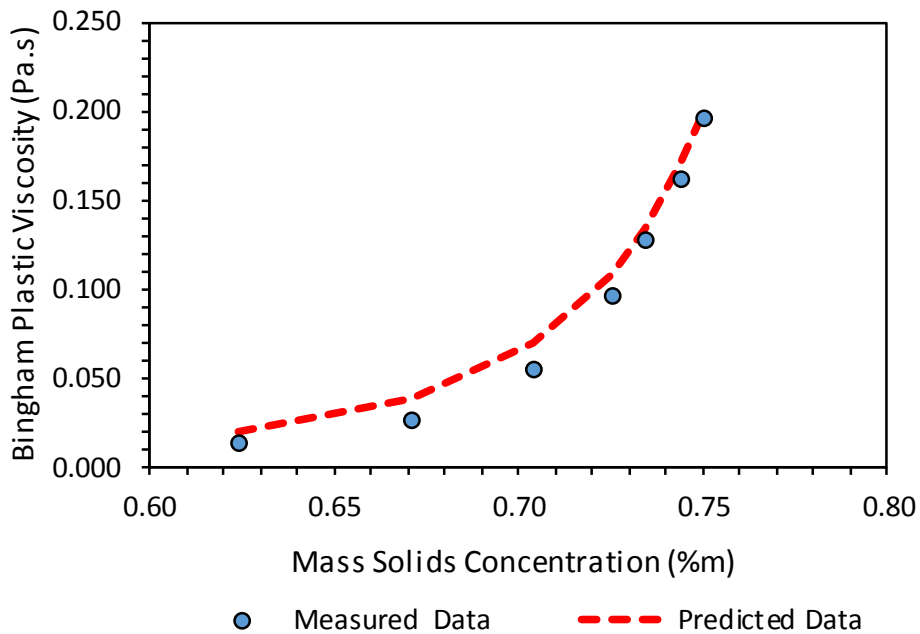


Figure 5-4: Comparison of Measured and Predicted Plastic Viscosity for Sample A

Figure 5-5 shows the rheogram for Sample B for mass solids concentrations ranging from 57.5%*m* to 72.7%*m*. The average pH and temperature measured were 8.4 at 17.6°C respectively for Sample B.

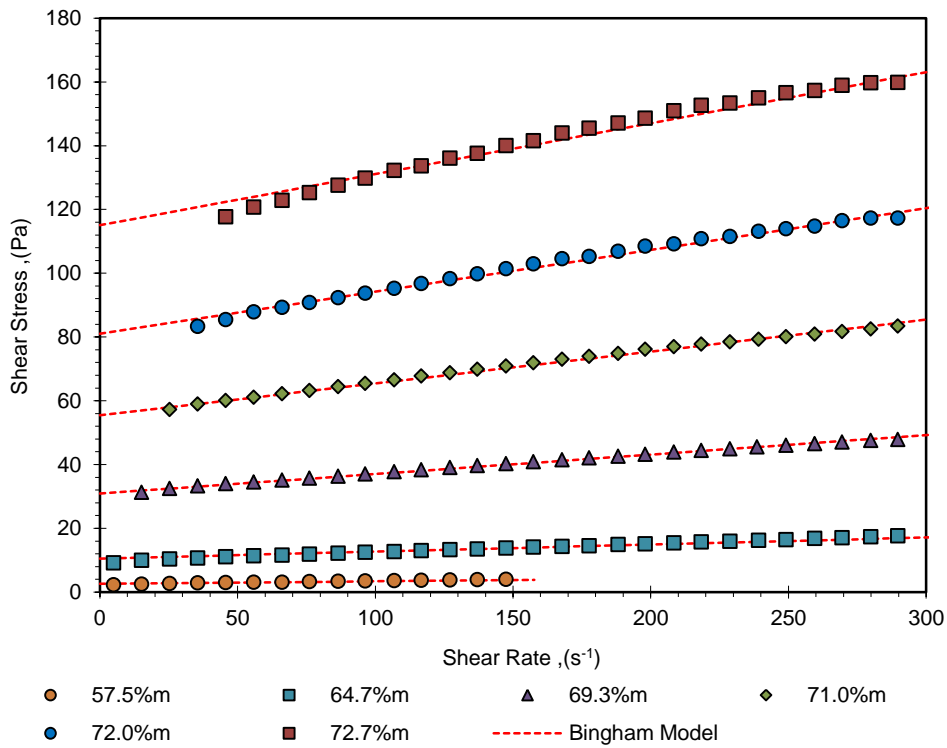


Figure 5-5: Rheogram of Sample B

Table 5-IV summarises the Bingham plastic parameters for the range of concentrations tested for sample B.

Table 5-IV: Sample B Rheology Test Results

Test Results for Sample B		
Mass Solids Concentration (%m)	Bingham Yield Stress, $\tau_{yB}$ (Pa)	Bingham Plastic Viscosity, $K_B$ (Pa.s)
57.5	2.6	0.008
64.7	10.5	0.002
69.3	30.9	0.061
71.0	55.4	0.100
72.0	81.1	0.131
72.7	115.1	0.160

Table 5-V presents the comparison between the measured and predicted data for sample B.

Table 5-V: Comparison of Predicted and Measured Data for Sample B

Sample B			
MPV	Predicted PV	MYS	Predicted YS
0.008	0.015	2.6	8.1
0.020	0.037	10.5	16.2
0.061	0.082	30.9	29.1
0.100	0.116	55.4	37.6
0.131	0.145	81.1	44.3
0.160	0.170	115.1	50.0

Figure 5-6 and Figure 5-7 present the comparison of the yield stress and plastic viscosity graphically.

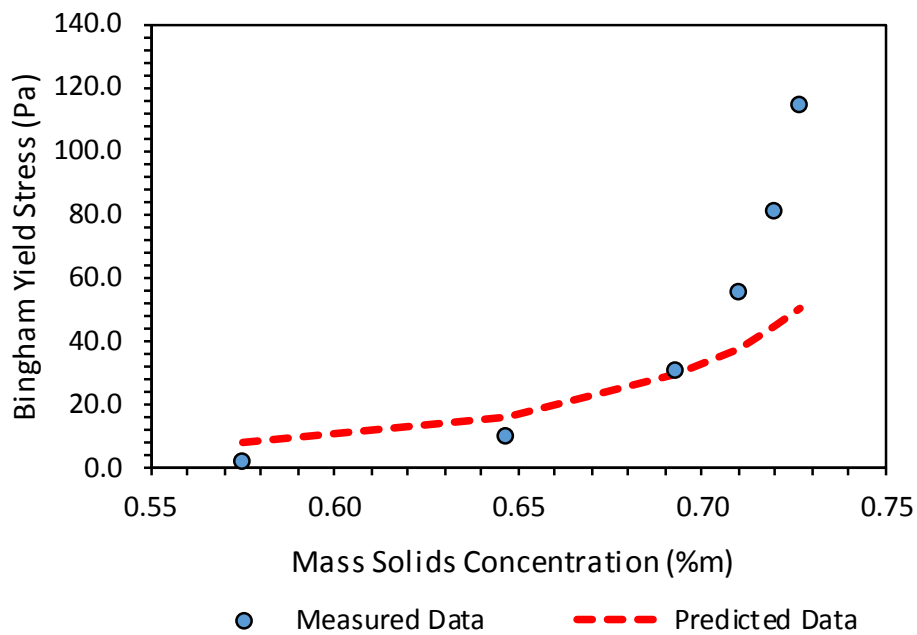


Figure 5-6: Comparison of Measured and Predicted Yield Stress for Sample B

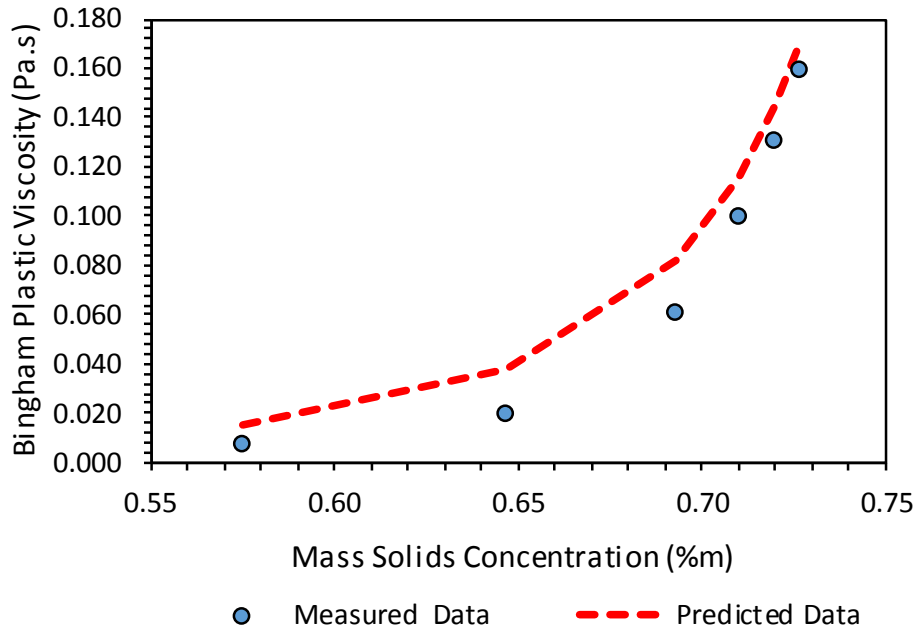


Figure 5-7: Comparison of Measured and Predicted Plastic Viscosity for Sample B

Figure 5-8 shows the rheogram for Sample C for mass solids concentrations ranging from 59.5%*m* to 69.6%*m*. The average pH and temperature measured were 8.7 at 16.4°C respectively for Sample C.

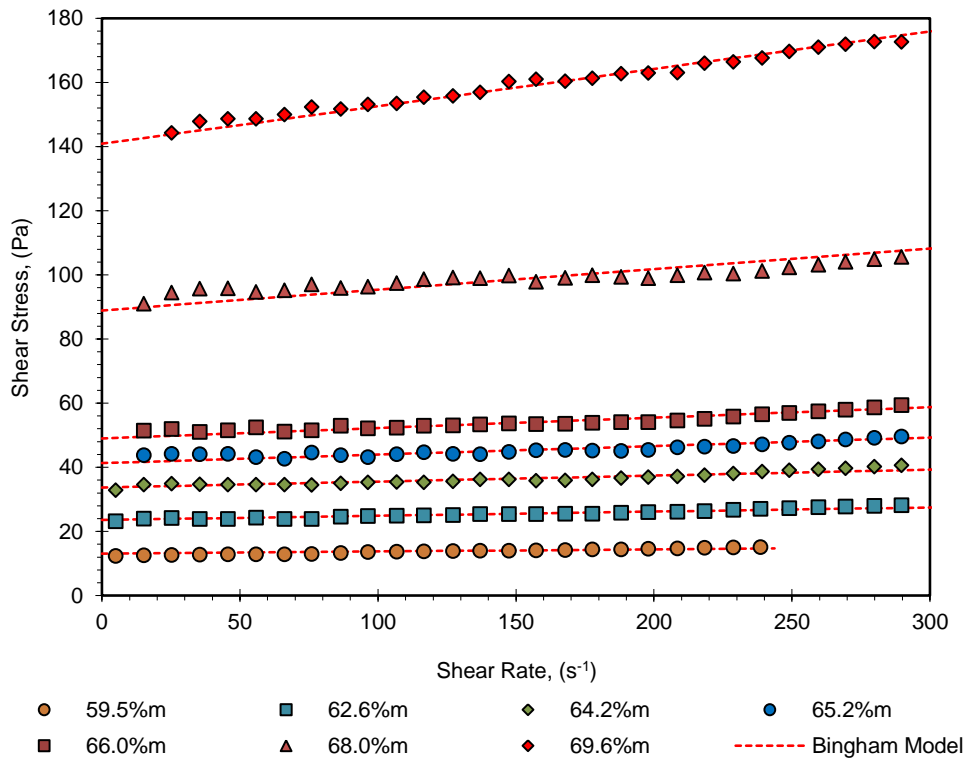


Figure 5-8: Rheogram of Sample C

Table 5-VI summarises the Bingham plastic parameters for the range of concentrations tested for sample C.

Table 5-VI: Sample C Rheology Test Results

<b>Test Results for Sample C</b>		
Mass Solids Concentration (%m)	Bingham Yield Stress, $\tau_{yB}$ (Pa)	Bingham Plastic Viscosity, $K_B$ (Pa.s)
59.5	13.1	0.007
62.6	23.6	0.013
64.2	33.7	0.019
65.2	41.3	0.027
66.0	49.0	0.033
68.0	88.9	0.064
69.6	140.9	0.117

Table 5-VII presents the comparison between the measured and predicted data for sample C.

Table 5-VII: Comparison of Predicted and Measured Data for Sample C

<b>Sample C</b>			
MPV	Predicted PV	MYS	Predicted YS
0.007	0.022	13.1	10.8
0.013	0.033	23.6	14.4
0.019	0.044	33.7	18.0
0.027	0.052	41.3	20.4
0.033	0.060	49.0	22.7
0.064	0.089	88.9	30.2
0.117	0.126	140.9	39.0

Figure 5-9 and Figure 5-10 present the comparison of the yield stress and plastic viscosity graphically.

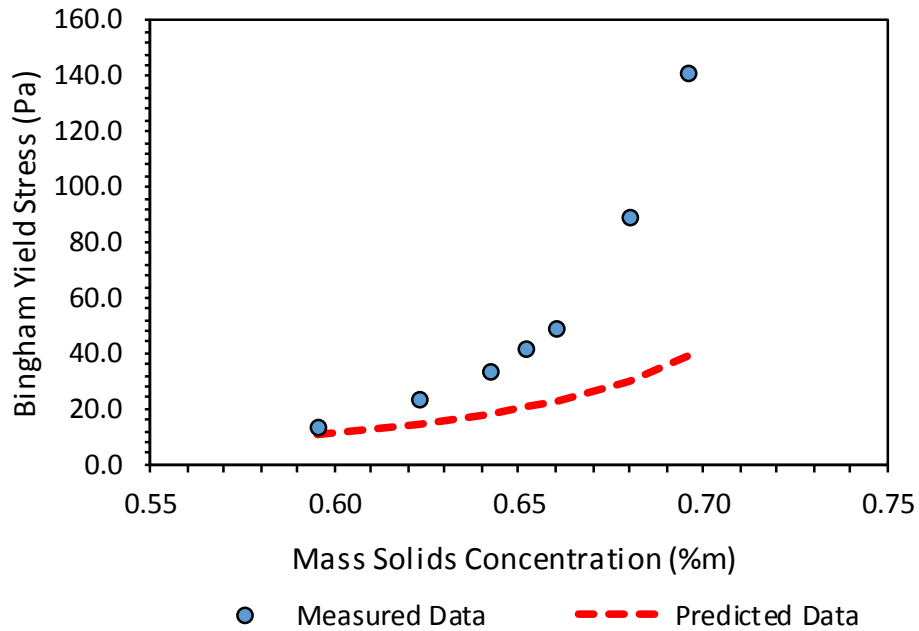


Figure 5-9: Comparison of Measured and Predicted Yield Stress for Sample C

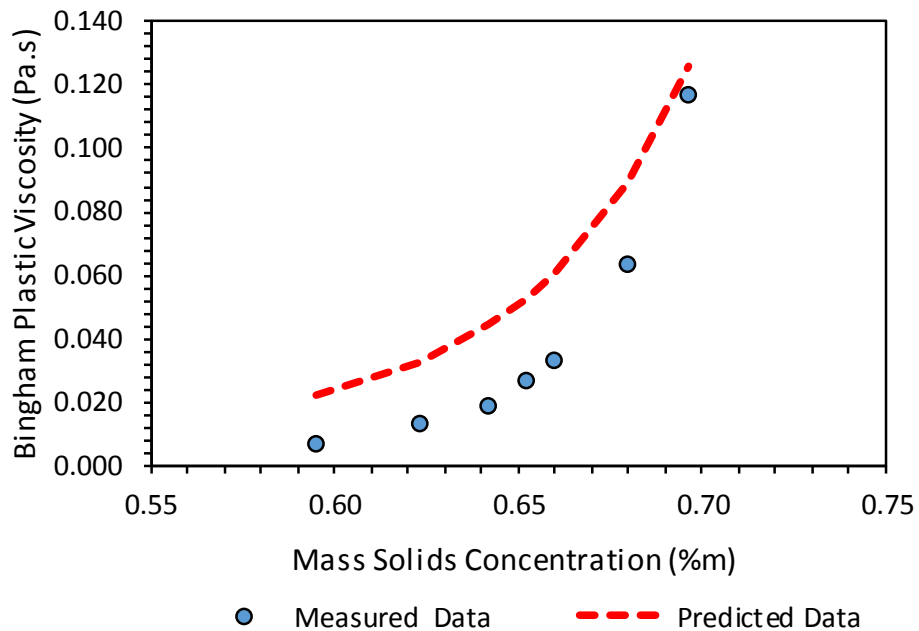


Figure 5-10: Comparison of Measured and Predicted Plastic Viscosity for Sample C

Figure 5-11 shows the rheogram for sample D for mass solids concentrations ranging from 65.0%*m* to 73.6%*m*. The average pH and temperature measured were 7.8 at 14.9°C respectively for sample D.

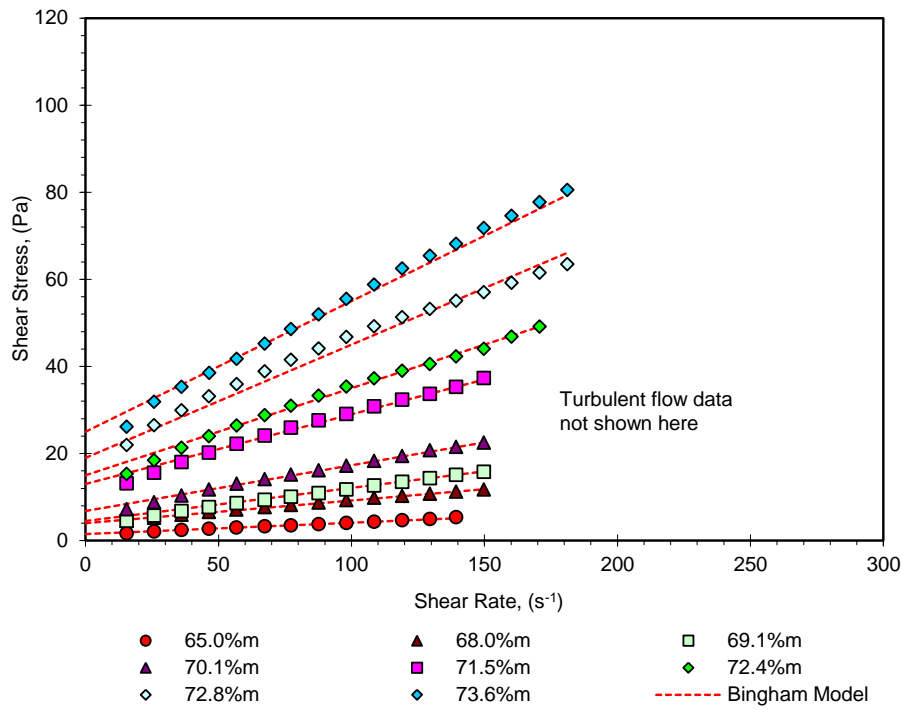


Figure 5-11: Rheogram of Sample D

Table 5-VIII summarises the Bingham plastic parameters for the range of concentrations tested for sample D.

Table 5-VIII: Sample 4 Rheology Test Results

Test Results for Sample D		
Mass Solids Concentration (%m)	Bingham Yield Stress, $\tau_{yB}$ (Pa)	Bingham Plastic Viscosity, $K_B$ (Pa.s)
65.0	1.5	0.026
68.0	4.0	0.052
69.1	4.5	0.076
70.1	6.8	0.105
71.5	13.0	0.160
72.4	15.0	0.200
72.8	19.0	0.260
73.6	25.0	0.300

Table 5-IX presents the comparison between the measured and predicted data for sample D.



Table 5-IX: Comparison of Predicted and Measured Data for Sample D

Sample D			
MPV	Predicted PV	MYS	Predicted YS
0.026	0.042	1.5	17.5
0.052	0.070	4.0	25.7
0.076	0.087	4.5	30.1
0.105	0.107	6.8	35.0
0.160	0.145	13.0	44.0
0.200	0.179	15.0	51.5
0.260	0.198	19.0	55.4
0.300	0.243	25.0	64.5

Figure 5-12 and Figure 5-13 present the comparison of the yield stress and plastic viscosity graphically.

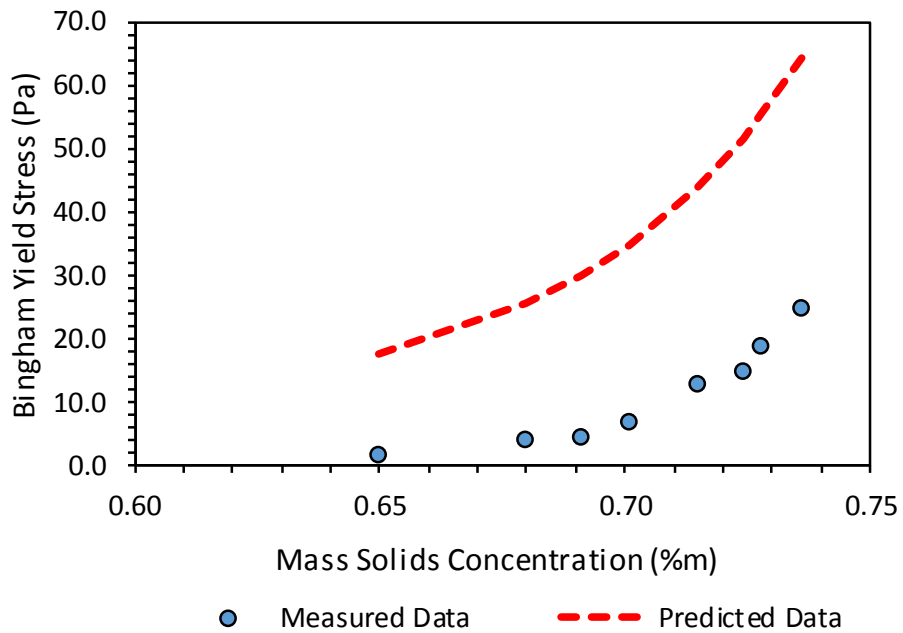


Figure 5-12: Comparison of Measured and Predicted Yield Stress for Sample D

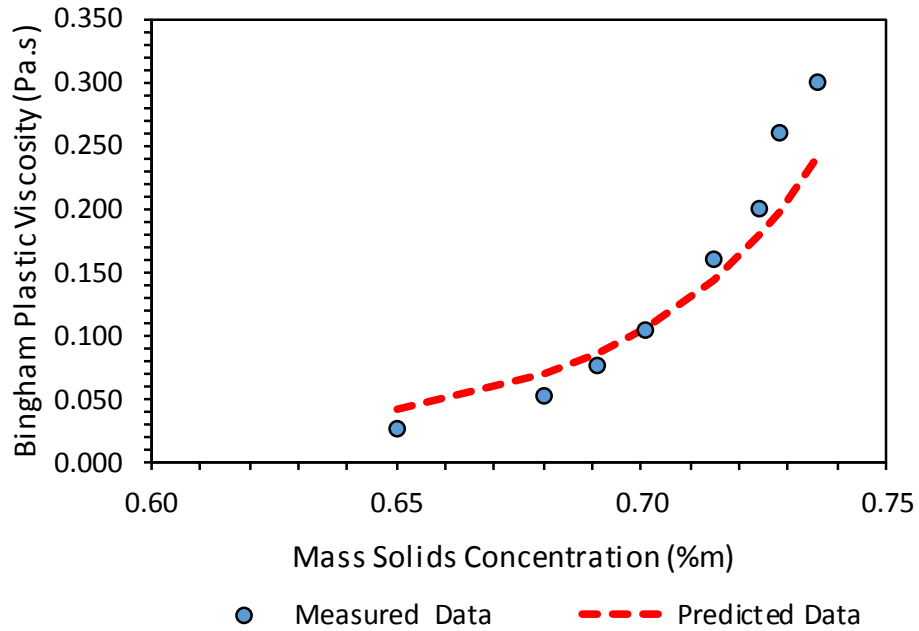


Figure 5-13: Comparison of Measured and Predicted Plastic Viscosity for Sample D

Figure 5-14 shows the rheogram for sample E for mass solids concentrations ranging from 49.3%*m* to 62.1%*m*. The average pH and temperature measured were 8.1 at 18.3°C respectively for sample E.

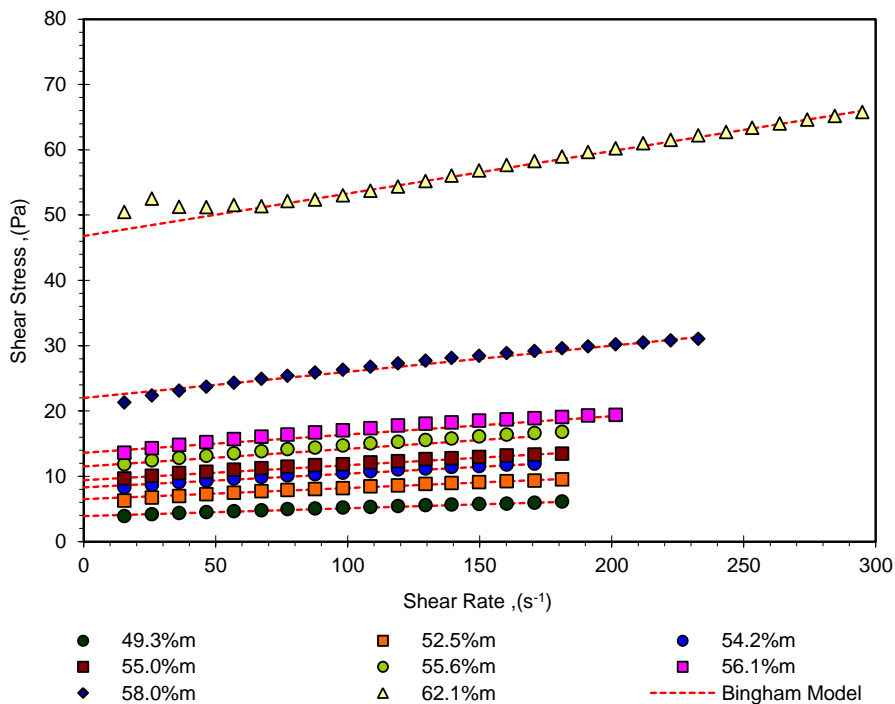


Figure 5-14: Rheogram of Sample E

Table 5-X summarises the Bingham plastic parameters for the range of concentrations tested for sample E.

Table 5-X: Sample E Rheology Test Results

<b>Test Results for Sample E</b>		
Mass Solids Concentration (%m)	Bingham Yield Stress, $\tau_{yB}$ (Pa)	Bingham Plastic Viscosity, $K_B$ (Pa.s)
49.3	3.9	0.012
52.5	6.5	0.017
54.2	8.3	0.021
55.0	9.4	0.023
55.6	11.50	0.027
56.1	13.60	0.028
58.0	22.0	0.040
62.1	46.8	0.065

Table 5-XI presents the comparison between the measured and predicted data for sample E.

Table 5-XI: Comparison of Predicted and Measured Data for Sample E

<b>Sample E</b>			
MPV	Predicted PV	MYS	Predicted YS
0.012	0.011	3.9	7.1
0.017	0.015	6.5	9.2
0.021	0.019	8.3	10.8
0.023	0.021	9.4	11.6
0.027	0.022	11.5	12.3
0.028	0.024	13.6	12.9
0.040	0.031	22.0	15.8
0.065	0.058	46.8	25.8

Figure 5-15 and Figure 5-16 present the comparison of the yield stress and plastic viscosity graphically.

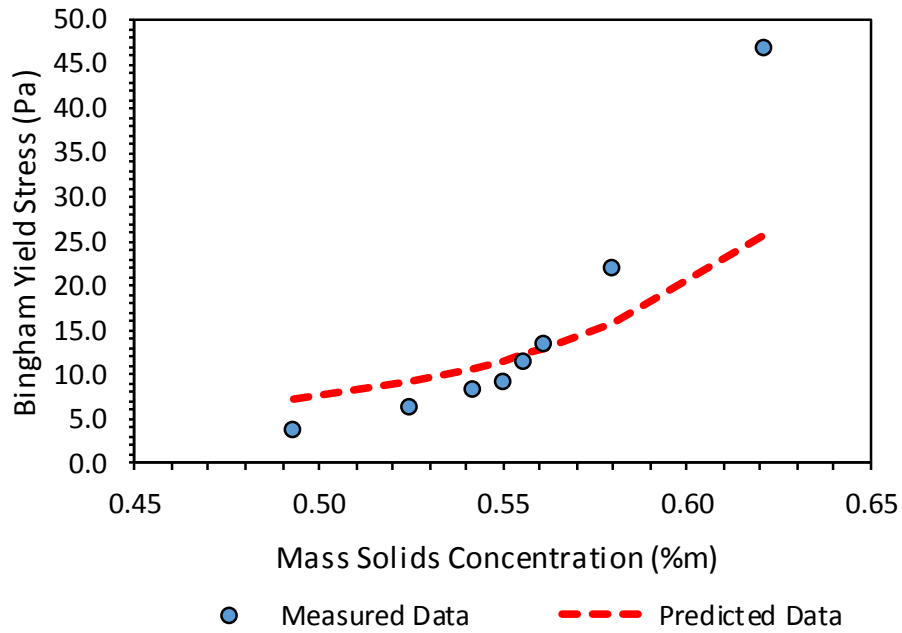


Figure 5-15: Comparison of Measured and Predicted Yield Stress for Sample E

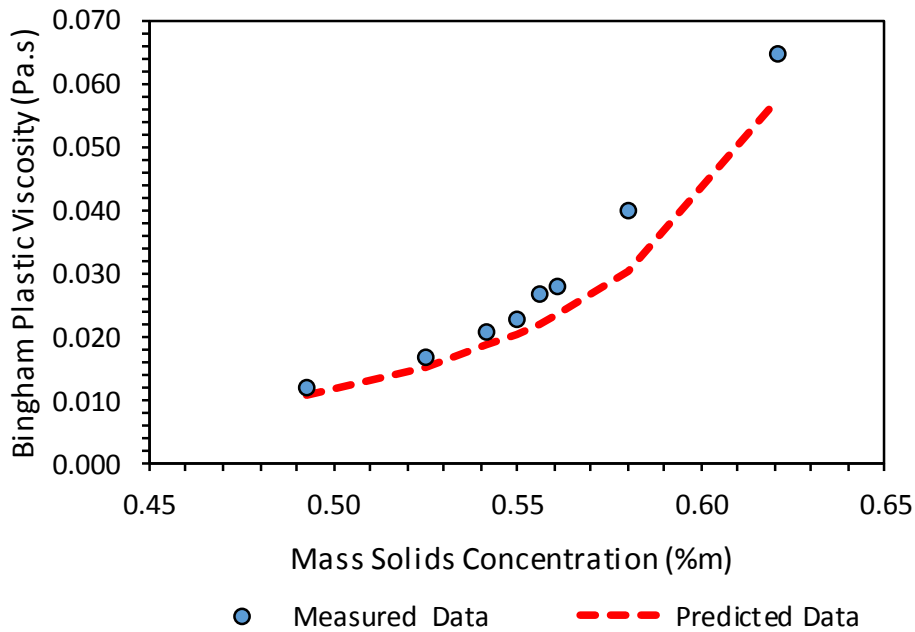


Figure 5-16: Comparison of Measured and Predicted Plastic Viscosity for Sample E

Figure 5-17 shows the rheogram for sample F for mass solids concentrations ranging from 46.6%*m* to 55.4%*m*. The average pH and temperature measured were 8.6 at 15.2°C respectively for sample F.

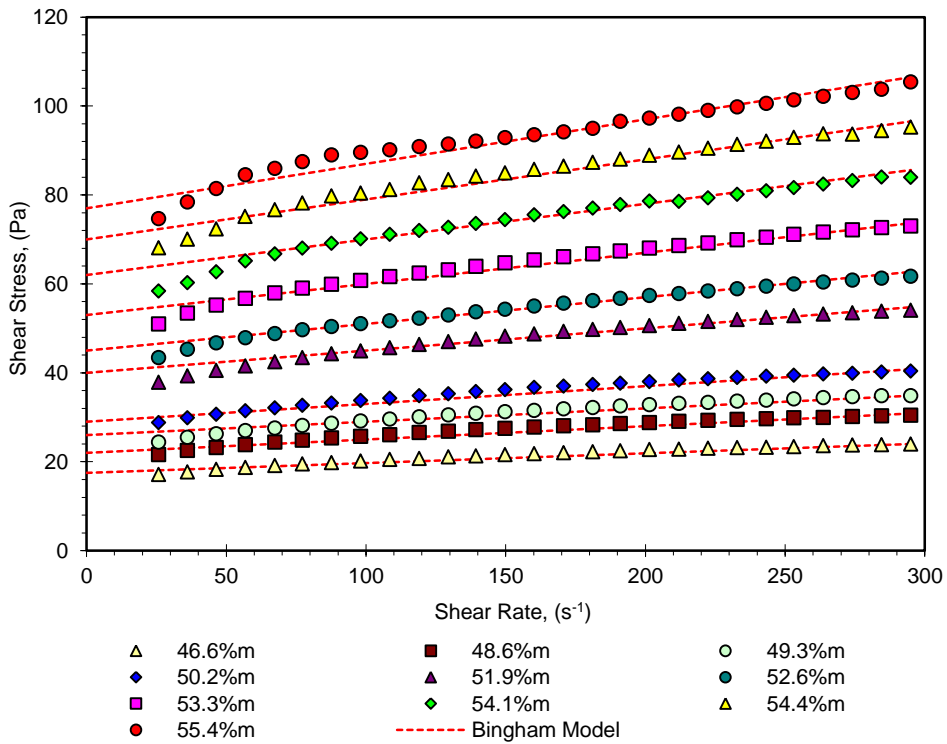


Figure 5-17: Rheogram of Sample F

Table 5-XII summarises the Bingham plastic parameters for the range of concentrations tested for sample F.

Table 5-XII: Sample F Rheology Test Results

Test Results for Sample F		
Mass Solids Concentration (%m)	Bingham Yield Stress, $\tau_{YB}$ (Pa)	Bingham Plastic Viscosity, $K_B$ (Pa.s)
46.6	17.5	0.022
48.6	22.0	0.028
49.3	26.0	0.030
50.2	29.0	0.040
51.9	40.0	0.050
52.6	45.0	0.060
53.3	53.0	0.070
54.1	62.0	0.080
54.4	70.0	0.090
55.4	77.0	0.100

Table 5-XIII presents the comparison between the measured and predicted data for sample F.

Table 5-XIII: Comparison of Predicted and Measured Data for Sample F

Sample F			
MPV	Predicted PV	MYS	Predicted YS
0.022	0.021	17.5	13.2
0.028	0.029	22.0	16.6
0.030	0.032	26.0	18.1
0.040	0.036	29.0	20.2
0.050	0.048	40.0	25.4
0.060	0.054	45.0	28.1
0.070	0.062	53.0	31.1
0.080	0.072	62.0	35.1
0.090	0.076	70.0	36.8
0.100	0.093	77.0	43.2

Figure 5-18 and Figure 5-19 present the comparison of the yield stress and plastic viscosity graphically.

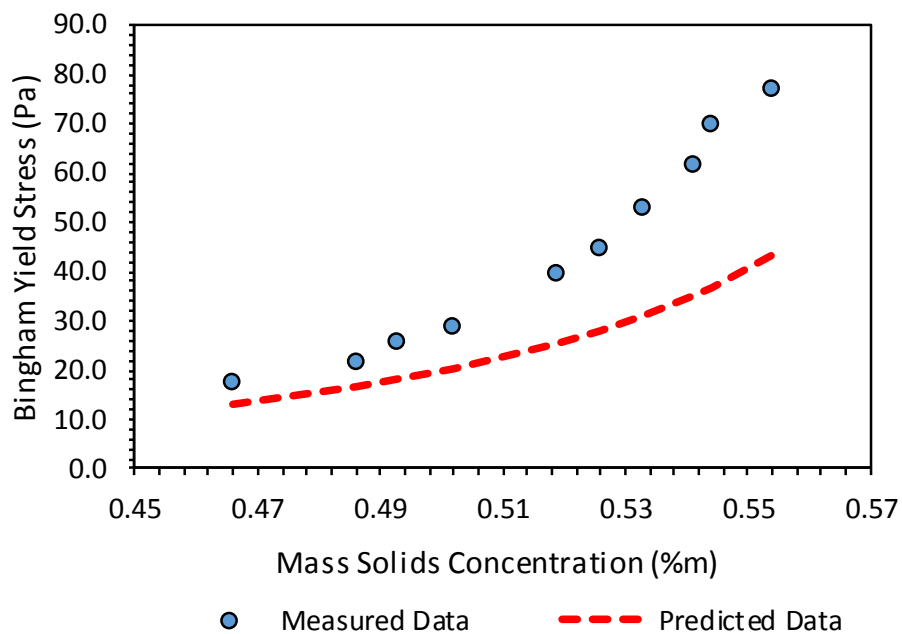


Figure 5-18: Comparison of Measured and Predicted Yield Stress for Sample F

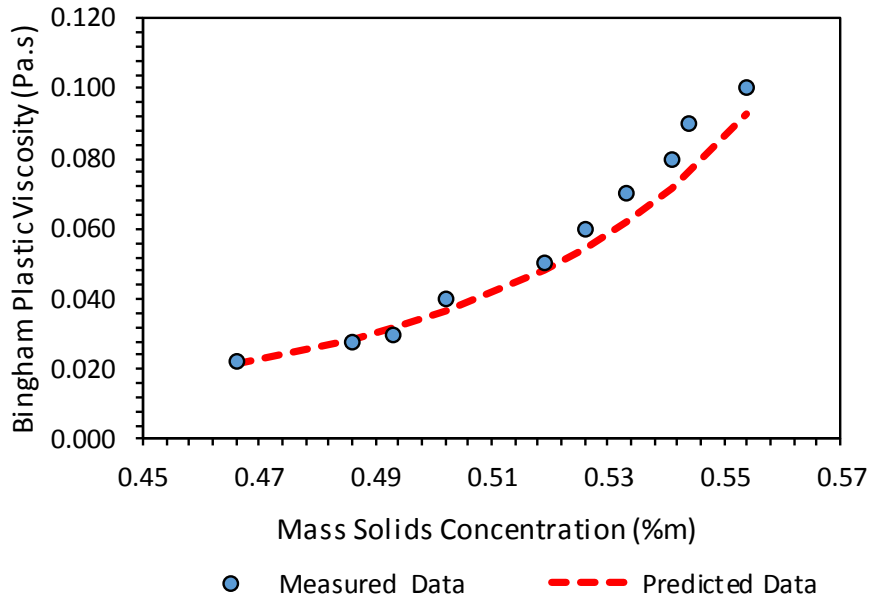


Figure 5-19: Comparison of Measured and Predicted Plastic Viscosity of Sample F

## 5.2 Evaluation of Model Predictions

The predictability of the model can be evaluated by calculating the average relative error between model predictions and new observations by the use of Equation 5-1.

$$\text{relative error} = \frac{|\text{predicted} - \text{actual}|}{\text{actual}} \quad \text{Equation 5-1}$$

The “relative error” is the amount by which the predicted value differs from the actual measured quantity as presented in Table 5-XIV.

Table 5-XIV: Average Relative Errors of Samples Tested

Sample A					
MPV	Predicted PV	MYS	Predicted YS	Relative Error YS	Relative Error PV
0.013	0.020	2.0	9.2	360%	54%
0.025	0.039	4.6	14.8	223%	57%
0.054	0.070	9.6	22.5	135%	30%
0.096	0.109	17.0	30.8	81%	13%
0.127	0.134	23.0	35.7	55%	5%
0.161	0.171	35.2	42.5	21%	6%
0.196	0.199	41.8	47.4	13%	2%
Average Relative Error				<b>127%</b>	<b>24%</b>

<b>Sample B</b>					
MPV	Predicted PV	MYS	Predicted YS	Relative Error YS	Relative Error PV
0.008	0.015	2.6	8.1	212%	86%
0.020	0.037	10.5	16.2	54%	87%
0.061	0.082	30.9	29.1	6%	35%
0.100	0.116	55.4	37.6	32%	16%
0.131	0.145	81.1	44.3	45%	10%
0.160	0.170	115.1	50.0	57%	6%
Average Relative Error				<b>68%</b>	<b>40%</b>
<b>Sample C</b>					
MPV	Predicted PV	MYS	Predicted YS	Relative Error YS	Relative Error PV
0.007	0.022	13.1	10.8	18%	216%
0.013	0.033	23.6	14.4	39%	152%
0.019	0.044	33.7	18.0	47%	132%
0.027	0.052	41.3	20.4	51%	94%
0.033	0.060	49.0	22.7	54%	83%
0.064	0.089	88.9	30.2	66%	39%
0.117	0.126	140.9	39.0	72%	7%
Average Relative Error				<b>49%</b>	<b>103%</b>
<b>Sample D</b>					
MPV	Predicted PV	MYS	Predicted YS	Relative Error YS	Relative Error PV
0.026	0.042	1.5	17.5	1067%	62%
0.052	0.070	4.0	25.7	542%	35%
0.076	0.087	4.5	30.1	568%	14%
0.105	0.107	6.8	35.0	415%	2%
0.160	0.145	13.0	44.0	238%	9%
0.200	0.179	15.0	51.5	243%	10%
0.260	0.198	19.0	55.4	192%	24%
0.300	0.243	25.0	64.5	158%	19%
Average Relative Error				<b>428%</b>	<b>22%</b>



<b>Sample E</b>					
MPV	Predicted PV	MYS	Predicted YS	Relative Error YS	Relative Error PV
0.012	0.011	3.9	7.1	83%	8%
0.017	0.015	6.5	9.2	42%	9%
0.021	0.019	8.3	10.8	30%	11%
0.023	0.021	9.4	11.6	23%	10%
0.027	0.022	11.5	12.3	7%	17%
0.028	0.024	13.6	12.9	5%	15%
0.040	0.031	22.0	15.8	28%	23%
0.065	0.058	46.8	25.8	45%	11%
Average Relative Error				<b>33%</b>	<b>13%</b>
<b>Sample F</b>					
MPV	Predicted PV	MYS	Predicted YS	Relative Error YS	Relative Error PV
0.022	0.021	17.5	13.2	25%	2%
0.028	0.029	22.0	16.6	25%	2%
0.030	0.032	26.0	18.1	30%	6%
0.040	0.036	29.0	20.2	30%	9%
0.050	0.048	40.0	25.4	36%	4%
0.060	0.054	45.0	28.1	38%	9%
0.070	0.062	53.0	31.1	41%	12%
0.080	0.072	62.0	35.1	43%	10%
0.090	0.076	70.0	36.8	47%	16%
0.100	0.093	77.0	43.2	44%	7%
Average Relative Error				<b>36%</b>	<b>8%</b>

### 5.3 Summary of Model Predictions

From Table 5-XIV above, from the average relative errors we can conclude that the Bingham plastic viscosity can be predicted with reasonable accuracy as compared to the Bingham yield stress. There is a need to improve the predictive accuracy of the prediction models as more data is generated in the slurry database.

## 6. CHAPTER SIX

### 6.1 Discussion and Conclusions

This chapter summarises the major research findings and discusses the limitations of this study and possible future work.

#### *6.1.1 Summary of This Research*

Transportation of mineral tailings through pipelines is an industrial reality. For bulk solids handling over long distances, it has proved to be more - economical than several other modes of transportation. For designing an economical and efficient pipeline system, a large amount of design data is required as an input. Rheological characteristics of the slurry at various concentrations and flow rate is one such parameter. This is needed to ensure a stable/energy efficient pipeline transportation and also for the prediction of the head requirement for pumping the slurry.

The review of the available literature has shown that the state of the knowledge about the rheological characteristics of the slurry and the effect of material properties on slurry pump performance is rather incomplete. Hence, a study of the rheological behaviour of slurries of solids of different particle size distribution and top particle size has been made, to get an insight into the subject.

The effect of slurry material properties on the rheological properties of thickened gold tailings slurries has been investigated in this dissertation. Identifying the most important material properties that can be used in the prediction models used to predict the slurry Bingham yield stress and plastic viscosity. 30 thickened gold tailings samples were tested and used to develop the models to predict the Bingham yield stress and plastic viscosity.

The freely settled bed packing concentration ( $C_{bfree}$ ) of a sample was found to be a very important parameter that can be used to predict the Beta coefficient of a sample that lies within the envelope of the tested data in the slurry database. The contribution of this study is to model a slurry by the use of its material properties. The rheology does not explain the variance in all the slurry properties and it will be useless to try and model certain slurry properties that are not related to the slurry rheological behaviour. Not all slurry material properties affect the rheology of a slurry and it will be useless to include these material properties in the model.

### *6.1.2 Limitations to the Study*

This study was limited to studying thickened gold tailings only. The number of samples tested was limited due to samples availability at the commercial test facility. The control of the quality of some of the test results was limited as some tests were outsourced to other test facilities and the researcher had to rely on these results.

### *6.1.3 Future Work*

This work showed that the models used to predict the yield stress and plastic viscosity provide varying degrees of accuracy. Although the models predicted the rheology of a number of samples with reasonable accuracy, care needs to be taken when using the models to estimate pipeline pressure losses. It is always preferable to measure the rheology of mineral tailings; however, this work does provide a means to estimate these properties with a reasonable level of accuracy. A thorough understanding of the limitations and applications of these models is needed.

## REFERENCES

- Alderman, N.J. 1996. Non-Newtonian Fluids: Obtaining Viscometric Data for Frictional Pressure Loss Estimation for Pipe flow. *ESDU95012*, September.
- Ancey, C., (2001), Geomorphological Fluid Mechanics. Producer: Balmforth, N.J.
- Barnes, H.A., Hutton, J.F. and Walters, K., (1989), An Introduction to Rheology, Elsevier, Amsterdam.
- Barnes, H.A., (1989), "Shear-thickening (dilatancy) in suspensions of non-aggregating particles", *Journal of Rheology*, vol 33(2).
- Bingham, E.C., (1922), Fluidity and Plasticity, McGraw-Hill, New York.
- Bingham, E. C. and Green, H., (1919), Plastic Material and not a Viscous Liquid; The Measurement of its Mobility and yield value. *Proc. Amer. Soc. Test Mater.*
- Bird, R.B., Stewart, W.E., Lightfoot, E.N., (1960), Transport Phenomena, Wiley, New York.
- Brown, N.P., and Heywood, N.I. (Editors)., (1991), Slurry Handling: Design of solid-liquid systems. Springer.
- Cheng Chang, Boger, D. V., and Nguyen, D., (1998), The Yielding of Waxy Crude Oils.
- Chhabra, R.P., and Richardson, J.F., (1999), *Non-Newtonian Flow in the Process Industries*. Oxford: Butterworth Heinemann.
- Chhabra, R.P. and Richardson, J.F. 2008. *Non-Newtonian flow and Applied Rheology: Engineering Applications*. Oxford: Butterworth-Heinemann.
- Coghill M (2003), "What is rheology?", First Mineral Processing & Tailings Rheology Workshop.
- Goodwin, J.W., (1975), "The Rheology of Dispersions", *Colloid Science*, vol. 7, pp.246-293.

Govier, G.W and Aziz, K., (1972), "*The Flow of Complex Mixtures in Pipes*", Van Nostrand Reinhold Company: New York.

Hackley, V.A, and Ferraris, C.F., (2001), *Guide to Rheological Nomenclature: Measurements in Ceramic Particulate Systems*. Washington: National Institute of Standards and Technology.

Haddas, P. Rheology. Saint Josephs' University, Available:  
<http://www.sju.edu/~phabdass/physics/rheo.html>

He, M., Wang, Y. & Forssberg, E., (2004), "Slurry rheology in wet ultra-fine grinding of industrial minerals: a review", *Powder Technology*. Vol. 147, pp. 267-304.

Jewell RJ, Fourie AB, Lord ER (2002), "Paste and Thickened Tailings – A Guide", Australian Centre for Geomechanics.

Litzenberger, C.G., (2003), Rheological Study of Kaolin Clay Slurries, M.Sc. Thesis, University of Saskatchewan, Canada.

Litzenberger, C.G., (2004), Sumner, R.J., "Flow behaviour of kaolin clay slurries", *Hydrotransport 16*, Santiago, Chile, v.1, 77-91.

Liu, D.M., (2000), "Particle packing and rheological property of highly-concentrated ceramic suspensions:  $\Phi$  determination and viscosity prediction", *Journal of Materials Science*, vol. 35, pp. 5503-5507 m.

Macdonald, E.H., (1983), *Alluvial Mining, The Geology, Technology and Economics of Placers*.

McClung, D. & Schaerer, P., (1993), *The Avalanche Handbook*. The Mountaineers. Seattle.

Nguyen, Q. D. and Boger D. V., (1992), Measuring the Flow Properties of Yield Stress Fluids. *Annu. Rev. Fluid Mech.*

Nguyen, Q.D., and Boger, D.V., (1987), "Characterization of yield stress with concentric cylinder viscometers", *Rheol. Acta*, v.26, 508-515.

Paterson & Cooke Consulting Engineers (2000), "Design of Slurry Pipeline Systems", Course notes.

Paterson & Cooke., (2007) "Paterson & Cooke Slurry Pipeline Design Course." The Design of Slurry Pipeline Systems. Cape Town.

Shook, C.A., Roco, M.C., (1991), Slurry Flow: Principles and Practice, Butterworth-Heinemann, Boston.

Slatter P, Malkin, Masalova I, Perrett D (2002), "Practical Rheology of Polymer Systems", Course notes, Cape Technikon Rheology Centre, Paar Physica.

Slatter, P.T, (1995), "Transitional and Turbulent flow of non-Newtonian Slurries in Pipelines" Ph.D. Thesis, University of Cape Town.

Steffe, J.F. 1996. Rheological methods in food process engineering. 2nd ed. East Lansing, USA: Freeman Press.

Sumner, R.S., Munkler, J.J., Carriere, S.M., Shook, C.A., (2000), "Rheology of Kaolin Slurries Containing Large Silica Particles", J. Hydrology and Hydromechanics, v.48 (2, 110-124.

Tadros, Th. F., (1988), "Rheology of Clays and Oxides", Applied Industrial Rheology, Somerset, NJ, 1-16.

Thomas, D.G., (1963), "Transport characteristics of suspensions VII", A.I.Ch.E. J., v.9, 310-316.

Usui, H., (1999), A rheological model for an agglomerative slurry of mono-modal silica particles, *Kagaku Kogaku Ronbunshu*.**25**, 459-465.

Usui, H., K. Kishimoto and H. Suzuki, (2000), A Viscosity prediction of agglomerative slurries with particle size distribution, *Kagaku Kogaku Ronbunshu*. **26**, 423-430.

Van Olphen, H., (1977), *An Introduction to Clay Colloid Chemistry*, 2nd Ed., Wiley, New York.

Weltmann, R.N. & Green, H., (1943), "Rheological Properties of Colloidal Solution, Pigment Suspensions and Oil mixtures", *Journal of Applied Physics*, vol.14, pp.569-576.

Wilson K. C, Addie G.R and Clift R (1992), *Slurry transport using centrifugal pumps*, Elsevier Science Publishers Ltd, Essex, England.

Xu, J., Gillies, R., Small, M., Shook, C.A., (1993) "Laminar and Turbulent Flow of Kaolin Slurries", *Hydrotransport 12*, Cranfield, UK, 595-613.

## APPENDIX A : PARTICLE SIZE DISTRIBUTION DATA



**CLIENT:** Paterson & Cooke  
P.O Box 23621  
Claremont  
7735

**PROJECT:**

**DATE:**

**ATT:** Brian Zengeni

**REF:**

### ASTM D422 SIEVE ANALYSIS

**DESCRIPTION :** \_\_\_\_\_  
**POSITION :** Sample A

**SAMPLE NO. :** 18885  
**CLIENT SAMPLE NO. :** \_\_\_\_\_

Sieve Analysis	Percent Passing
75.00	
63.00	
53.00	
37.50	
26.50	
19.00	
13.20	
9.50	
6.70	
4.75	
2.36	
2.00	
1.18	
0.600	
0.425	
0.300	100
0.150	95
0.0750	72

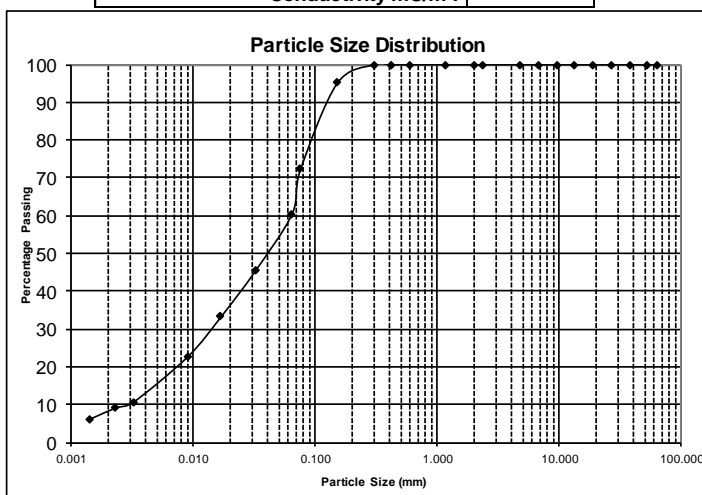
Hydrometer Analysis	
Diameter of particle (mm)	Percentage of soil suspension
0.0605	60
0.0320	45
0.0167	33
0.0090	23
0.0032	11
0.0023	9
0.0014	6

SCS Dispersion Test	
Diameter of particle (mm)	Percentage of soil suspension

<b>Specific Gravity:</b>	2.839
<b>Initial Moisture Content (%):</b>	
<b>pH:</b>	
<b>Conductivity mS/m:</b>	

<i>Atterberg Limits :</i> <i>TMH1 A2, A3 &amp; A4</i>	
Liquid Limit	
Plastic Index	
Linear Shrinkage	

<i>MOD AASHTO ; C.B.R. :</i> <i>TMH1 A7 &amp; A8</i>	
MOD AASHTO (Kg/m <sup>3</sup> )	
O.M.C. (%)	
C.B.R. @ 100% Comp.	
C.B.R. @ 98 % Comp.	
C.B.R. @ 95 % Comp.	
C.B.R. @ 93 % Comp.	
C.B.R. @ 90 % Comp.	
Swell ( max ) %	



Tabulated Summary	Percentage
<b>Gravel :</b> Percentage - 4.75 mm	0
<b>Sand :</b> Percentage - 4.75mm and + 0.075mm	28
<b>Silt :</b> Percentage - 0.075mm and + 0.002mm	64
<b>Clay :</b> Percentage - 0.002mm	8

The above test results are pertinent to the samples received and tested only. For Geoscience:  
While the tests are carried out according to recognized standards Geoscience shall not  
be liable for erroneous testing or reporting thereof. This report may not be reproduced except in full without prior consent of Geoscience.

Remarks:

ConSR22



**CLIENT:** Paterson & Cooke  
P.O Box 23621  
Claremont  
7735

**PROJECT:**

**DATE:**

**ATT:** Brian Zengeni

**REF:**

## ASTM D422 SIEVE ANALYSIS

**DESCRIPTION:** Tailings  
**POSITION:** Sample B

**SAMPLE NO.:** 18883

**CLIENT SAMPLE NO.:**

Sieve Analysis	Percent Passing
75.00	
63.00	
53.00	
37.50	
26.50	
19.00	
13.20	
9.50	
6.70	
4.75	
2.36	
2.00	
1.18	
0.600	
0.425	100
0.300	99
0.150	90
0.0750	71

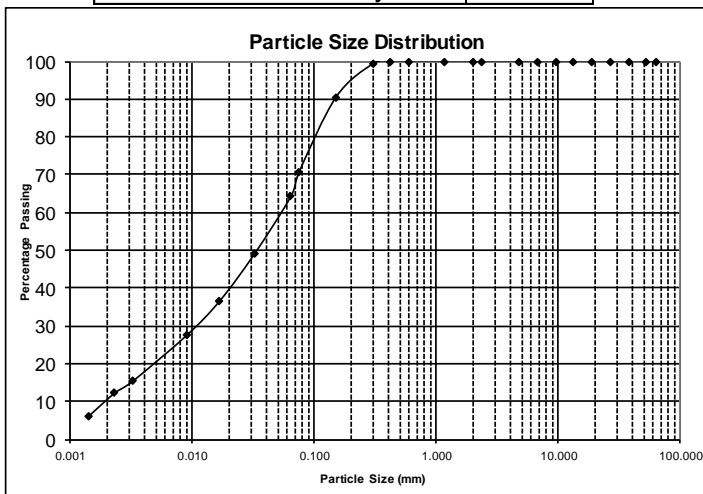
Hydrometer Analysis	
Diameter of particle (mm)	Percentage of soil suspension
0.0605	64
0.0317	49
0.0165	37
0.0089	28
0.0032	15
0.0023	12
0.0014	6

SCS Dispersion Test	
Diameter of particle (mm)	Percentage of soil suspension

<b>Specific Gravity:</b>	2.875
<b>Initial Moisture Content (%):</b>	
<b>pH:</b>	
<b>Conductivity mS/m:</b>	

Atterberg Limits : TMH1 A2, A3 & A4	
Liquid Limit	
Plastic Index	
Linear Shrinkage	

MOD AASHTO ; C.B.R. : TMH1 A7 & A8	
MOD AASHTO (Kg/m <sup>3</sup> )	
O.M.C. (%)	
C.B.R. @ 100% Comp.	
C.B.R. @ 98 % Comp.	
C.B.R. @ 95 % Comp.	
C.B.R. @ 93 % Comp.	
C.B.R. @ 90 % Comp.	
Swell ( max ) %	



Tabulated Summary	Percentage
<b>Gravel</b> : Percentage - 4.75 mm	0
<b>Sand</b> : Percentage - 4.75mm and + 0.075mm	29
<b>Silt</b> : Percentage - 0.075mm and + 0.002mm	61
<b>Clay</b> : Percentage - 0.002mm	10

The above test results are pertinent to the samples received and tested only. For Geoscience:  
While the tests are carried out according to recognized standards Geoscience shall not  
be liable for erroneous testing or reporting thereof. This report may not be reproduced except in full without prior consent of Geoscience.

Remarks:

ConSR22

**CLIENT:** Paterson & Cooke  
P.O Box 23621  
Claremont  
7735

**PROJECT:**

**DATE:**

**ATT:** Brian Zengeni

**REF:**

## ASTM D422 SIEVE ANALYSIS

**DESCRIPTION:** Tailings  
**POSITION:** Sample C

**SAMPLE NO.:** 18884  
**CLIENT SAMPLE NO.:**

Sieve Analysis	Percent Passing
75.00	
63.00	
53.00	
37.50	
26.50	
19.00	
13.20	
9.50	
6.70	
4.75	
2.36	
2.00	
1.18	
0.600	
0.425	
0.300	100
0.150	95
0.0750	73

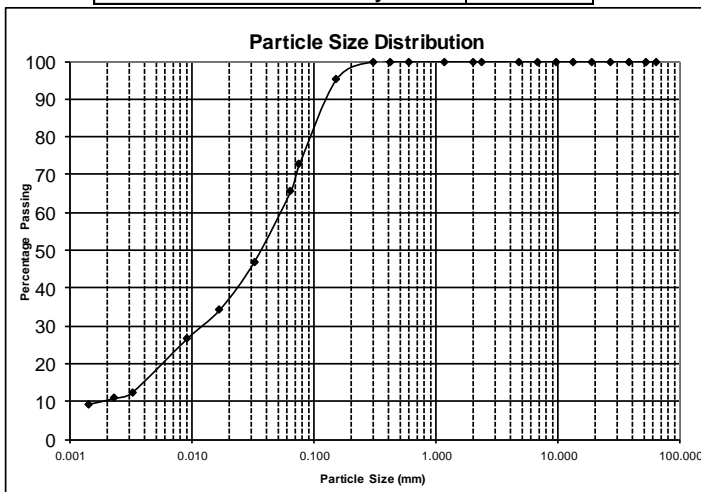
Hydrometer Analysis	
Diameter of particle (mm)	Percentage of soil suspension
0.0621	66
0.0329	47
0.0171	35
0.0092	27
0.0033	13
0.0024	11
0.0014	9

SCS Dispersion Test	
Diameter of particle (mm)	Percentage of soil suspension

<b>Specific Gravity:</b>	2.788
<b>Initial Moisture Content (%):</b>	
<b>pH:</b>	
<b>Conductivity mS/m:</b>	

<i>Atterberg Limits :</i> <i>TMH1 A2, A3 &amp; A4</i>	
Liquid Limit	
Plastic Index	
Linear Shrinkage	

<i>MOD AASHTO ; C.B.R. :</i> <i>TMH1 A7 &amp; A8</i>	
MOD AASHTO (Kg/m <sup>3</sup> )	
O.M.C. (%)	
C.B.R. @ 100% Comp.	
C.B.R. @ 98 % Comp.	
C.B.R. @ 95 % Comp.	
C.B.R. @ 93 % Comp.	
C.B.R. @ 90 % Comp.	
Swell ( max ) %	



Tabulated Summary	Percentage
<b>Gravel :</b> Percentage - 4.75 mm	0
<b>Sand :</b> Percentage - 4.75mm and + 0.075mm	27
<b>Silt :</b> Percentage - 0.075mm and + 0.002mm	63
<b>Clay :</b> Percentage - 0.002mm	10

The above test results are pertinent to the samples received and tested only. For Geoscience:  
While the tests are carried out according to recognized standards Geoscience shall not  
be liable for erroneous testing or reporting thereof. This report may not be reproduced except in full without prior consent of Geoscience.

Remarks:

ConSR22

**CLIENT:** Paterson & Cooke  
P.O Box 23621  
Claremont  
7735

**PROJECT:**

**DATE:**

**ATT:** Brian Zengeni

**REF:**

## ASTM D422 SIEVE ANALYSIS

**DESCRIPTION:**   
**POSITION:** Sample D

**SAMPLE NO.:** 11927  
**CLIENT SAMPLE NO.:**

Sieve Analysis	Sieve Size (mm)	Percent Passing
	75.00	
	63.00	
	53.00	
	37.50	
	26.50	
	19.00	
	13.20	
	9.50	
	6.70	
	4.75	
	2.36	
	2.00	
	1.18	
	0.600	
	0.425	
	0.300	100
	0.150	97
	0.0750	77

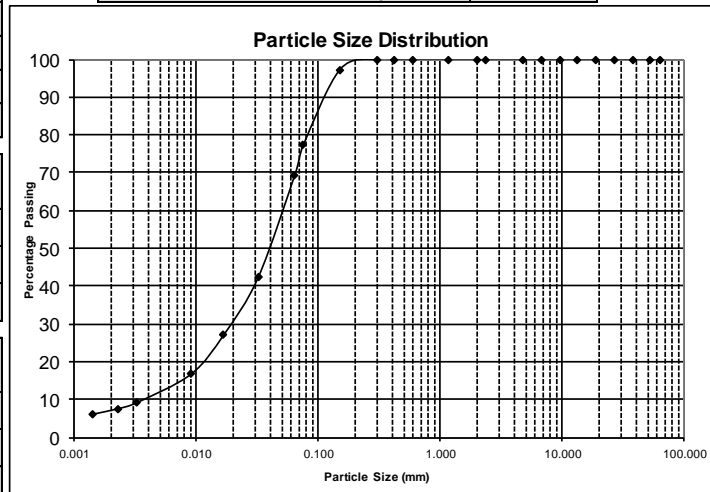
Hydrometer Analysis	
Diameter of particle (mm)	Percentage of soil suspension
0.0596	70
0.0324	42
0.0170	27
0.0091	17
0.0032	9
0.0023	8
0.0014	6

SCS Dispersion Test	
Diameter of particle (mm)	Percentage of soil suspension

<b>Specific Gravity:</b>	2.853
<b>Initial Moisture Content (%):</b>	
<b>pH:</b>	
<b>Conductivity mS/m:</b>	

Atterberg Limits : TMH1 A2, A3 & A4	
Liquid Limit	
Plastic Index	
Linear Shrinkage	

MOD AASHTO ; C.B.R. : TMH1 A7 & A8	
MOD AASHTO (Kg/m <sup>3</sup> )	
O.M.C. (%)	
C.B.R. @ 100% Comp.	
C.B.R. @ 98 % Comp.	
C.B.R. @ 95 % Comp.	
C.B.R. @ 93 % Comp.	
C.B.R. @ 90 % Comp.	
Swell ( max ) %	



Tabulated Summary	Percentage
<b>Gravel</b> : Percentage - 4.75 mm	0
<b>Sand</b> : Percentage - 4.75mm and + 0.075mm	23
<b>Silt</b> : Percentage - 0.075mm and + 0.002mm	69
<b>Clay</b> : Percentage - 0.002mm	8

The above test results are pertinent to the samples received and tested only. For Geoscience:  
While the tests are carried out according to recognized standards Geoscience shall not  
be liable for erroneous testing or reporting thereof. This report may not be reproduced except in full without prior consent of Geoscience.

Remarks:

ConSR22

**CLIENT:** Paterson & Cooke  
 P.O Box 23621  
 Claremont  
 7735

**PROJECT:**

**DATE:**

**ATT:** Brian Zengeni

**REF:**

**ASTM D422 SIEVE ANALYSIS**

**DESCRIPTION:** \_\_\_\_\_  
**POSITION:** Sample E

**SAMPLE NO.:** 11928  
**CLIENT SAMPLE NO.:** \_\_\_\_\_

Sieve Analysis	Percent Passing
75.00	
63.00	
53.00	
37.50	
26.50	
19.00	
13.20	
9.50	
6.70	
4.75	
2.36	
2.00	
1.18	
0.600	
0.425	
0.300	100
0.150	95
0.0750	75

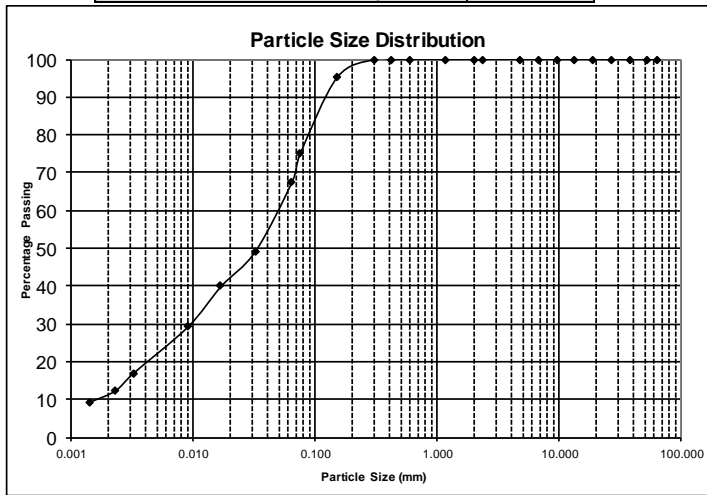
Hydrometer Analysis	
Diameter of particle (mm)	Percentage of soil suspension
0.0605	68
0.0317	49
0.0164	40
0.0088	29
0.0032	17
0.0022	12
0.0014	9

SCS Dispersion Test	
Diameter of particle (mm)	Percentage of soil suspension

<b>Specific Gravity:</b>	2.825
<b>Initial Moisture Content (%):</b>	
<b>pH:</b>	
<b>Conductivity mS/m:</b>	

Atterberg Limits : TMH1 A2, A3 & A4	
Liquid Limit	
Plastic Index	
Linear Shrinkage	

MOD AASHTO ; C.B.R. : TMH1 A7 & A8	
MOD AASHTO (Kg/m <sup>3</sup> )	
O.M.C. (%)	
C.B.R. @ 100% Comp.	
C.B.R. @ 98 % Comp.	
C.B.R. @ 95 % Comp.	
C.B.R. @ 93 % Comp.	
C.B.R. @ 90 % Comp.	
Swell ( max ) %	



Tabulated Summary	Percentage
<b>Gravel :</b> Percentage - 4.75 mm	0
<b>Sand :</b> Percentage - 4.75mm and + 0.075mm	25
<b>Silt :</b> Percentage - 0.075mm and + 0.002mm	60
<b>Clay :</b> Percentage - 0.002mm	15

The above test results are pertinent to the samples received and tested only. For Geoscience:  
 While the tests are carried out according to recognized standards Geoscience shall not  
 be liable for erroneous testing or reporting thereof. This report may not be reproduced except in full without prior consent of Geoscience.

Remarks:

ConSR22

**CLIENT:** Paterson & Cooke  
 P.O Box 23621  
 Claremont  
 7735

**PROJECT:**

**DATE:**

**ATT:** Brian Zengeni

**REF:**

**ASTM D422 SIEVE ANALYSIS**

**DESCRIPTION:** \_\_\_\_\_  
**POSITION:** Sample F

**SAMPLE NO.:** 11929  
**CLIENT SAMPLE NO.:** \_\_\_\_\_

Sieve Analysis	Percent Passing
75.00	
63.00	
53.00	
37.50	
26.50	
19.00	
13.20	
9.50	
6.70	
4.75	
2.36	
2.00	
1.18	
0.600	
0.425	
0.300	100
0.150	95
0.0750	81

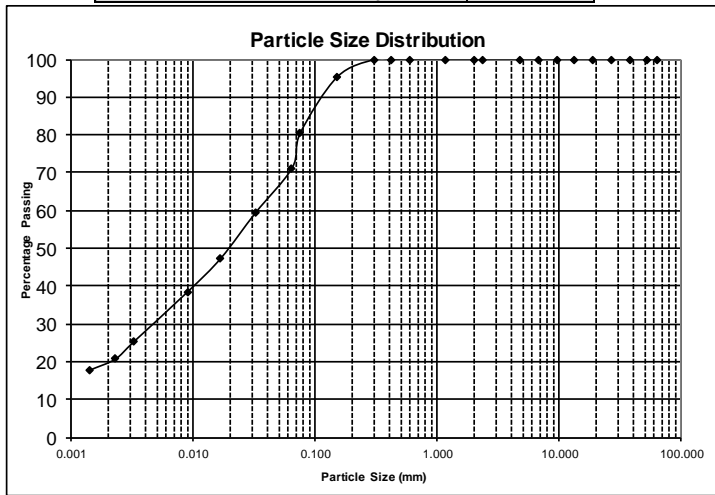
Hydrometer Analysis	
Diameter of particle (mm)	Percentage of soil suspension
0.0576	71
0.0302	59
0.0159	47
0.0085	39
0.0031	25
0.0022	21
0.0013	18

SCS Dispersion Test	
Diameter of particle (mm)	Percentage of soil suspension

<b>Specific Gravity:</b>	2.585
<b>Initial Moisture Content (%):</b>	
<b>pH:</b>	
<b>Conductivity mS/m:</b>	

Atterberg Limits : TMH1 A2, A3 & A4	
Liquid Limit	
Plastic Index	
Linear Shrinkage	

MOD AASHTO ; C.B.R. : TMH1 A7 & A8	
MOD AASHTO (Kg/m <sup>3</sup> )	
O.M.C. (%)	
C.B.R. @ 100% Comp.	
C.B.R. @ 98 % Comp.	
C.B.R. @ 95 % Comp.	
C.B.R. @ 93 % Comp.	
C.B.R. @ 90 % Comp.	
Swell ( max ) %	



Tabulated Summary	Percentage
<b>Gravel</b> : Percentage - 4.75 mm	0
<b>Sand</b> : Percentage - 4.75mm and + 0.075mm	19
<b>Silt</b> : Percentage - 0.075mm and + 0.002mm	58
<b>Clay</b> : Percentage - 0.002mm	23

The above test results are pertinent to the samples received and tested only. For Geoscience:  
 While the tests are carried out according to recognized standards Geoscience shall not  
 be liable for erroneous testing or reporting thereof. This report may not be reproduced except in full without prior consent of Geoscience.

Remarks:

ConSR22

## APPENDIX B : ROTATIONAL VISCOMETER TEST DATA

Rotational Viscometer	Rheolab QC
Measuring System	CC39 and CC35/HR
Test Procedure	ISO 3219
Bob Radius (mm)	17.5
Cup Internal Radius (mm)	21
Bob Height (mm)	52.5

### 1. Sample A

Mass Solids Concentration = 62.4% <i>m</i>				
Meas. Pts.	Speed	Torque	Shear Rate	Shear Stress
	[1/min]	[Nm]	[1/s]	[Pa]
1	271	0.000572	157	4.80
2	254	0.000531	148	4.45
3	236	0.000484	137	4.06
4	219	0.000459	127	3.85
5	201	0.000436	117	3.66
6	184	0.000410	107	3.44
7	166	0.000390	96	3.27
8	149	0.000370	87	3.10
9	131	0.000357	76	2.99
10	114	0.000333	66	2.79
11	96	0.000318	56	2.67
12	79	0.000297	46	2.49
13	61	0.000270	36	2.27
14	44	0.000249	25	2.09
15	26	0.000218	15	1.83
16	9	0.000172	5	1.44

<b>Mass Solids Concentration = 67.1%<i>m</i></b>				
Meas. Pts.	Speed	Torque	Shear Rate	Shear Stress
	[1/min]	[Nm]	[1/s]	[Pa]
1	412	0.001293	239	10.84
2	394	0.001246	229	10.45
3	376	0.001201	218	10.07
4	359	0.001158	208	9.71
5	341	0.001123	198	9.42
6	324	0.001101	188	9.24
7	306	0.001078	178	9.04
8	289	0.001049	168	8.80
9	271	0.001011	157	8.48
10	254	0.000986	148	8.27
11	236	0.000957	137	8.02
12	219	0.000928	127	7.78
13	201	0.000894	117	7.50
14	184	0.000861	107	7.22
15	166	0.000830	96	6.96
16	149	0.000796	87	6.68
17	131	0.000764	76	6.41
18	114	0.000729	66	6.11
19	96	0.000693	56	5.81
20	79	0.000653	46	5.47
21	61	0.000614	36	5.15
22	44	0.000570	25	4.78
23	26	0.000523	15	4.39
24	9	0.000440	5	3.69

<b>Mass Solids Concentration = 70.4%<i>m</i></b>				
Meas. Pts.	Speed	Torque	Shear Rate	Shear Stress
	[1/min]	[Nm]	[1/s]	[Pa]
1	517	0.003097	300	25.97
2	499	0.003024	290	25.36
3	482	0.002955	280	24.78
4	464	0.002877	269	24.13
5	447	0.002808	260	23.55
6	429	0.002746	249	23.03
7	412	0.002676	239	22.44
8	394	0.002602	229	21.82
9	376	0.002545	218	21.34
10	359	0.002471	208	20.72
11	341	0.002410	198	20.21
12	324	0.002345	188	19.67
13	306	0.002296	178	19.26
14	289	0.002231	168	18.71
15	271	0.002176	157	18.25
16	254	0.002124	148	17.81
17	236	0.002054	137	17.23
18	219	0.002001	127	16.78
19	201	0.001933	117	16.21
20	184	0.001867	107	15.66
21	166	0.001801	96	15.10
22	149	0.001735	87	14.55
23	131	0.001666	76	13.97
24	114	0.001590	66	13.33
25	96	0.001525	56	12.79
26	79	0.001442	46	12.09
27	61	0.001355	36	11.36
28	44	0.001276	25	10.70
29	26	0.001160	15	9.73
30	9	0.001091	5	9.15



<b>Mass Solids Concentration = 72.5%<math>\rho</math></b>				
Meas. Pts.	Speed	Torque	Shear Rate	Shear Stress
	[1/min]	[Nm]	[1/s]	[Pa]
1	517	0.005405	300	45.33
2	499	0.005307	290	44.51
3	482	0.005164	280	43.31
4	464	0.005038	269	42.25
5	447	0.004919	260	41.25
6	429	0.004810	249	40.34
7	412	0.004702	239	39.43
8	394	0.004598	229	38.56
9	376	0.004487	218	37.63
10	359	0.004375	208	36.69
11	341	0.004285	198	35.94
12	324	0.004190	188	35.14
13	306	0.004086	178	34.27
14	289	0.003982	168	33.40
15	271	0.003883	157	32.56
16	254	0.003780	148	31.70
17	236	0.003683	137	30.89
18	219	0.003570	127	29.94
19	201	0.003470	117	29.10
20	184	0.003352	107	28.11
21	166	0.003241	96	27.18
22	149	0.003123	87	26.19
23	131	0.003006	76	25.21
24	114	0.002879	66	24.14
25	96	0.002751	56	23.07
26	79	0.002616	46	21.94
27	61	0.002462	36	20.65
28	44	0.002299	25	19.28
29	26	0.002082	15	17.46

<b>Mass Solids Concentration = 73.4%<math>\rho</math></b>				
Meas. Pts.	Speed	Torque	Shear Rate	Shear Stress
	[1/min]	[Nm]	[1/s]	[Pa]
1	517	0.007495	300	62.86
2	499	0.007225	290	60.59
3	482	0.006984	280	58.57
4	464	0.006778	269	56.84
5	447	0.006596	260	55.32
6	429	0.006441	249	54.02
7	412	0.006296	239	52.80
8	394	0.006138	229	51.48
9	376	0.006001	218	50.33
10	359	0.005850	208	49.06
11	341	0.005713	198	47.91
12	324	0.005574	188	46.75
13	306	0.005427	178	45.51
14	289	0.005288	168	44.35
15	271	0.005139	157	43.10
16	254	0.005003	148	41.96
17	236	0.004855	137	40.72
18	219	0.004707	127	39.48
19	201	0.004550	117	38.16
20	184	0.004397	107	36.88
21	166	0.004241	96	35.57
22	149	0.004076	87	34.18
23	131	0.003916	76	32.84
24	114	0.003741	66	31.37
25	96	0.003558	56	29.84
26	79	0.003357	46	28.15
27	61	0.003154	36	26.45
28	44	0.002904	25	24.35

<b>Mass Solids Concentration = 74.4%<i>m</i></b>				
Meas. Pts.	Speed	Torque	Shear Rate	Shear Stress
	[1/min]	[Nm]	[1/s]	[Pa]
1	517	0.009947	300	83.42
2	499	0.009764	290	81.89
3	482	0.009472	280	79.44
4	464	0.009290	269	77.91
5	447	0.009084	260	76.18
6	429	0.008906	249	74.69
7	412	0.008729	239	73.21
8	394	0.008556	229	71.76
9	376	0.008383	218	70.30
10	359	0.008208	208	68.84
11	341	0.008023	198	67.29
12	324	0.007841	188	65.76
13	306	0.007656	178	64.21
14	289	0.007473	168	62.67
15	271	0.007302	157	61.24
16	254	0.007116	148	59.68
17	236	0.006933	137	58.14
18	219	0.006740	127	56.53
19	201	0.006550	117	54.93
20	184	0.006363	107	53.36
21	166	0.006159	96	51.65
22	149	0.005949	87	49.89
23	131	0.005730	76	48.05
24	114	0.005504	66	46.16
25	96	0.005258	56	44.10
26	79	0.004995	46	41.89
27	61	0.004703	36	39.44
28	44	0.004344	25	36.43

<b>Mass Solids Concentration = 75.0%<math>\rho</math></b>				
Meas. Pts.	Speed	Torque	Shear Rate	Shear Stress
	[1/min]	[Nm]	[1/s]	[Pa]
1	517	0.012000	300	100.64
2	499	0.011730	290	98.37
3	482	0.011440	280	95.94
4	464	0.011150	269	93.51
5	447	0.010970	260	92.00
6	429	0.010690	249	89.65
7	412	0.010510	239	88.14
8	394	0.010230	229	85.79
9	376	0.010050	218	84.28
10	359	0.009870	208	82.78
11	341	0.009590	198	80.43
12	324	0.009410	188	78.92
13	306	0.009230	178	77.41
14	289	0.008960	168	75.14
15	271	0.008780	157	73.63
16	254	0.008570	148	71.87
17	236	0.008333	137	69.88
18	219	0.008113	127	68.04
19	201	0.007879	117	66.08
20	184	0.007636	107	64.04
21	166	0.007376	96	61.86
22	149	0.007129	87	59.79
23	131	0.006851	76	57.46
24	114	0.006576	66	55.15
25	96	0.006273	56	52.61
26	79	0.005937	46	49.79
27	61	0.005566	36	46.68
28	44	0.005092	25	42.70

## 2. Sample B

<b>Mass Solids Concentration = 57.5%<i>m</i></b>				
Meas. Pts.	Speed	Torque	Shear Rate	Shear Stress
	[1/min]	[Nm]	[1/s]	[Pa]
1	517	0.001213	300	10.17
2	499	0.001126	290	9.44
3	482	0.001044	280	8.76
4	464	0.000994	269	8.34
5	447	0.000949	260	7.96
6	429	0.000902	249	7.56
7	412	0.000861	239	7.22
8	394	0.000817	229	6.85
9	376	0.000768	218	6.44
10	359	0.000727	208	6.10
11	341	0.000687	198	5.76
12	324	0.000644	188	5.40
13	306	0.000595	178	4.99
14	289	0.000550	168	4.61
15	271	0.000509	157	4.27
16	254	0.000473	148	3.96
17	236	0.000457	137	3.83
18	219	0.000445	127	3.73
19	201	0.000435	117	3.65
20	184	0.000425	107	3.56
21	166	0.000415	96	3.48
22	149	0.000401	87	3.36
23	131	0.000387	76	3.24
24	114	0.000371	66	3.11
25	96	0.000360	56	3.02
26	79	0.000349	46	2.92
27	61	0.000336	36	2.82
28	44	0.000319	25	2.68
29	26	0.000299	15	2.51
30	9	0.000271	5	2.27

<b>Mass Solids Concentration = 64.7%<i>m</i></b>				
Meas. Pts.	Speed	Torque	Shear Rate	Shear Stress
	[1/min]	[Nm]	[1/s]	[Pa]
1	517	0.002136	300	17.91
2	499	0.002096	290	17.58
3	482	0.002060	280	17.28
4	464	0.002033	269	17.05
5	447	0.002003	260	16.80
6	429	0.001960	249	16.44
7	412	0.001930	239	16.19
8	394	0.001892	229	15.87
9	376	0.001868	218	15.67
10	359	0.001832	208	15.36
11	341	0.001799	198	15.09
12	324	0.001775	188	14.89
13	306	0.001733	178	14.53
14	289	0.001707	168	14.32
15	271	0.001684	157	14.12
16	254	0.001644	148	13.79
17	236	0.001611	137	13.51
18	219	0.001585	127	13.29
19	201	0.001547	117	12.97
20	184	0.001511	107	12.67
21	166	0.001488	96	12.48
22	149	0.001454	87	12.19
23	131	0.001418	76	11.89
24	114	0.001384	66	11.61
25	96	0.001348	56	11.31
26	79	0.001313	46	11.01
27	61	0.001271	36	10.66
28	44	0.001238	25	10.38
29	26	0.001181	15	9.90
30	9	0.001091	5	9.15

<b>Mass Solids Concentration = 69.3%<math>\rho</math></b>				
Meas. Pts.	Speed	Torque	Shear Rate	Shear Stress
	[1/min]	[Nm]	[1/s]	[Pa]
1	517	0.005657	300	47.44
2	499	0.005704	290	47.84
3	482	0.005663	280	47.49
4	464	0.005604	269	47.00
5	447	0.005546	260	46.51
6	429	0.005487	249	46.02
7	412	0.005424	239	45.49
8	394	0.005351	229	44.88
9	376	0.005294	218	44.40
10	359	0.005233	208	43.89
11	341	0.005152	198	43.21
12	324	0.005079	188	42.60
13	306	0.005017	178	42.08
14	289	0.004946	168	41.48
15	271	0.004868	157	40.83
16	254	0.004795	148	40.21
17	236	0.004723	137	39.61
18	219	0.004651	127	39.01
19	201	0.004570	117	38.33
20	184	0.004496	107	37.71
21	166	0.004415	96	37.03
22	149	0.004333	87	36.34
23	131	0.004257	76	35.70
24	114	0.004187	66	35.11
25	96	0.004117	56	34.53
26	79	0.004048	46	33.95
27	61	0.003972	36	33.31
28	44	0.003872	25	32.47
29	26	0.003725	15	31.24

<b>Mass Solids Concentration = 71.0%<math>\rho</math></b>				
Meas. Pts.	Speed	Torque	Shear Rate	Shear Stress
	[1/min]	[Nm]	[1/s]	[Pa]
1	517	0.009640	300	80.85
2	499	0.009940	290	83.36
3	482	0.009840	280	82.52
4	464	0.009740	269	81.68
5	447	0.009640	260	80.85
6	429	0.009550	249	80.09
7	412	0.009450	239	79.25
8	394	0.009360	229	78.50
9	376	0.009270	218	77.74
10	359	0.009170	208	76.90
11	341	0.009080	198	76.15
12	324	0.008920	188	74.81
13	306	0.008810	178	73.89
14	289	0.008700	168	72.96
15	271	0.008574	157	71.91
16	254	0.008455	148	70.91
17	236	0.008325	137	69.82
18	219	0.008204	127	68.80
19	201	0.008077	117	67.74
20	184	0.007938	107	66.57
21	166	0.007800	96	65.41
22	149	0.007675	87	64.37
23	131	0.007539	76	63.23
24	114	0.007411	66	62.15
25	96	0.007285	56	61.10
26	79	0.007162	46	60.06
27	61	0.007025	36	58.92
28	44	0.006825	25	57.24



<b>Mass Solids Concentration = 72.0%<math>\rho</math></b>				
Meas. Pts.	Speed	Torque	Shear Rate	Shear Stress
	[1/min]	[Nm]	[1/s]	[Pa]
1	517	0.013900	300	116.57
2	499	0.013980	290	117.24
3	482	0.013980	280	117.24
4	464	0.013880	269	116.40
5	447	0.013680	260	114.73
6	429	0.013580	249	113.89
7	412	0.013490	239	113.13
8	394	0.013300	229	111.54
9	376	0.013210	218	110.79
10	359	0.013020	208	109.19
11	341	0.012930	198	108.44
12	324	0.012740	188	106.84
13	306	0.012550	178	105.25
14	289	0.012460	168	104.50
15	271	0.012270	157	102.90
16	254	0.012090	148	101.39
17	236	0.011900	137	99.80
18	219	0.011720	127	98.29
19	201	0.011540	117	96.78
20	184	0.011360	107	95.27
21	166	0.011180	96	93.76
22	149	0.011000	87	92.25
23	131	0.010820	76	90.74
24	114	0.010640	66	89.23
25	96	0.010470	56	87.81
26	79	0.010190	46	85.46
27	61	0.009930	36	83.28

<b>Mass Solids Concentration = 72.7%<math>\rho</math></b>				
Meas. Pts.	Speed	Torque	Shear Rate	Shear Stress
	[1/min]	[Nm]	[1/s]	[Pa]
1	517	0.018660	300	156.49
2	499	0.019050	290	159.76
3	482	0.019040	280	159.68
4	464	0.018950	269	158.92
5	447	0.018760	260	157.33
6	429	0.018670	249	156.58
7	412	0.018480	239	154.98
8	394	0.018290	229	153.39
9	376	0.018200	218	152.63
10	359	0.018000	208	150.96
11	341	0.017720	198	148.61
12	324	0.017540	188	147.10
13	306	0.017340	178	145.42
14	289	0.017160	168	143.91
15	271	0.016870	157	141.48
16	254	0.016690	148	139.97
17	236	0.016410	137	137.62
18	219	0.016220	127	136.03
19	201	0.015940	117	133.68
20	184	0.015760	107	132.17
21	166	0.015480	96	129.82
22	149	0.015210	87	127.56
23	131	0.014930	76	125.21
24	114	0.014650	66	122.86
25	96	0.014390	56	120.68
26	79	0.014030	46	117.66

### 3. Sample C

<b>Mass Solids Concentration = 51.7%<i>m</i></b>				
Meas. Pts.	Speed	Torque	Shear Rate	Shear Stress
	[1/min]	[Nm]	[1/s]	[Pa]
1	271	0.000513	157	4.30
2	254	0.000513	148	4.30
3	236	0.000507	137	4.25
4	219	0.000503	127	4.22
5	201	0.000498	117	4.18
6	184	0.000489	107	4.10
7	166	0.000480	96	4.03
8	149	0.000474	87	3.97
9	131	0.000471	76	3.95
10	114	0.000464	66	3.89
11	96	0.000457	56	3.84
12	79	0.000447	46	3.75
13	61	0.000433	36	3.63
14	44	0.000426	25	3.57
15	26	0.000419	15	3.52
16	9	0.000406	5	3.41

<b>Mass Solids Concentration = 59.5%<i>m</i></b>				
Meas. Pts.	Speed	Torque	Shear Rate	Shear Stress
	[1/min]	[Nm]	[1/s]	[Pa]
1	411	0.001799	239	15.09
2	394	0.001788	229	15.00
3	376	0.001767	218	14.82
4	359	0.001754	208	14.71
5	341	0.001734	198	14.54
6	324	0.001717	188	14.40
7	306	0.001707	178	14.32
8	289	0.001683	168	14.11
9	271	0.001671	157	14.01
10	254	0.001660	148	13.92
11	236	0.001658	137	13.90
12	219	0.001654	127	13.87
13	201	0.001645	117	13.80
14	184	0.001625	107	13.63
15	166	0.001615	96	13.54
16	149	0.001582	87	13.27
17	131	0.001547	76	12.97
18	114	0.001525	66	12.79
19	96	0.001531	56	12.84
20	79	0.001526	46	12.80
21	61	0.001517	36	12.72
22	44	0.001504	25	12.61
23	26	0.001499	15	12.57
24	9	0.001470	5	12.33

<b>Mass Solids Concentration = 62.6%<math>\rho</math></b>				
Meas. Pts.	Speed	Torque	Shear Rate	Shear Stress
	[1/min]	[Nm]	[1/s]	[Pa]
1	517	0.003372	300	28.28
2	499	0.003359	290	28.17
3	482	0.003330	280	27.93
4	464	0.003300	269	27.68
5	447	0.003282	260	27.52
6	429	0.003250	249	27.26
7	412	0.003222	239	27.02
8	394	0.003184	229	26.70
9	376	0.003135	218	26.29
10	359	0.003113	208	26.11
11	341	0.003100	198	26.00
12	324	0.003077	188	25.81
13	306	0.003042	178	25.51
14	289	0.003033	168	25.44
15	271	0.003025	157	25.37
16	254	0.003031	148	25.42
17	236	0.003023	137	25.35
18	219	0.002991	127	25.08
19	201	0.002973	117	24.93
20	184	0.002967	107	24.88
21	166	0.002957	96	24.80
22	149	0.002932	87	24.59
23	131	0.002848	76	23.88
24	114	0.002848	66	23.88
25	96	0.002889	56	24.23
26	79	0.002847	46	23.88
27	61	0.002846	36	23.87
28	44	0.002874	25	24.10
29	26	0.002859	15	23.98
30	9	0.002758	5	23.13

<b>Mass Solids Concentration = 64.2%<math>\rho</math></b>				
Meas. Pts.	Speed	Torque	Shear Rate	Shear Stress
	[1/min]	[Nm]	[1/s]	[Pa]
1	517	0.004834	300	40.54
2	499	0.004838	290	40.57
3	482	0.004784	280	40.12
4	464	0.004734	269	39.70
5	447	0.004687	260	39.31
6	429	0.004653	249	39.02
7	412	0.004607	239	38.64
8	394	0.004538	229	38.06
9	376	0.004469	218	37.48
10	359	0.004422	208	37.09
11	341	0.004405	198	36.94
12	324	0.004366	188	36.62
13	306	0.004317	178	36.20
14	289	0.004277	168	35.87
15	271	0.004272	157	35.83
16	254	0.004309	148	36.14
17	236	0.004317	137	36.20
18	219	0.004248	127	35.63
19	201	0.004204	117	35.26
20	184	0.004216	107	35.36
21	166	0.004211	96	35.32
22	149	0.004168	87	34.96
23	131	0.004113	76	34.49
24	114	0.004115	66	34.51
25	96	0.004126	56	34.60
26	79	0.004119	46	34.54
27	61	0.004133	36	34.66
28	44	0.004157	25	34.86
29	26	0.004120	15	34.55
30	9	0.003911	5	32.80

<b>Mass Solids Concentration = 65.2%<math>\rho</math></b>				
Meas. Pts.	Speed	Torque	Shear Rate	Shear Stress
	[1/min]	[Nm]	[1/s]	[Pa]
1	517	0.005827	300	48.87
2	499	0.005910	290	49.56
3	482	0.005855	280	49.10
4	464	0.005796	269	48.61
5	447	0.005729	260	48.05
6	429	0.005678	249	47.62
7	412	0.005620	239	47.13
8	394	0.005550	229	46.55
9	376	0.005536	218	46.43
10	359	0.005502	208	46.14
11	341	0.005413	198	45.40
12	324	0.005369	188	45.03
13	306	0.005387	178	45.18
14	289	0.005408	168	45.35
15	271	0.005399	157	45.28
16	254	0.005338	148	44.77
17	236	0.005257	137	44.09
18	219	0.005260	127	44.11
19	201	0.005329	117	44.69
20	184	0.005249	107	44.02
21	166	0.005138	96	43.09
22	149	0.005209	87	43.69
23	131	0.005308	76	44.52
24	114	0.005086	66	42.65
25	96	0.005138	56	43.09
26	79	0.005269	46	44.19
27	61	0.005257	36	44.09
28	44	0.005260	25	44.11
29	26	0.005215	15	43.74

<b>Mass Solids Concentration = 66.0%<math>\rho</math></b>				
Meas. Pts.	Speed	Torque	Shear Rate	Shear Stress
	[1/min]	[Nm]	[1/s]	[Pa]
1	517	0.007231	300	60.64
2	499	0.007073	290	59.32
3	482	0.006996	280	58.67
4	464	0.006905	269	57.91
5	447	0.006842	260	57.38
6	429	0.006790	249	56.94
7	412	0.006738	239	56.51
8	394	0.006652	229	55.79
9	376	0.006567	218	55.07
10	359	0.006503	208	54.54
11	341	0.006445	198	54.05
12	324	0.006442	188	54.03
13	306	0.006423	178	53.87
14	289	0.006379	168	53.50
15	271	0.006375	157	53.46
16	254	0.006399	148	53.67
17	236	0.006357	137	53.31
18	219	0.006323	127	53.03
19	201	0.006314	117	52.95
20	184	0.006231	107	52.26
21	166	0.006218	96	52.15
22	149	0.006305	87	52.88
23	131	0.006142	76	51.51
24	114	0.006094	66	51.11
25	96	0.006251	56	52.42
26	79	0.006141	46	51.50
27	61	0.006081	36	51.00
28	44	0.006194	25	51.95
29	26	0.006122	15	51.34

<b>Mass Solids Concentration = 68.0%<math>\rho</math></b>				
Meas. Pts.	Speed	Torque	Shear Rate	Shear Stress
	[1/min]	[Nm]	[1/s]	[Pa]
1	517	0.012660	300	106.17
2	499	0.012590	290	105.59
3	482	0.012500	280	104.83
4	464	0.012400	269	103.99
5	447	0.012300	260	103.15
6	429	0.012200	249	102.32
7	412	0.012060	239	101.14
8	394	0.011960	229	100.30
9	376	0.012000	218	100.64
10	359	0.011910	208	99.88
11	341	0.011790	198	98.88
12	324	0.011850	188	99.38
13	306	0.011900	178	99.80
14	289	0.011810	168	99.04
15	271	0.011660	157	97.79
16	254	0.011890	148	99.72
17	236	0.011790	137	98.88
18	219	0.011820	127	99.13
19	201	0.011760	117	98.63
20	184	0.011610	107	97.37
21	166	0.011480	96	96.28
22	149	0.011430	87	95.86
23	131	0.011570	76	97.03
24	114	0.011350	66	95.19
25	96	0.011280	56	94.60
26	79	0.011420	46	95.77
27	61	0.011410	36	95.69
28	44	0.011260	25	94.43
29	26	0.010850	15	90.99



<b>Mass Solids Concentration = 69.6%<math>\rho</math></b>				
Meas. Pts.	Speed	Torque	Shear Rate	Shear Stress
	[1/min]	[Nm]	[1/s]	[Pa]
1	517	0.020590	300	172.89
2	499	0.020580	290	172.68
3	482	0.020750	280	172.59
4	464	0.020490	269	171.84
5	447	0.020380	260	170.92
6	429	0.020220	249	169.58
7	412	0.019980	239	167.56
8	394	0.019840	229	166.39
9	376	0.019790	218	165.97
10	359	0.019440	208	163.03
11	341	0.019420	198	162.87
12	324	0.019400	188	162.70
13	306	0.019230	178	161.27
14	289	0.019120	168	160.35
15	271	0.019190	157	160.94
16	254	0.019100	148	160.18
17	236	0.018710	137	156.91
18	219	0.018570	127	155.74
19	201	0.018520	117	155.32
20	184	0.018290	107	153.39
21	166	0.018250	96	153.05
22	149	0.018080	87	151.63
23	131	0.018160	76	152.30
24	114	0.017880	66	149.95
25	96	0.017720	56	148.61
26	79	0.017720	46	148.61
27	61	0.017620	36	147.77
28	44	0.017190	25	144.16

#### 4. Sample D

<b>Mass Solids Concentration = 49.3%<i>m</i></b>				
Meas. Pts.	Speed	Torque	Shear Rate	Shear Stress
	[1/min]	[Nm]	[1/s]	[Pa]
1	26	0.000462	15	3.88
2	44	0.000497	26	4.17
3	61	0.000520	36	4.36
4	79	0.000537	46	4.50
5	96	0.000555	57	4.65
6	114	0.000571	67	4.79
7	131	0.000592	77	4.96
8	149	0.000605	88	5.08
9	166	0.000618	98	5.18
10	184	0.000633	109	5.30
11	201	0.000648	119	5.43
12	219	0.000662	130	5.56
13	236	0.000676	139	5.67
14	254	0.000684	150	5.73
15	271	0.000692	160	5.80
16	289	0.000709	171	5.95
17	306	0.000728	181	6.11

<b>Mass Solids Concentration = 52.5%<i>m</i></b>				
Meas. Pts.	Speed	Torque	Shear Rate	Shear Stress
	[1/min]	[Nm]	[1/s]	[Pa]
1	26.1	0.000747	15	6.26
2	43.7	0.000802	26	6.72
3	61.2	0.000830	36	6.96
4	78.7	0.000865	46	7.26
5	96.2	0.000890	57	7.46
6	114	0.000916	67	7.68
7	131	0.000942	77	7.90
8	149	0.000958	88	8.03
9	166	0.000976	98	8.18
10	184	0.001008	109	8.45
11	201	0.001023	119	8.58
12	219	0.001052	130	8.82
13	236	0.001069	139	8.97
14	254	0.001084	150	9.09
15	271	0.001099	160	9.21
16	289	0.001114	171	9.34
17	306	0.001132	181	9.49

<b>Mass Solids Concentration = 54.2%<math>\rho</math>m</b>				
Meas. Pts.	Speed	Torque	Shear Rate	Shear Stress
	[1/min]	[Nm]	[1/s]	[Pa]
1	26	0.000988	15	8.29
2	44	0.001034	26	8.67
3	61	0.001083	36	9.08
4	79	0.001110	46	9.31
5	96	0.001150	57	9.64
6	114	0.001180	67	9.89
7	131	0.001208	77	10.13
8	149	0.001228	88	10.30
9	166	0.001258	98	10.55
10	184	0.001285	109	10.78
11	201	0.001316	119	11.04
12	219	0.001335	130	11.20
13	236	0.001360	139	11.41
14	254	0.001377	150	11.55
15	271	0.001402	160	11.76
16	289	0.001421	171	11.91

<b>Mass Solids Concentration = 55.0%<math>\rho</math>m</b>				
Meas. Pts.	Speed	Torque	Shear Rate	Shear Stress
	[1/min]	[Nm]	[1/s]	[Pa]
1	26	0.001149	15	9.63
2	44	0.001200	26	10.06
3	61	0.001247	36	10.46
4	79	0.001273	46	10.67
5	96	0.001312	57	11.00
6	114	0.001338	67	11.22
7	131	0.001367	77	11.46
8	149	0.001394	88	11.69
9	166	0.001413	98	11.85
10	184	0.001441	109	12.08
11	201	0.001467	119	12.30
12	219	0.001502	130	12.60
13	236	0.001519	139	12.74
14	254	0.001543	150	12.94
15	271	0.001570	160	13.17
16	289	0.001589	171	13.33
17	306	0.001604	181	13.45

<b>Mass Solids Concentration = 55.6%<math>\rho</math>m</b>				
Meas. Pts.	Speed	Torque	Shear Rate	Shear Stress
	[1/min]	[Nm]	[1/s]	[Pa]
1	26	0.001411	15	11.83
2	44	0.001482	26	12.43
3	61	0.001528	36	12.81
4	79	0.001564	46	13.12
5	96	0.001612	57	13.52
6	114	0.001649	67	13.83
7	131	0.001688	77	14.16
8	149	0.001717	88	14.40
9	166	0.001754	98	14.71
10	184	0.001792	109	15.03
11	201	0.001817	119	15.24
12	219	0.001855	130	15.56
13	236	0.001882	139	15.78
14	254	0.001919	150	16.09
15	271	0.001953	160	16.38
16	289	0.001979	171	16.60
17	306	0.002003	181	16.80

<b>Mass Solids Concentration = 56.1%<math>\rho</math>m</b>				
Meas. Pts.	Speed	Torque	Shear Rate	Shear Stress
	[1/min]	[Nm]	[1/s]	[Pa]
1	26	0.001619	15	13.58
2	44	0.001701	26	14.27
3	61	0.001766	36	14.81
4	79	0.001812	46	15.20
5	96	0.001867	57	15.66
6	114	0.001914	67	16.05
7	131	0.001954	77	16.39
8	149	0.001992	88	16.71
9	166	0.002031	98	17.03
10	184	0.002068	109	17.34
11	201	0.002116	119	17.75
12	219	0.002150	130	18.03
13	236	0.002172	139	18.22
14	254	0.002204	150	18.48
15	271	0.002229	160	18.69
16	289	0.002251	171	18.88
17	306	0.002275	181	19.08
18	324	0.002300	191	19.29
19	341	0.002311	202	19.38

<b>Mass Solids Concentration = 58.0%<i>m</i></b>				
Meas. Pts.	Speed	Torque	Shear Rate	Shear Stress
	[1/min]	[Nm]	[1/s]	[Pa]
1	26	0.002539	15	21.29
2	44	0.002664	26	22.34
3	61	0.002755	36	23.11
4	79	0.002826	46	23.70
5	96	0.002895	57	24.28
6	114	0.002968	67	24.89
7	131	0.003028	77	25.39
8	149	0.003086	88	25.88
9	166	0.003138	98	26.32
10	184	0.003190	109	26.75
11	201	0.003250	119	27.26
12	219	0.003300	130	27.67
13	236	0.003351	139	28.10
14	254	0.003390	150	28.43
15	271	0.003441	160	28.86
16	289	0.003478	171	29.16
17	306	0.003528	181	29.59
18	324	0.003564	191	29.89
19	341	0.003598	202	30.17
20	359	0.003635	212	30.48
21	376	0.003674	222	30.81
22	394	0.003701	233	31.04

<b>Mass Solids Concentration = 62.1%<i>m</i></b>				
Meas. Pts.	Speed	Torque	Shear Rate	Shear Stress
	[1/min]	[Nm]	[1/s]	[Pa]
1	26	0.006017	15	50.46
2	44	0.006262	26	52.52
3	61	0.006110	36	51.24
4	79	0.006103	46	51.18
5	96	0.006147	57	51.55
6	114	0.006120	67	51.33
7	131	0.006216	77	52.13
8	149	0.006245	88	52.37
9	166	0.006323	98	53.03
10	184	0.006402	109	53.69
11	201	0.006481	119	54.35
12	219	0.006579	130	55.17
13	236	0.006679	139	56.01
14	254	0.006772	150	56.79
15	271	0.006874	160	57.65
16	289	0.006948	171	58.27
17	306	0.007027	181	58.93
18	324	0.007112	191	59.64
19	341	0.007179	202	60.21
20	359	0.007272	212	60.99
21	376	0.007333	222	61.50
22	394	0.007417	233	62.20
23	412	0.007476	243	62.70
24	429	0.007553	253	63.34
25	447	0.007631	264	64.00
26	464	0.007703	274	64.60
27	482	0.007770	285	65.16
28	499	0.007840	295	65.75

## 5. Sample E

<b>Mass Solids Concentration = 49.3%<i>m</i></b>				
Meas. Pts.	Speed	Torque	Shear Rate	Shear Stress
	[1/min]	[Nm]	[1/s]	[Pa]
1	26	0.000462	15	3.88
2	44	0.000497	26	4.17
3	61	0.000520	36	4.36
4	79	0.000537	46	4.50
5	96	0.000555	57	4.65
6	114	0.000571	67	4.79
7	131	0.000592	77	4.96
8	149	0.000605	88	5.08
9	166	0.000618	98	5.18
10	184	0.000633	109	5.30
11	201	0.000648	119	5.43
12	219	0.000662	130	5.56
13	236	0.000676	139	5.67
14	254	0.000684	150	5.73
15	271	0.000692	160	5.80
16	289	0.000709	171	5.95
17	306	0.000728	181	6.11

<b>Mass Solids Concentration = 52.5%<i>m</i></b>				
Meas. Pts.	Speed	Torque	Shear Rate	Shear Stress
	[1/min]	[Nm]	[1/s]	[Pa]
1	26.1	0.000747	15	6.26
2	43.7	0.000802	26	6.72
3	61.2	0.000830	36	6.96
4	78.7	0.000865	46	7.26
5	96.2	0.000890	57	7.46
6	114	0.000916	67	7.68
7	131	0.000942	77	7.90
8	149	0.000958	88	8.03
9	166	0.000976	98	8.18
10	184	0.001008	109	8.45
11	201	0.001023	119	8.58
12	219	0.001052	130	8.82
13	236	0.001069	139	8.97
14	254	0.001084	150	9.09
15	271	0.001099	160	9.21
16	289	0.001114	171	9.34
17	306	0.001132	181	9.49

<b>Mass Solids Concentration = 54.2%<math>\rho</math></b>				
Meas. Pts.	Speed	Torque	Shear Rate	Shear Stress
	[1/min]	[Nm]	[1/s]	[Pa]
1	26	0.000988	15	8.29
2	44	0.001034	26	8.67
3	61	0.001083	36	9.08
4	79	0.001110	46	9.31
5	96	0.001150	57	9.64
6	114	0.001180	67	9.89
7	131	0.001208	77	10.13
8	149	0.001228	88	10.30
9	166	0.001258	98	10.55
10	184	0.001285	109	10.78
11	201	0.001316	119	11.04
12	219	0.001335	130	11.20
13	236	0.001360	139	11.41
14	254	0.001377	150	11.55
15	271	0.001402	160	11.76
16	289	0.001421	171	11.91

<b>Mass Solids Concentration = 55.0%<math>\rho</math></b>				
Meas. Pts.	Speed	Torque	Shear Rate	Shear Stress
	[1/min]	[Nm]	[1/s]	[Pa]
1	26	0.001149	15	9.63
2	44	0.001200	26	10.06
3	61	0.001247	36	10.46
4	79	0.001273	46	10.67
5	96	0.001312	57	11.00
6	114	0.001338	67	11.22
7	131	0.001367	77	11.46
8	149	0.001394	88	11.69
9	166	0.001413	98	11.85
10	184	0.001441	109	12.08
11	201	0.001467	119	12.30
12	219	0.001502	130	12.60
13	236	0.001519	139	12.74
14	254	0.001543	150	12.94
15	271	0.001570	160	13.17
16	289	0.001589	171	13.33
17	306	0.001604	181	13.45



<b>Mass Solids Concentration = 55.6%<math>\rho</math>m</b>				
Meas. Pts.	Speed	Torque	Shear Rate	Shear Stress
	[1/min]	[Nm]	[1/s]	[Pa]
1	26	0.001411	15	11.83
2	44	0.001482	26	12.43
3	61	0.001528	36	12.81
4	79	0.001564	46	13.12
5	96	0.001612	57	13.52
6	114	0.001649	67	13.83
7	131	0.001688	77	14.16
8	149	0.001717	88	14.40
9	166	0.001754	98	14.71
10	184	0.001792	109	15.03
11	201	0.001817	119	15.24
12	219	0.001855	130	15.56
13	236	0.001882	139	15.78
14	254	0.001919	150	16.09
15	271	0.001953	160	16.38
16	289	0.001979	171	16.60
17	306	0.002003	181	16.80

<b>Mass Solids Concentration = 56.1%<math>\rho</math>m</b>				
Meas. Pts.	Speed	Torque	Shear Rate	Shear Stress
	[1/min]	[Nm]	[1/s]	[Pa]
1	26	0.001619	15	13.58
2	44	0.001701	26	14.27
3	61	0.001766	36	14.81
4	79	0.001812	46	15.20
5	96	0.001867	57	15.66
6	114	0.001914	67	16.05
7	131	0.001954	77	16.39
8	149	0.001992	88	16.71
9	166	0.002031	98	17.03
10	184	0.002068	109	17.34
11	201	0.002116	119	17.75
12	219	0.002150	130	18.03
13	236	0.002172	139	18.22
14	254	0.002204	150	18.48
15	271	0.002229	160	18.69
16	289	0.002251	171	18.88
17	306	0.002275	181	19.08
18	324	0.002300	191	19.29
19	341	0.002311	202	19.38

<b>Mass Solids Concentration = 58.0%<i>m</i></b>				
Meas. Pts.	Speed	Torque	Shear Rate	Shear Stress
	[1/min]	[Nm]	[1/s]	[Pa]
1	26	0.002539	15	21.29
2	44	0.002664	26	22.34
3	61	0.002755	36	23.11
4	79	0.002826	46	23.70
5	96	0.002895	57	24.28
6	114	0.002968	67	24.89
7	131	0.003028	77	25.39
8	149	0.003086	88	25.88
9	166	0.003138	98	26.32
10	184	0.003190	109	26.75
11	201	0.003250	119	27.26
12	219	0.003300	130	27.67
13	236	0.003351	139	28.10
14	254	0.003390	150	28.43
15	271	0.003441	160	28.86
16	289	0.003478	171	29.16
17	306	0.003528	181	29.59
18	324	0.003564	191	29.89
19	341	0.003598	202	30.17
20	359	0.003635	212	30.48
21	376	0.003674	222	30.81
22	394	0.003701	233	31.04

<b>Mass Solids Concentration = 62.1%<i>m</i></b>				
Meas. Pts.	Speed	Torque	Shear Rate	Shear Stress
	[1/min]	[Nm]	[1/s]	[Pa]
1	26	0.006017	15	50.46
2	44	0.006262	26	52.52
3	61	0.006110	36	51.24
4	79	0.006103	46	51.18
5	96	0.006147	57	51.55
6	114	0.006120	67	51.33
7	131	0.006216	77	52.13
8	149	0.006245	88	52.37
9	166	0.006323	98	53.03
10	184	0.006402	109	53.69
11	201	0.006481	119	54.35
12	219	0.006579	130	55.17
13	236	0.006679	139	56.01
14	254	0.006772	150	56.79
15	271	0.006874	160	57.65
16	289	0.006948	171	58.27
17	306	0.007027	181	58.93
18	324	0.007112	191	59.64
19	341	0.007179	202	60.21
20	359	0.007272	212	60.99
21	376	0.007333	222	61.50
22	394	0.007417	233	62.20
23	412	0.007476	243	62.70
24	429	0.007553	253	63.34
25	447	0.007631	264	64.00
26	464	0.007703	274	64.60
27	482	0.007770	285	65.16
28	499	0.007840	295	65.75

## 6. Sample F

<b>Mass Solids Concentration = 46.6%<i>m</i></b>				
Meas. Pts.	Speed	Torque	Shear Rate	Shear Stress
	[1/min]	[Nm]	[1/s]	[Pa]
1	44	0.002038	26	17.09
2	62	0.002108	36	17.68
3	80	0.002175	46	18.24
4	98	0.002233	57	18.73
5	116	0.002280	67	19.12
6	133	0.002325	77	19.50
7	151	0.002362	88	19.81
8	169	0.002398	98	20.11
9	187	0.002444	109	20.50
10	205	0.002471	119	20.72
11	223	0.002509	130	21.04
12	240	0.002536	139	21.27
13	258	0.002569	150	21.54
14	276	0.002595	160	21.76
15	294	0.002626	171	22.02
16	312	0.002650	181	22.22
17	329	0.002676	191	22.44
18	347	0.002710	202	22.73
19	365	0.002720	212	22.81
20	383	0.002745	222	23.02
21	401	0.002759	233	23.14
22	419	0.002773	243	23.26
23	436	0.002789	253	23.39
24	454	0.002811	264	23.57
25	472	0.002828	274	23.72
26	490	0.002843	285	23.84
27	508	0.002854	295	23.94

<b>Mass Solids Concentration = 48.6%<math>\rho</math></b>				
Meas. Pts.	Speed	Torque	Shear Rate	Shear Stress
	[1/min]	[Nm]	[1/s]	[Pa]
1	44	0.002576	26	21.60
2	62	0.002681	36	22.48
3	80	0.002766	46	23.20
4	98	0.002841	57	23.83
5	116	0.002906	67	24.37
6	133	0.002961	77	24.83
7	151	0.003016	88	25.30
8	169	0.003061	98	25.67
9	187	0.003106	109	26.05
10	205	0.003161	119	26.51
11	223	0.003196	130	26.81
12	240	0.003242	139	27.19
13	258	0.003277	150	27.48
14	276	0.003312	160	27.77
15	294	0.003347	171	28.07
16	312	0.003372	181	28.28
17	329	0.003407	191	28.57
18	347	0.003432	202	28.78
19	365	0.003467	212	29.08
20	383	0.003492	222	29.29
21	401	0.003517	233	29.50
22	419	0.003532	243	29.62
23	436	0.003558	253	29.84
24	454	0.003573	264	29.96
25	472	0.003598	274	30.17
26	490	0.003613	285	30.30
27	508	0.003628	295	30.42

<b>Mass Solids Concentration = 49.3%<math>\rho</math></b>				
Meas. Pts.	Speed	Torque	Shear Rate	Shear Stress
	[1/min]	[Nm]	[1/s]	[Pa]
1	44	0.002909	26	24.40
2	62	0.003034	36	25.44
3	80	0.003129	46	26.24
4	98	0.003214	57	26.95
5	116	0.003288	67	27.58
6	133	0.003353	77	28.12
7	151	0.003418	88	28.67
8	169	0.003473	98	29.13
9	187	0.003528	109	29.58
10	205	0.003582	119	30.04
11	223	0.003637	130	30.50
12	240	0.003682	139	30.88
13	258	0.003727	150	31.26
14	276	0.003762	160	31.55
15	294	0.003797	171	31.84
16	312	0.003831	181	32.13
17	329	0.003876	191	32.51
18	347	0.003911	202	32.80
19	365	0.003946	212	33.09
20	383	0.003971	222	33.30
21	401	0.004005	233	33.59
22	419	0.004030	243	33.80
23	436	0.004065	253	34.09
24	454	0.004100	264	34.39
25	472	0.004125	274	34.59
26	490	0.004150	285	34.80
27	508	0.004154	295	34.84

<b>Mass Solids Concentration = 50.2%<math>\rho</math></b>				
Meas. Pts.	Speed	Torque	Shear Rate	Shear Stress
	[1/min]	[Nm]	[1/s]	[Pa]
1	44	0.003434	26	28.80
2	62	0.003559	36	29.85
3	80	0.003655	46	30.65
4	98	0.003748	57	31.43
5	116	0.003828	67	32.10
6	133	0.003899	77	32.70
7	151	0.003958	88	33.19
8	169	0.004021	98	33.72
9	187	0.004084	109	34.25
10	205	0.004150	119	34.80
11	223	0.004203	130	35.25
12	240	0.004261	139	35.73
13	258	0.004318	150	36.21
14	276	0.004373	160	36.67
15	294	0.004409	171	36.98
16	312	0.004454	181	37.35
17	329	0.004488	191	37.64
18	347	0.004530	202	37.99
19	365	0.004574	212	38.36
20	383	0.004609	222	38.65
21	401	0.004642	233	38.93
22	419	0.004675	243	39.21
23	436	0.004703	253	39.44
24	454	0.004734	264	39.70
25	472	0.004757	274	39.89
26	490	0.004786	285	40.14
27	508	0.004814	295	40.37

<b>Mass Solids Concentration = 51.9%<math>\rho</math></b>				
Meas. Pts.	Speed	Torque	Shear Rate	Shear Stress
	[1/min]	[Nm]	[1/s]	[Pa]
1	44	0.004510	26	37.83
2	62	0.004684	36	39.29
3	80	0.004828	46	40.49
4	98	0.004952	57	41.53
5	116	0.005066	67	42.49
6	133	0.005170	77	43.36
7	151	0.005274	88	44.23
8	169	0.005358	98	44.93
9	187	0.005442	109	45.64
10	205	0.005526	119	46.34
11	223	0.005600	130	46.96
12	240	0.005674	139	47.58
13	258	0.005748	150	48.20
14	276	0.005812	160	48.74
15	294	0.005875	171	49.27
16	312	0.005929	181	49.73
17	329	0.005983	191	50.18
18	347	0.006037	202	50.63
19	365	0.006091	212	51.08
20	383	0.006145	222	51.54
21	401	0.006199	233	51.99
22	419	0.006253	243	52.44
23	436	0.006297	253	52.81
24	454	0.006341	264	53.18
25	472	0.006375	274	53.46
26	490	0.006419	285	53.83
27	508	0.006443	295	54.03




<b>Mass Solids Concentration = 53.3%<math>\rho</math></b>				
Meas. Pts.	Speed	Torque	Shear Rate	Shear Stress
	[1/min]	[Nm]	[1/s]	[Pa]
1	44	0.006075	26	50.94
2	62	0.006368	36	53.40
3	80	0.006581	46	55.19
4	98	0.006764	57	56.73
5	116	0.006908	67	57.93
6	133	0.007041	77	59.05
7	151	0.007144	88	59.92
8	169	0.007248	98	60.78
9	187	0.007351	109	61.65
10	205	0.007444	119	62.43
11	223	0.007527	130	63.13
12	240	0.007621	139	63.91
13	258	0.007714	150	64.69
14	276	0.007797	160	65.39
15	294	0.007880	171	66.09
16	312	0.007954	181	66.70
17	329	0.008037	191	67.40
18	347	0.008110	202	68.02
19	365	0.008184	212	68.63
20	383	0.008247	222	69.16
21	401	0.008330	233	69.86
22	419	0.008403	243	70.47
23	436	0.008477	253	71.09
24	454	0.008540	264	71.62
25	472	0.008603	274	72.15
26	490	0.008657	285	72.60
27	508	0.008700	295	72.96

<b>Mass Solids Concentration = 54.1%<math>\rho</math></b>				
Meas. Pts.	Speed	Torque	Shear Rate	Shear Stress
	[1/min]	[Nm]	[1/s]	[Pa]
1	44	0.006963	26	58.39
2	62	0.007186	36	60.26
3	80	0.007479	46	62.72
4	98	0.007772	57	65.18
5	116	0.007955	67	66.71
6	133	0.008108	77	68.00
7	151	0.008241	88	69.11
8	169	0.008364	98	70.14
9	187	0.008476	109	71.09
10	205	0.008579	119	71.95
11	223	0.008672	130	72.73
12	240	0.008775	139	73.59
13	258	0.008878	150	74.46
14	276	0.009001	160	75.49
15	294	0.009094	171	76.27
16	312	0.009187	181	77.05
17	329	0.009280	191	77.83
18	347	0.009373	202	78.61
19	365	0.009366	212	78.55
20	383	0.009459	222	79.32
21	401	0.009551	233	80.10
22	419	0.009644	243	80.88
23	436	0.009738	253	81.66
24	454	0.009830	264	82.44
25	472	0.009923	274	83.22
26	490	0.010016	285	84.00
27	508	0.010009	295	83.94

<b>Mass Solids Concentration = 55.4%<math>\rho</math></b>				
Meas. Pts.	Speed	Torque	Shear Rate	Shear Stress
	[1/min]	[Nm]	[1/s]	[Pa]
1	44	0.008900	26	74.64
2	62	0.009350	36	78.41
3	80	0.009710	46	81.43
4	98	0.010080	57	84.54
5	116	0.010250	67	85.96
6	133	0.010430	77	87.47
7	151	0.010610	88	88.98
8	169	0.010680	98	89.57
9	187	0.010750	109	90.16
10	205	0.010830	119	90.83
11	223	0.010900	130	91.41
12	240	0.010980	139	92.08
13	258	0.011070	150	92.84
14	276	0.011150	160	93.51
15	294	0.011230	171	94.18
16	312	0.011320	181	94.94
17	329	0.011510	191	96.53
18	347	0.011600	202	97.28
19	365	0.011700	212	98.12
20	383	0.011800	222	98.96
21	401	0.011900	233	99.80
22	419	0.011990	243	100.55
23	436	0.012090	253	101.39
24	454	0.012180	264	102.15
25	472	0.012280	274	102.99
26	490	0.012370	285	103.74
27	508	0.012570	295	105.42

# Appendix C : VISCOSITY AND DENSITY REFERENCE STANDARD






**Anton Paar**

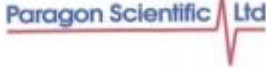
Anton-Paar-Str. 20  
A-8054 Graz  
Austria - Europe  
Tel: +43 (0) 316 2570  
Fax: +43 (0) 316 257 257  
www.anton-paar.com

The parent batch for this sample was manufactured, tested, packaged and stored on our behalf in accordance with the requirements of ISO 17025 and ISO Guide 34 by Paragon Scientific Ltd. The calibration certificate issued by Paragon Scientific Ltd for this product is reproduced below.


**CERTIFICATE OF CALIBRATION**  
ISSUED BY PARAGON SCIENTIFIC LIMITED

Date of Issue: **07-Oct-14**      Certificate No. **AP1662**



UKAS accredited calibration laboratory No.0649 accredited to ISO/IEC 17025  
UKAS accredited reference material producer No.4589 accredited to ISO Guide 34  
6 Prenton Way, North Cheshire Trading Estate, Prenton, Wirral, UK. CH43 3DU.  
Telephone: +44 (0) 151 649 9955 Fax: +44 (0) 151 649 9977  
e-mail: sales@paragon-sci.com Web Site: www.paragon-sci.com

Approved Signatory  
Name: Mr. J. Morris  
Signature: 

**ISO 17025 / ISO Guide 34 VISCOSITY AND DENSITY REFERENCE STANDARD**


Standard type: **APN26**      Lot No: **2122308**      Expiry Date: **06-Oct-16**

Temperature		Viscosity				Density
(°C)	(°F)	mm <sup>2</sup> /s (cSt) Kinematic	mPa.s (cP) Dynamic	SUS	SFS	(g/mL)
20.00	68.00	61.09	50.14			0.8207
25.00	77.00	48.59	39.72			0.8175
37.78	100.00	28.84	23.34			0.8094
40.00	104.00	26.56	21.46			0.8081
50.00	122.00	18.82	15.09			0.8018
60.00	140.00	13.87	11.03			0.7956
80.00	176.00	8.279	6.482			0.7830
98.89	210.00	5.572	4.297			0.7712
100.00	212.00	5.453	4.202			0.7705

Paragon Scientific Ltd. certifies that the kinematic viscosity measurements have been made in accordance with ASTM D2162 using long capillary Master Viscometers at all temperatures. See also ASTM D445, D446, D2171, ISO 3104, ISO 3105, IP 71 Sections 1 and 2 and IP 222. The viscosity data reported is based on the primary standard of pure water at 20°C (ITS-90) having a value of 1.0034 mm<sup>2</sup>/s (cSt) ± 0.17%, as adopted by NIST, ASTM, IP and ISO (ISO 3668). Density measurements were made in accordance with ASTM D1480. Temperature measurements were made using thermometers specified in ASTM D2162 which have a current calibration traceable to the National Physical Laboratory (NPL), National Institute Standards and Technology (NIST) and other recognised national standards laboratories. SUS and SFS values have been calculated in accordance with ASTM D2161 where stated. The calibrations of this product are traceable to NIST.

**Uncertainties:**

Viscosity Range	Expanded Uncertainty	
	Kinematic Viscosity mm <sup>2</sup> /s (cSt)	Dynamic Viscosity mPa.s (cP)
0.3 to 7.4	± 0.07 %	± 0.07 %
7.4 to 10	± 0.09 %	± 0.09 %
10 to 30	± 0.12 %	± 0.12 %
30 to 72	± 0.14 %	± 0.14 %
72 to 180	± 0.15 %	± 0.15 %
180 to 520	± 0.17 %	± 0.17 %
520 to 1000	± 0.19 %	± 0.19 %
1000 to 2700	± 0.20 %	± 0.20 %
2700 to 8000	± 0.22 %	± 0.22 %
8000 to 82 500	± 0.23 %	± 0.23 %



Uncertainties stated on this certificate do not include the uncertainty for the value of the viscosity of water at 20°C (ITS-90) having a value of 1.0034 mm<sup>2</sup>/s (cSt) ± 0.17%.

**Density Uncertainties:** Expanded Uncertainty ± 0.01 %

The reported expanded uncertainty is based on a combined standard uncertainty multiplied by a coverage factor of *k*=2, providing a level of confidence of approximately 95%.

**Notes:** The shelf life of this product is guaranteed until the expiry date, provided the bottle is unopened and stored at ambient temperature (15 to 30°C). The guarantee is void if the bottle seal is broken but the product should remain stable for 3 months after opening if stored correctly. Filtration of product before use is not necessary. No minimum volume is required to guarantee homogeneity.

**Units:**  
Kinematic Viscosity: 1 cSt = 10<sup>-6</sup> St = 10<sup>-6</sup> m<sup>2</sup>/s = 1 mm<sup>2</sup>/s  
Dynamic Viscosity: 1 mPa.s = 10<sup>-3</sup> Pa.s = 1 cP = 10<sup>-2</sup> P  
Dynamic Viscosity = Kinematic Viscosity x Density (at the same temperature)

This certificate is issued in accordance with the laboratory accreditation requirements of the United Kingdom Accreditation Service (UKAS). It provides traceability of measurement to recognised national standards, and to units of measurement realised at the National Physical Laboratory (NPL) or other recognised national standards laboratories. This certificate may not be reproduced other than in full, except with the prior written approval of the issuing laboratory. UKAS is one of the signatories to the Multilateral Agreement of European co-operation for Accreditation (EA) for the mutual recognition of calibration certificates issued by accredited laboratories.

